Durham E-Theses

Solid solution studies of the molecular nonlinear optical properties of organic chromophores

Healy, David

How to cite:

Healy, David (1996) *Solid solution studies of the molecular nonlinear optical properties of organic chromophores*, Durham theses, Durham University. Available at Durham E-Theses Online: http://etheses.dur.ac.uk/5435/

ABSTRACT

The work presented in this thesis describes an investigation into the properties and behaviour of nonlinear optical guest molecules doped into polymeric matrices.

The interactions of the guest molecule 2-(N, N dimethylamino)-5-nitroacetanilide (DAN) with a polycarbonate and polymethyl methacrylate (PMMA) host are compared. A detailed characterisation of the two systems is described employing infra red spectroscopy and analysis of the chromophore alignment during electric field poling. The study reveals that hydrogen bond formation between the guest and the polar polycarbonate backbone accounts for the unusually good alignment stability previously reported in the polycarbonate system. The molecular hyperpolarisibility of DAN in PMMA is also measured and the apparent enhancement compared with solution measurements is accounted for by the more polar nature of the polymer environment.

A new technique allowing the measurement of the dipole moment of polar molecules doped into thin polymer films is also presented. The technique is demonstrated on a series of zwitterionic chromophores whose measured dipole moments range from 30 to 40 D. Electrochroism measurements are performed to account for aggregation of the monomer species which then permits the first hyperpolarisibility of the molecules to be calculated. The values of dipole moment and hyperpolarisibility are found to be very sensitive to the choice of dielectric cavity shape used when deriving the local field correction factors. The measured values are therefore compared with theoretical calculations and a preferred cavity shape is proposed.

DECLARATION AND COPYRIGHT

I hereby declare that the work presented in this thesis has not previously been submitted for any degree and is not being currently submitted in candidature for any other degree.

The work reported in this thesis was carried out by the candidate. Any work not carried out by the candidate is acknowledged in the main text.

The copyright of this thesis rests with the author. No quotation should be published without his prior written consent and information derived from it should be acknowledged.

ACKNOWLEDGEMENTS

SOLID SOLUTION STUDIES OF THE MOLECULAR NONLINEAR OPTICAL PROPERTIES OF ORGANIC CHROMOPHORES

DAVID HEALY

Thesis submitted for the Degree of Ph.D

Department of Physics

University of Durham

1996

1 3 JAN 1997

TABLE OF CONTENTS

LIST OF FIGURES

LIST OF TABLES

CHAPTER 1

INTRODUCTION

Until 1960 and the invention of the laser by Maiman [1], none of the nonlinear phenomena studied had been at optical wavelengths [2-4]. Only the laser could provide the coherent intense light source necessary to elicit nonlinear effects at these wavelengths. The first demonstration of a nonlinear optical effect was performed one year after Maiman's invention by Franken et al. in 1961 who doubled the frequency of a ruby laser with a piece of crystalline quartz [5]. This experiment opened up the research field of nonlinear optics and provided a possible means of reproducing, optically, the effects associated with active electronic devices such as transistors.

In order to realise the possibilities of optical processors, a means had to be found by which properties of a light beam such as its amplitude, phase and frequency could be changed. To this end more emphasis was placed on exploring new optical phenomena during the early stages in the development of nonlinear optics rather than on the materials. As a result nonlinear optical research was mostly confined to the investigation of phenomena such as sum-frequency generation [6], parametric amplification [7, 8], two photon absorption [9], four wave mixing [10], intensity dependent refractive index [11] and surface nonlinear optical effects [12].

As more was understood about each phenomenon investigated it became clear that the properties of the available materials were far from ideal if effective devices were to be realised. At this point the materials studied were the inorganic crystals such as potassium dihydrogen phosphate (KDP) and ammonium dihydrogen phosphate

1

(ADP). These materials were originally developed for applications in ultrasonic transducers and therefore satisfied the symmetry constraints imposed on second order nonlinear optical compounds. Although very little research is conducted on compounds such as these today, they are still very important in large scale applications with the deuterated form of KDP still the most common frequency doubling crystal in commercial laser systems [13].

Organic material research was not a consideration during the early development of nonlinear optics due to the scarcity of experiments carried out on such materials. This however changed upon the introduction in 1968 of the Kurtz powder second harmonic generation (SHG) technique [14] which provided a simple means of comparing both organic and inorganic crystalline materials without the need for growing large crystals. A systematic study of the properties of organic materials followed in 1970 [15] which confirmed theoretical proposals, first made in 1965 by Bloembergen [16], that the quadratic nonlinearity could be predicted using a two level model. This work further showed that the organic materials containing longer conjugation lengths led to a higher quadratic nonlinearity. As a result of these experiments and others like them, an understanding of organic nonlinear optical materials quickly developed and their potential was soon realised.

In 1971, Hauchecorne et al. developed the technique of electric field induced second harmonic generation (EFISH) [17] which provided a means of measuring the first hyperpolarisability, β, of molecules dissolved in solution. This technique, coupled with the powder SHG technique, allowed a systematic study of a large number of organic materials [18]. However, much of this research was carried out on existing materials and no attempt was initially made to deliberately synthesise materials whose nonlinear properties were optimised, despite the great deal of knowledge already collected on the origin of organic nonlinear responses. This changed in the 1980's when two major groups (Bell Labs and CNET) worked on molecules designed and synthesised specifically for use in nonlinear optics. Not only were the nonlinearities optimised but the molecules were also tailored to allow easy growth of a desired crystal structure. This work culminated in the development of the molecule

2

N-(4-nitrophenyl)-(L)-prolinol (NPP) [19, 20] and provoked a new molecular engineering approach to materials research.

For many years, research was based around materials which could be grown into large crystals. Not only is this very time consuming and expensive but in the case of second order effects, materials are restricted to the few which crystallise noncentrosymmetrically. For practical devices a thin film [21] or doped fibre [22] approach is more appropriate in order to allow integration with existing technologies. Further to this, longer interaction lengths than in large crystals are possible at high optical power densities [23, 24]. The growing of thin film crystals has been attempted on a number of occasions [25-27], however achieving growth in the correct orientation with low optical waveguide losses has proven very difficult.

As a result of the problems associated with thin film crystal growth, the nonlinear optical research community started to concentrate on polymeric systems. By the late 1970's a great deal of work had been done on polymers and as such they were well understood and had proven far easier to synthesise and process than crystals. The use of polymers doped with nonlinearly active chromophores also opened up the possibility of using those materials previously excluded due to non-favourable crystal formation. The first guest-host polymeric systems of this type were studied in 1979 by Havinga and Van Pelt as a means of probing the local molecular environment [28]. It was not until 1982 when Meredith and Williams extended the idea and used these polymeric systems as nonlinear optical materials [29]. In order to induce the noncentrosymmetry required for second order nonlinearities in these systems, the active constituents are aligned using an electric field [30]. It is in this process that the disadvantages of these materials lie since the induced alignment does not remain indefinitely. As a result much research has been carried out in order to understand the relaxation processes involved and reduce the response loss to acceptable levels [31-33]. This led to the development of polymeric systems wherein the active chromophores are chemically bonded to the polymer chains in the form of either side groups [34] or main-chain sub-units [35, 36]. These systems, in conjunction with the process of cross-linking [37, 38], have led to very stable

nonlinear responses. Although there is still much work to be done on this class of material, their low cost and ease of processing make them the most likely candidates for use in integrated optical devices.

Until relatively recently the only methods of characterising the properties of new nonlinear materials were the Kurtz powder technique and EFISH. The powder technique, although simple, gives information only on those compounds which crystallise noncentrosymmetrically and does not yield accurate values by which materials can be characterised. As a result EFISH was the only technique which made quantitative analysis of the nonlinear response of new molecules possible. It was therefore modified and optimised following its original development in 1971 and by the late 1970's had become the standard technique by which all new molecules were compared [39, 40]. In 1981 the EFISH technique was advanced still further by Singer who improved its accuracy by introducing a concentration dependence technique [41-42].

There has been a recent development of new material classes such as those made up of octopolar [43] or ionic molecules [44]. The EFISH technique is unsuitable for characterising systems such as these and therefore the technique of Hyper Rayleigh Scattering (HRS) [45] must be employed. This again is a technique carried out in solution and has the advantage that it yields the first hyperpolarisability alone without the need for calculating any other molecular parameters such as the dipole moment.

Another technique enabling the determination of the first hyperpolarisability also attempted involved the use of Langmuir Blodgett (LB) films. LB films have received considerable attention during recent years that has included the investigation of the nonlinear optical properties of suitable molecular layers [46, 47]. In theory the molecular ordering in LB films is controllable and very regular and thus the idea of using them to determine the nonlinear optical properties of the component molecules has been considered [48]. However, it was found that in reality the molecular ordering is far from regular and difficult to model or predict. As a result the values of

the molecular hyperpolarisability obtained by this method were unreliable and the technique lost favour.

Although using LB films to measure the nonlinear optical properties of a molecule is no longer considered, the concept of measuring molecular properties in the solid state is still important. Recent evidence has shown that the properties of molecules, such as the dipole moment and polarisability, are very sensitive to the molecular environment [49-51]. The conclusion to be drawn from these calculations is that the values for dipole moment and molecular polarisability measured in solution can no longer be considered a reliable representation of their values in the solid state. In view of the fact that most future devices are likely to be manufactured using thin film technology, it is therefore important to develop techniques to measure the molecular properties in this solid state form.

Early attempts have been made to characterise the properties of molecules doped into thin films using electro-optic measurements [52]. Along with some important observations made with regard to the interaction of the guest and host in the polymer system studied, an attempt was also made to calculate the first hyperpolarisability of the dopant. However, there is no simple relationship between the electro-optic coefficient and the nonlinear susceptibility, only an approximate expression is obtainable employing various simplifying assumptions and the two-level model. Further to this the dipole moment used in the calculations was not obtained from a solid state measurement. As a result care must be taken when interpreting results from measurements such as these.

It is clear therefore that an alternative approach must be taken if the properties and behaviour of thin polymer films and their constituents are to be characterised accurately. In particular a technique must be found which allows determination of the molecular dipole moment of the chromophores contained within a polymer film. The subject of the studies reported in this body of work is therefore concerned with the nonlinear optical characterisation of guest molecules doped into polymer thin films and their interaction with the surrounding host media.

The nonlinearities of interest in this work are those associated with the first molecular hyperpolarisability (i.e. second order nonlinear optics) which encompasses effects such as second harmonic generation and the electro-optic effect. Chapter 2 thus presents an introduction to second order nonlinear optics in organics. The relevant theory is addressed, both on a microscopic scale, concerned with the molecular response and a macroscopic scale concerned with the bulk material response. Following this the specific material properties required to observe the desired effects are presented and the material classes investigated to date are discussed.

Chapter 3 is concerned with the technique of electric field poling, the application of which is necessary to induce the noncentrosymmetric molecular alignment required by second order nonlinear optical materials. The chapter begins with a summary of the various poling techniques available with a discussion of the relative merits of each. The chapter then concludes with a presentation of the theory used to model the orientation of the aligned dipoles contained within the film following the application of the electric field.

Chapter 4 contains details of the experimental techniques used throughout the study. The chapter begins with a description of the sample preparation methods employed and includes details of the spin coating and substrate withdrawal techniques used to deposit the films. Sample characterisation is then discussed and includes the methods used to determine the linear optical and physical properties of the prepared films. The two electric field poling techniques used are described and details are given of the new constant current corona triode (CCCT) built to monitor the molecular alignment processes during corona charging. The chapter concludes with a summary of the optical effects chosen to characterise the nonlinear properties of each film. The experimental arrangements required to observe the electro-optic effect and second harmonic generation are described and the theory used to extract the relevant film efficiency coefficients from each response is presented.

Chapter 5 is concerned with the characterisation of hydrogen bonding guest host polymeric thin films. A number of authors have observed unusual molecular alignment stability following the poling of certain guest host systems and attributed the effect to intermolecular interactions thought to be a result of hydrogen bond formation [32, 33, 52, 53]. Through the use of infra-red spectroscopy and electric field poling studies, these intermolecular interactions are characterised and a mechanism to explain the stable alignment is proposed. An attempt to further improve this alignment stability through modification of the system components is also described. Second harmonic generation studies are reported along with calculations of the molecular hyperpolarisibilities of the guest molecules, the results from which are compared with measurements made previously in solution.

Chapter 6 presents results obtained from the solid state molecular characterisation of a series of highly polar zwitterionic chromophores. A new technique is presented which allows the determination of the molecular dipole moment of the guest molecules doped into thin polymer films. The technique is based on angle resolved second harmonic generation and results in a concentration independent calculation of the local dipole moment. Second harmonic generation results are also analysed and, after taking into account the effects of chromophore dimerisation, estimates are made of the local first hyperpolarisability of the molecules. The resultant values of dipole moment and hyperpolarisability are found to be very sensitive to the local field model used. The experimental values of dipole moment and hyperpolarisability are therefore compared with theoretical models and a favoured local field model is proposed.

1.1 References

1.   T.H. Maiman, *Stimulated Optical Radiation in Ruby*. Nature, 1960. **187**: p. 493.

2.   L.D. Landau and E.M. Lifshitz, *Electrodynamics of Continuous Media*. 1960: Pergamon Press.

3.   M.E. Lines and A.M. Glass, *Principals and Applications of Ferroelectrics and Related Materials*. 1977: Clarendon Press.

4.   C.G. Le Fevre and R.J.W. Le Fevre, *The Kerr Effect - Its Measurement and Application in Chemistry*. Rev. of Pure and Appl. Chem., 1955. **5**: p. 261.

5.   P.A. Franken, A.E. Hill, C.W. Peters and G. Weinreich, *Generation of Optical Harmonics*. Phys. Rev. Lett., 1961. **7**: p. 118-119.

6.   M. Bass, P.A. Franken, A.E. Hill, C.W. Peters and G. Weinreich, *Optical Mixing*. Phys. Rev. Lett., 1962. **8**: p. 18.

7.   W.H. Louisell, *Coupled Mode and Parametric Electronics*. 1960, New York: Wiley.

8.   J.A. Giordmaine and R.C. Miller, *Tunable, Coherent Parametric Oscillation in LiNbO₃ at Optical Frequencies*. Phys. Rev. Lett., 1965. **14**: p. 973-976.

9.   M.W. McClain and D.M. Friedrich, *Two Photon Molecular Electronic Spectroscopy*. Ann. Rev. Phys. Chem., 1980. **31**: p. 559-577.

10.   P.D. Maker and R.W. Terhune, *Study of Optical Effects due to an Induced Polarization Third Order in the Electric Field Strength*. Phys. Rev., 1965. **137** A(801-818).

11.   T.Y. Chang, *Fast Self-Induced Refractive-Index Changes In Optical Media - a Survey*. Optical Engineering, 1981. **20**(2): p. 220-232.

12.   V.M. Agranovich and D.L. Mills, *Surface Polarons*. 1982, Amsterdam: North Holland Publishing Co.

13.   P. Thomas, *Inorganic Nonlinear Materials*. Physics World, 1990. **March**: p. 34-38.

14.   S.K. Kurtz and T.T. Perry, *A Powder Technique for the Evaluation of Nonlinear Optical Materials*. J. Appl. Phys., 1968. **39**: p. 3798-3813.

15.   B.L. Davydov, L.D. Derkacheva, V.V. Dunina, M.E. Zhabotinskii, V.F. Zolin, L.G. Koreneva and M.A. Samokhina, *Connection Between Charge Transfer and Laser Second Harmonic Generation*. ZhEFT Pis. Red., 1970. **12**: p. 24-26.

16.   N. Bloembergen, *Nonlinear Optics*. 1965: Benjamin.

17.   G. Hauchecorne, F. Kerherve and G. Mayer, *Mesure des Interactions Entre ondes Lumineuses dans Diverse Substances*. J. de Phys., 1971. **32**: p. 47.

18.   D.S. Chemla and J. Zyss, *Nonlinear Properties of Organic Molecules and Crystals (volume 2 of Quntum Electron)*. 1987: Academic Press.

19.   D.S. Chemla and J. Zyss, *Nonlinear Properties of Organic Molecules and Crystals (volume 1 of Quntum Electron)*. 1987: Academic Press.

20.   J. Zyss, J.F. Nicoud and M. Coquillay, *Chirality and Hydrogen-Bonding In Molecular-Crystals For Phase- Matched 2nd-Harmonic Generation - N-(4-Nitrophenyl)-(L)-Prolinol (Npp)*. Journal Of Chemical Physics, 1984. **81**(9): p. 4160-4167.

21.   P.K. Tien, *Light Waves in Thin Films and Integrated Optics*. Applied Optics, 1971. **10**: p. 2395.

22.   B.K. Nayer and R.C. Booth, *An Introduction to Integrated Optics*. Br. Telecom. Tech. J., 1986. **4**: p. 5-15.

23.   G.I. Stegeman and C.T. Seaton, *Nonlinear Integrated Optics*. J. Appl. Phys., 1985. **58**: p. R57-R78.

24.   M. De Micheli and D. Ostrowski, *Nonlinear Integrated Optics*. Physics World, 1990. **March**: p. 56-60.

25.   P.A. Norman, D. Bloor, J.S. Obhi, S.A. Karaulov, M.B. Hursthouse, P.V. Kolinsky, R.J. Jones and S.R. Hall, *Efficient 2nd-Harmonic Generation In Single-Crystals Of 2-(N,N- Dimethylamino)-5-Nitroacetanilide*. Journal Of the Optical Society Of America B-Optical Physics, 1987. **4**(6): p. 1013-1017.

26.   J.C. Baumert, R.J. Tweig, G.C. Bjorklund, J.A. Logan and C.W. Dirk, *Crystal Growth and Characterisation of 4 - (N,N-dimethylamino) - 3 - acetamidonitrobenzene, a New Organic material for Nonlinear Optics*. Appl. Phys. Lett., 1987. **51**: p. 1484-1486.

27.   J. Zyss, *Nonlinear Organic Materials for Integrated Optics: a Review*. J. Mol. Electron., 1985. **1**(25-45).

28.   E.E. Havinga and P. Van Pelt, *Intramolecular Charge Transfer Studied by Electrochroism of Organic Molecules in Polymer Matrices*. Mol. Cryst. Liq. Cryst, 1979. **52**: p. 145-156.

29.   G.R. Meredith, J.G. Vandusen and D.J. Williams, *Optical and Non-Linear Optical Characterization Of Molecularly Doped Thermotropic Liquid-Crystalline Polymers*. Macromolecules, 1982. **15**(5): p. 1385-1389.

30.   S. Keilich, *Optical SGH by Electrically Polarised Isotropic Media*. IEEE J. of Quantum Electronics, 1969. **QE-5**: p. 562.

31.   M. Stahelin, D.M. Burland, M. Ebert, R.D. Miller, B.A. Smith, R.J. Twieg, W. Volksen and C.A. Walsh, *Reevaluation Of the Thermal-Stability Of*

Optically Nonlinear Polymeric Guest-Host Systems. Applied Physics Letters, 1992. **61**(14): p. 1626-1628.

32. H.L. Hampsch, J. Yang, G.K. Wong and J.M. Torkelson, *2nd Harmonic Generation In Doped Glassy Polymer-Films As a Function Of Physical Aging and Dopant Size.* Polymer Communications, 1989. **30**(2): p. 40-43.

33. G.T. Boyd, C.V. Francis, J.E. Trend and D.A. Ender, *2nd-Harmonic Generation As a Probe Of Rotational Mobility In Poled Polymers.* Journal Of the Optical Society Of America B-Optical Physics, 1991. **8**(4): p. 887-894.

34. K.D. Singer, M.G. Kuzyk, W.R. Holland, J.E. Sohn, S.J. Lalama, R.B. Comizzoli, H.E. Katz and M.L. Schilling, *Electro-Optic Phase Modulation and Optical 2nd-Harmonic Generation In Corona-Poled Polymer-Films.* Applied Physics Letters, 1988. **53**(19): p. 1800-1802.

35. H.K. Hall, T.M. Kuo and T.M. Leslie, *New Ab Polyesters and a Polymethacrylate Containing Dipolar Para- Phenyleneazo Groups.* Macromolecules, 1989. **22**(9): p. 3525-3529.

36. I. Teraoka, D. Jungbauer, B. Reck, D.Y. Yoon, R. Twieg and C.G. Willson, *Stability Of Nonlinear Optical Characteristics and Dielectric Relaxations Of Poled Amorphous Polymers With Main-Chain Chromophores.* Journal Of Applied Physics, 1991. **69**(4): p. 2568-2576.

37. R.J. Morgan, *Advances in Polymer Science,* . 1985, Springer-Verlag: Berlin. p. 72.

38. D.R. Robello, C. Willand, M. Scozzafava, A. Ullman and D.J. Williams, *Materials for Nonlinear Optics, Chemical Perspectives,* , S.R. Marder, J. Sohn and G. Stucky, Editors. 1991, ACS. p. 279.

39. J. Oudar, *Optical Nonlinearities of Conjugated Molecules. Stilbene Derivatives and Highly Polar Aromatic Compounds.* J. Chem Phys., 1977. **63**: p. 2666-2682.

40. B.F. Levine and C.G. Bethea, *Second and Third Order hyperpolarisibilities of Organic Molecules.* J. Chem. Phys., 1975. **75**: p. 3572-3580.

41. K.D. Singer and A.F. Garito, *Measurements Of Molecular 2nd Order Optical Susceptibilities Using Dc Induced 2nd Harmonic-Generation.* Journal Of Chemical Physics, 1981. **75**(7): p. 3572-3580.

42. K.D. Singer, *Experimental Studies of Second Order Nonlinear Optical Susceptibilities in Organic Systems,* . 1981: Pennsylvania.

43.   T. Verbiest, K. Clays, A. Persoons, F. Meyers and J.L. Bredas, *Determination of the hyperpolarisability of an Octopolar Molecular Ion by Hyper Rayleigh Scattering.* Optics Letters, 1993. **18**: p. 525-527.

44.   X.M. Duan, S. Okada, H. Oikawa, H. Matsuda and H. Nakanishi, *Comparatively Large Second Order Hyperpolarisability of Aromatic Sulphonate Anion with Short Cut-off wavelength.* Jap. J. Appl. Phys. II - Lett., 1994. **33**: p. L1559-L1561.

45.   K. Clays and A. Persoons, *Hyper Rayleigh Scattering in Solution.* Rev. Sci. Instr., 1992. **63**: p. 3285-3289.

46.   O.A. Aktsipetrov, N.N. Achmediev, E.D. Mishina and V.R. Novak, *Second Harmonic Generation on Reflection from a Monomolecular Langmuir Layer.* JETP Lett, 1983. **37**: p. 207-209.

47.   G.J. Ashwell, *Photochromic and Nonlinear Optical-Properties Of C16h33-P3cnq and C16h33-Q3cnq Langmuir-Blodgett-Films.* Thin Solid Films, 1990. **186**(1): p. 155-165.

48.   I.R. Girling, N.A. Cade, P.V. Kolinsky and C.M. Montgomery, *Observation of Second Harmonic Generation from a Langmuir Blodgett Monolayer of a Merocyanine Dye.* Electronics letters, 1985. **21**: p. 169-170.

49.   J.L. Bredas, F. Meyers, C. Dehu, B.M. Pierce and S.R. Marder, *Nonlinear-Optical Response Of Organic Conjugated Compounds - Theoretical Description Of Solvent Mediated Enhancement Of Hyperpolarizabilities.* Abstracts Of Papers Of the American Chemical Society, 1994. **208**(Pt1): p. 8-COMP.

50.   F. Meyers, S.R. Marder, B.M. Pierce and J.L. Bredas, *Tuning Of Large 2nd Hyperpolarizabilities In Organic Conjugated Compounds.* Chemical Physics Letters, 1994. **228**(1-3): p. 171-176.

51.   F. Meyers, S.R. Marder, J.W. Perry, J.L. Bredas and B.M. Pierce, *Optimizing Molecular Polarizabilities In Linear Conjugated Organic- Molecules.* Abstracts Of Papers Of the American Chemical Society, 1994. **208**(Pt2): p. 169-POLY.

52.   Y. Karakus, D. Bloor and G.H. Cross, *Enhanced Linear Electrooptic Response and Enhanced Stability Of Thermo-Poled Guest Host Polycarbonate Thin-Films.* Journal Of Physics D-Applied Physics, 1992. **25**(6): p. 1014-1018.

53.   F. Wan, G.O. Carlisle, K. Koch, D.R. Martinez and T.A. W, *Enhanced 2nd-Harmonic Response and Stability Of Corona-Poled Guest- Host Polycarbonate Thin-Films.* Journal Of Materials Science-Materials In Electronics, 1995. **6**(4): p. 228-234.

CHAPTER 2

NONLINEAR OPTICS IN ORGANIC SYSTEMS

2.1 Introduction

In this chapter the origins of nonlinear optical effects are described along with the material properties required to observe them. The chapter will begin with an introduction to the linear and nonlinear interactions of electromagnetic radiation with matter, both on a microscopic scale, dealing with individual molecules, and with the bulk media. Following this a more detailed description of these effects, specific to organic media, will be given. The chapter will conclude with a brief summary of the classes of organic material systems studied to date including a short discussion on their development within the field of nonlinear optics.

2.2 Microscopic Nonlinearities

Nonlinear optical effects result from a change in the properties of a material induced by the presence of an electric field. Therefore, in order to understand the origins of these effects, the interaction of the field with the system components, i.e. the molecules, must first be considered.

In the presence of an electric field, such as those of electromagnetic radiation, charges within a molecule are displaced from their equilibrium position and a dipole moment, μ_{ind}, is induced [1]:

$$\mu_{ind} = -qr$$

(2.1)

where q is the charge and r is the field induced displacement. The negative sign indicates that the direction of polarisation is opposite to the electron displacement direction. When the field strength is small in comparison to the atomic field ($\sim 10^{11}$ Vm^{-1}) then the induced polarisation is linearly dependent on the field and can be expressed as follows [2]:

$$p_i(\omega) = \alpha_{ij}(\omega)E_j(\omega)$$

(2.2)

where $\alpha_{ij}(\omega)$ is the linear molecular polarisability and is independent of the local field, $E_j(\omega)$. $\alpha_{ij}(\omega)$ is a second rank tensor where i and j refer to the molecular co-ordinate system. It is a complex value where the real part provides the origin of refractive index and the imaginary part the origin of absorption.

When the applied electric field becomes much greater, the induced polarisation is nonlinearly dependent on the field and can be expanded in powers of the electric field strength [3]:

$$p_i(\omega) = \sum_j \alpha_{ij}(\omega)E_j(\omega) + \sum_j \sum_k \beta_{ijk}(-\omega; \omega_1, \omega_2)E_j(\omega_1)E_k(\omega_2) +$$
$$\sum_j \sum_k \sum_l \gamma_{ijkl}(-\omega; \omega_1', \omega_2', \omega_3')E_j(\omega_1')E_k(\omega_2')E_l(\omega_3') + ..$$

(2.3)

where $\beta_{ijk}(-\omega;\omega_1,\omega_2)$ and $\gamma_{ijkl}(-\omega;\omega_1',\omega_2',\omega_3')$ are the frequency dependent first and second hyperpolarisabilities and E_j, E_k, etc. are the components of the applied local field. β and γ are third and fourth rank tensors respectively and each is the origin of two distinct groups of nonlinear optical effects.

2.2.1 The Nonlinear Optical Effects Associated with β and γ

As mentioned above, the more common nonlinear optical responses can be divided into two general groups, those associated with the first molecular hyperpolarisibility, β, known as second order responses, and those associated with the second hyperpolarisibility, γ, known as third order responses. Although other effects can be

exhibited, associated with higher order hyperpolarisibilities related to higher powers of electric field, the responses are usually very weak and as such require electric field strengths higher than are usually practical for most applications.

Probably the most well known second order response involves the frequency conversion of the incident radiation. Sum frequency generation is indicated by $\beta_{ijk}(-\omega; \omega_1, \omega_2)$ where the minus sign denotes the radiated energy. ω, ω_1 and ω_2 can take any value provided that energy conservation is satisfied, i.e. $\omega = \omega_1 + \omega_2$. A special case of this is second harmonic generation (SHG) where $\omega_1 = \omega_2$ resulting in the output radiation having twice the frequency of the input. $\beta_{ijk}(-\omega; \omega_1, -\omega_3)$ indicates difference frequency generation where $\omega_3 = \omega_1 - \omega_2$ the special case of which is when $\omega_1 = \omega_2$ resulting in optical rectification. The other well known second order response is the linear electro-optic effect (or Pockels effect) denoted by $\beta_{ijk}(-\omega; \omega, 0)$. This is where the refractive index of the medium can be adjusted by application of a dc electric field. Provided that the molecule satisfies certain symmetry requirements, which will be discussed in section **2.2.2**, the second order response is usually the strongest of all the nonlinear optical responses and as such is typically the easiest to probe.

Third order responses are usually far weaker than the second order responses mentioned above. One of the more common third order effects is four wave mixing described by $\gamma_{ijkl}(-\omega; \omega_1, \omega_2, \omega_3)$ where again energy must be conserved such that $\omega = \omega_1 + \omega_2 + \omega_3$. A special case of this is third harmonic generation where $\omega_1 = \omega_2 = \omega_3$ resulting in the output radiation having three times the frequency of the input. A common use of a third order effect is in the technique of field induced second harmonic generation (EFISH), denoted by $\gamma_{ijkl}(-2\omega; \omega, \omega, 0)$. This is where second harmonic light is generated on the application of a dc electric field and can be used to characterise the nonlinear optical properties of molecules dissolved in solution. Another well known third order effect is the DC Kerr effect denoted by $\gamma_{ijkl}(-\omega; \omega, 0, 0)$ where two dc electric fields interact with an optical field.

2.2.2 Symmetry and Nonlinear Optical Responses

It can be seen from careful examination of equation 2.3 that certain symmetry requirements must be satisfied if molecules are to exhibit the second order nonlinear optical responses associated with β. If a centrosymmetric molecule is considered and an electric field +E is applied, then equation 2.3 predicts that the polarisation induced by the first nonlinear term is given by $+\beta E^2$. Similarly, if the electric field -E is applied to the same molecule, equation 2.3 also predicts the second order polarisation to be $+\beta E^2$. This is clearly not possible for a completely symmetric molecule and as such $\beta \equiv 0$. As a result, for a molecule to exhibit a second order nonlinear optical response it must also exhibit some form of asymmetry. If the same argument is applied to polarisations associated with the second nonlinear term, γE^3, it can be seen that the same contradiction does not occur, meaning that all molecules, both symmetric and asymmetric, can exhibit a third order nonlinear optical response.

2.3 Macroscopic Nonlinearities

The nonlinear optical response of a material is directly related to the response of the individual molecules which make up the medium. To understand the bulk response not only must the relationship between the macroscopic response and the molecular response be found but also the relationship between the electric field applied externally and that experienced by the individual molecule. The polarisation induced in a bulk medium can be expanded out in terms of powers of the applied electric field, in a similar manner to the microscopic polarisation, resulting in the following expression [3]:

$$P_I(\omega) = \sum_J \chi_{IJ}^{(1)}(\omega)E_J(\omega) + \sum_J \sum_K \chi_{IJK}^{(2)}(-\omega;\omega_1,\omega_2)E_J(\omega_1)E_K(\omega_2)+$$
$$\sum_J \sum_K \sum_L \chi_{IJKL}^{(3)}(-\omega;\omega_1',\omega_2',\omega_3')E_J(\omega_1')E_K(\omega_2')E_L(\omega_3') + .. \qquad (2.4)$$

where I,J,K now refer to the co-ordinate system of the bulk material and E_J, E_K and E_L are the components of the externally applied field. $\chi^{(1)}$ is the linear susceptibility of the medium and $\chi^{(2)}$ and $\chi^{(3)}$ are the second and third order nonlinear

susceptibilities of the medium respectively. The odd ordered susceptibilities, $\chi^{(1)}$ and $\chi^{(3)}$, are directly related to their corresponding molecular polarisabilities in equation 2.3 by the following [3]:

$$\chi_{IJ}^{(1)}(\omega) = Nf(\omega)\alpha_{ij}(\omega) \qquad (2.5)$$

$$\chi_{IJKL}^{(3)}(-\omega; \omega_1', \omega_2', \omega_3') = Nf(\omega)f(\omega_1')f(\omega_2')f(\omega_3')\gamma_{IJKL}(-\omega; \omega_1', \omega_2', \omega_3') \qquad (2.6)$$

where N is the number density of the component molecules and $f(\omega)$ is the local field factor at frequency ω which relates the externally applied field to the field experienced by the molecule, as described in section **2.3.1**.

It can be seen by comparing equations 2.3 and 2.4 that the symmetry arguments which apply to β must also apply to $\chi^{(2)}$. As such not only must a second order nonlinearly active medium contain noncentrosymmetric molecules but also the molecular arrangement must also be asymmetric. As a result, the relationship between the second order bulk susceptibility and the first hyperpolarisability is far more complicated due to the need to project the components of β_{ijk} onto the bulk co-ordinate system. This is obviously dependent on the material system in question and the means by which the bulk asymmetry was introduced into the system. In a simplified representation, however, the two terms can be related by the following [3]:

$$\chi_{IJK}^{(2)}(-\omega; \omega_1, \omega_2) = Nf(\omega)f(\omega_1)f(\omega_2)\langle \beta_{ijk}(-\omega; \omega_1, \omega_2)\rangle_{IJK} \qquad (2.7)$$

where $\langle\beta_{ijk}(-\omega; \omega_1, \omega_2)\rangle_{IJK}$ is the weighted sum of values of the first molecular hyperpolarisability components averaged over all orientations of the molecule [4, 5]. For a second order nonlinearly active crystal where the active components are fixed with respect to each other by the crystal matrix, $\langle\beta_{ijk}(-\omega; \omega_1, \omega_2)\rangle_{IJK}$ is dependent only on the projection of the crystal lattice onto the incident fields. When considering samples such as doped polymers, however, where the preferential molecular alignment has been introduced by some other means such as electric field

poling (Chapter 3), the calculation of this term is far more complicated and a model such as the oriented gas model [6] (section **3.3**) must be employed.

2.3.1 Local Field Factors

Equation 2.4 is expressed in terms of the externally applied fields. In a dielectric medium containing polarisable particles, the fields experienced by an individual molecule differs from the externally applied fields due to the presence of the dipole fields generated by the surrounding medium. In order to take this into account, therefore, the externally applied fields must be adjusted by the local field factors introduced in equations (2.5) to (2.7). It is common practice to employ the Lorentz-Lorenz local field factor in the case of optical or high frequency fields. The guest molecule is considered to be embedded within a spherical volume external to which the surrounding medium is described as a uniform dielectric. The system is assumed to be a pure non-polar medium and furthermore the dielectric properties of the guest molecule are neglected. If the Lorentz-Lorenz local field ($F_L(\omega)$) is defined in terms of a local field factor ($f_L(\omega)$) such that:

(2.8)

$$F_L(\omega) = f_L(\omega)E(\omega)$$

where $E(\omega)$ is the external field of frequency ω, then the Lorentz-Lorenz local field factor is given by [7]:

$$f_L(\omega) = \frac{(\varepsilon_h(\omega) + 2)}{3} \qquad (2.9)$$

where $\varepsilon_h(\omega)$ is the relative permittivity of the host medium at frequency ω. Although equation (2.9) has proven a good approximation for optical fields, it is not necessarily accurate for low frequency fields applied to solutions since the dielectric properties of the guest molecule are not accounted for and may, for the molecules studied, be substantially different to those of the solvent. Furthermore, both the solvent and solute may have permanent dipole moments.

As a result of these limitations a theory was developed by Onsager [8] who derived an expression which takes account of the dipolar nature of both the solvent and solute. Furthermore a description of the reaction field was introduced which is a field generated by polarisations in the surrounding host medium brought about by the dipole field of the guest (see section **3.3.1**). The theory was then further extended by Scholte [9] and Bottcher [7] who accounted for the shape of the molecule, describing it in terms of an ellipsoid. As before the host is assumed to be an isotropic dielectric with a uniform relative permittivity, $\varepsilon_h(\omega)$, across which is applied a homogeneous external field $E_I(\omega)$. The guest molecule is assumed to be represented by an ellipsoidal volume whose semi-principal axes are a, b and c and whose relative permittivity tensor at frequency ω is $\varepsilon_{ij}(\omega)$. If the ellipsoidal semi-axis, a, is aligned in the direction of the applied field then the field acting on the guest is given by [10]:

$$F_1(\omega)\frac{\varepsilon_h(\omega)}{\varepsilon_h(\omega)+(\varepsilon_{11}(\omega)-\varepsilon_h(\omega))A_1}E_I(\omega) \qquad (2.10)$$

where

$$A_1 = \frac{abc}{2}\int_0^\infty \frac{ds}{\left(s+a^2\right)^{3/2}\left(s+b^2\right)^{1/2}\left(s+c^2\right)^{1/2}} \qquad (2.11)$$

Similarly if the ellipsoidal axis, b, is aligned with the electric field then the field inside the cavity is:

$$F_2(\omega) = \frac{\varepsilon_h(\omega)}{\varepsilon_h(\omega)+(\varepsilon_{22}(\omega)-\varepsilon_h(\omega))A_2}E_I(\omega \qquad (2.12)$$

where
$$A_2 = \frac{abc}{2}\int_0^\infty \frac{ds}{\left(s+a^2\right)^{1/2}\left(s+b^2\right)^{3/2}\left(s+c^2\right)^{1/2}} \qquad (2.13)$$

and similarly for the c axis:

$$F_3(\omega) = \frac{\varepsilon_h(\omega)}{\varepsilon_h(\omega)+(\varepsilon_{33}(\omega)-\varepsilon_h(\omega))A_3}E_I(\omega) \qquad (2.14)$$

18

where (2.15)

$$A_3 = \frac{abc}{2} \int_0^\infty \frac{ds}{\left(s+a^2\right)^{1/2}\left(s+b^2\right)^{1/2}\left(s+c^2\right)^{3/2}}$$

The terms F_1, F_2 and F_3 define three perpendicular components of the local field and since the molecules are randomly oriented within the host matrix the resultant local field is the average of these components:

$$F_l(\omega) = \frac{1}{3}[F_1(\omega) + F_2(\omega) + F_3(\omega)] \qquad (2.16)$$

The relative permittivity within the cavity, $\varepsilon_{ij}(\omega)$, is defined as the internal relative permittivity and can be expressed in terms of three perpendicular components. If the polarisability components along the axes of the ellipsoid are the diagonal polarisability components of the guest molecule, α_{ij} (where $i = j = 1, 2, 3$), then $\varepsilon_{ij}(\omega)$ can be defined as follows [9]:

$$\varepsilon_{ij}(\omega) = \frac{abc + 3(1 - A_i)\alpha_{ij}(\omega)}{abc - 3A_i\alpha_{ij}(\omega)} \qquad (2.17)$$

The values of a, b and c are taken from the van-der-Waals dimensions of the guest molecule which can be obtained from one of several molecular modelling packages such as 'Nemesis'. The polarisability components of the molecule can be calculated using a number of methods including the finite field method within MOPAC (v.6) employing the AM1 Hamiltonian*. For the case of optical fields, when the frequencies are high, the approximation $\varepsilon_h(\omega) = n_\omega^2$ is made where n_ω is the refractive index of the host at frequency ω. For a spherical dielectric volume, where $A_1 = A_2 = A_3 = 1/3$, the obtained values of local field factor should be comparable to those calculated using the Lorentz-Lorenz formula (equation 2.9) if the approximations made in the derivation of (2.9) are valid. However, this is not the case since the medium is polar and the dielectric properties of the guest cannot be neglected in a large number of cases. The case of low frequency and dc applied fields will be discussed in section **3.3.1**.

---

* Note: Other Hamiltonians are available within MOPAC.

2.4 Material Requirements

All optical materials are capable of exhibiting nonlinear optical phenomena. The efficiency of the effect, however, is governed by factors such as the electronic structure of the atomic and molecular constituents, their dynamic behaviour, their symmetry and their geometrical arrangement within the medium. As a result each of these factors must be optimised in order to maximise the efficiency of the desired effect and reduce the strength of the optical fields required to observe them. Since the main topic of the work presented here centres around second order effects, the discussion which follows mainly concentrates on material systems suitable for second order nonlinear optics. As a result the first and foremost material requirement is the need to satisfy the symmetry conditions as discussed in section **2.2.2**. Not only must the molecules themselves be asymmetric but they must also be arranged in a noncentrosymmetric manner. This clearly puts a heavy constraint on possible second order material systems unlike materials for third order nonlinear optical applications where it is theoretically possible for any material to exhibit an effect.

One of the first classes of materials considered in the past were those where the nonlinearities arise from the polarisation of electrons not associated with specific nuclei, such as semiconductor based materials. In this case the nonlinearities derive from the electronic characteristics of the bulk medium and since they originate from the motion of free moving unbound electrons, nonlinear efficiencies can be very high. Although semiconductors are generally studied for their third order effects, the group II-VI and III-V systems form into the noncentrosymmetric "zincblende" structure and are therefore capable of exhibiting second order effects. However, their poor transparency and lack of birefringence, used to achieve phase matching, means that their usefulness is very limited.

Another class of materials which are also regarded as falling into this bulk response category are the noncentrosymmetric inorganic crystals such as lithium niobate, $LiNbO_3$, potassium dihydrogen phosphate, KDP, and potassium titanyl phosphate, KTP. Although their nonlinearities are believed to originate from individual bond

20

polarisabilities, no single molecular unit in the ionic lattice can be identified and as such they are considered to behave as bulk media. The examples mentioned above have proved to be very efficient second order materials and are still used as electro-optic modulators [11] and second harmonic generators [12, 13]. Due to the bulk nature of the response in both the inorganic crystals and the semiconductor materials, the origins of the response are less understood and as such the theoretical models described earlier in this chapter are less easy to apply.

Other material systems under investigation are the nonlinear glasses. Like the semiconductor systems, these were traditionally considered third order materials due to their amorphous structure. However, recent evidence has shown that it is possible to induce a second order response from silica glasses through the application of electric field poling and charge injection [14, 15]. This is clearly an important breakthrough since it opens up the possibility of manufacturing active devices using current optical fibre technology.

Probably the most promising group of materials for second order nonlinear optics, however, is that of organic materials. The nonlinearities in this class derive from the electronic structure of individual molecules and as such fit the theory described earlier in this chapter very well. Their ease of synthesis and ease by which molecules can be tailored to specific requirements opens up many more possibilities for optimising system nonlinearities than are currently available. Further to this, the nonlinearities expected from such systems exceed those of existing materials such as the inorganic crystals, probably their nearest rivals.

2.5 Organic Materials for Nonlinear Optics

2.5.1 The Microscopic Origins of Nonlinear Responses in Organic Media

As discussed above, the origin of the nonlinear response in organic media lies at the molecular level and as such can be modelled using the theory outlined earlier in this chapter. Since the nonlinearities are determined primarily by the nonlinear optical

21

properties of the individual molecules, an understanding of the electronic origins of the response is necessary.

In general, organic nonlinear optical molecules can be described as being constructed of three functional groups as shown in figure 2.1.

$$\text{ED} \quad — \quad \boxed{\begin{array}{c}\pi\text{ - Electron} \\ \text{System}\end{array}} \quad — \quad \text{EA}$$
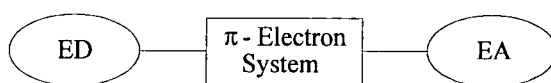
Figure 2.1 Fundamental molecular structure required for second order
nonlinear optical responses.

These are an electron donor group (ED), such as NH_2, $N(CH_3)$, etc., an electron acceptor group (EA), such as NO_2, CN, etc. and these are connected by a conjugated system. In a conjugated system, where the carbon - carbon bonds are alternating single and double bonds and the four valency of carbon cannot be satisfied with single σ–bonds, the orbitals associated with the remaining non-bonding electrons cannot overlap along the internuclear axis and as a result overlap laterally leading to π–bonds. The electrons associated with these π–bonds are highly delocalised, that is they are not bound specifically to one particular atom, and as such are free to move along the length of the conjugated system. Provided that the conjugated system is planar enough, in order that there is sufficient overlap of the π–orbitals, these structures will clearly lead to a high degree of polarisability and as a result give rise to large optical nonlinearities. The differing electronic characters of the two end groups result in the required molecular noncentrosymmetry and also a finite dipole moment, necessary if they are to be aligned in an electric field to induce bulk anisotropy.

This π-bonded structure leads to some important properties, unique to this class of materials. Firstly, unlike their inorganic counterparts, organic molecules are capable of exhibiting very large non-resonant nonlinearities. Operating on, or near, absorption bands can lead to problems of pump depletion and the absorbed light can result in thermally induced nonlinearities which can often dominate over the

electronic effects. Furthermore, response times of a system can be much slower on resonance since they are governed by the excitation lifetime of the transition.

In a second order nonlinear optical system, the relative permittivity (ε_r) of the material is an important parameter when considering its response. In low frequency electric fields, ionic displacements contribute towards ε_r in an inorganic system resulting in much higher values of ε_r than those observed in organic systems where the response is purely electronic and therefore much faster. These ionic contributions are frozen out as the frequency increases leading to a marked difference in ε_r in the two frequency regimes not seen in organic media. In an organic electro-optic modulator the low values of ε_r result in a low RC time constant which permits the modulator to be operated over a much wider bandwidth than a corresponding inorganic device. The marked difference in ε_r in inorganic media in the two frequency regime also makes phase matching in waveguide devices considerably more difficult. Furthermore, it results in a marked difference in the behaviour of inorganic materials depending on whether they are used as harmonic generators, where the response at optical frequencies is important, or electro-optic modulators, where dc frequency response is important.

As a direct result of the structural nature of the majority of organic chromophores, an important simplifying assumption can be made about the first hyperpolarisability tensor, β_{ijk}. Since the nonlinear response of the molecules shown schematically in figure 1.1 increases as the conjugated system lengthens, molecules in this class are often long and very linear and as a result can be considered to be one dimensional. Considerable simplification therefore results with regard to β_{ijk}, since now only one of its components, the one projected onto the dipole moment, β_{vec}, need be considered.

2.5.2 The Macroscopic Properties of Organic Media

One of the clear advantages organic media have over other nonlinear materials is the variety in which they can be prepared. Like inorganic materials, organic molecules can be grown into crystals for applications in nonlinear optics including

noncentrosymmetric crystals when second order properties need to be exploited. However this is only one of the many ways in which organic nonlinearly active media can be prepared. These include growth of thin crystalline layers, fabrication into structures so that they can be deposited as ultra-thin films such as Langmuir-Blodgett (LB) films and incorporation into polymeric media for thin film deposition. Growing crystalline layers, like growing full size optical crystals is very time consuming and difficult from a device point of view. LB films, although far simpler to manufacture than crystals, suffer from very time consuming deposition techniques and the molecular alignment is far from ideal and difficult to quantify. In contrast, polymers are easy to handle and are already manufactured on a large scale. As a result it is this last option that probably shows the greatest promise and as such has been the subject of the work reported here.

Introducing the nonlinearly active molecules into a polymeric system offers many advantages. The mechanical strength of polymers is very good, offering high thermal and environmental stability along with very high optical damage thresholds well in excess of some of the inorganic and semiconductor based media. Their ease of fabrication and inexpensive mass production is clearly another advantage and possibly one of their most important particularly when considering the future possibilities of integrated optical devices and waveguides. The optical quality of polymers is also very high and their basic optical properties such as refractive index can be easily tailored through some careful chemistry. Finally the existence of a glass transition temperature, the temperature at which a polymer softens without melting, in many of the common polymers can be exploited when introducing anisotropic molecular ordering, required for second order effects, through the application of the electric field poling technique (Chapter 3).

2.5.3 $\chi^{(2)}_{IJK}$ and Poled Polymer Systems

When organic chromophores are introduced into an amorphous polymer system, their initial orientation is usually completely random and as a result symmetry requirements of the second order response are not satisfied. Usually to overcome this the dipolar nature of the molecules is exploited and the molecules are aligned in an

electric field using the technique of electric field poling (chapter 3). This introduces preferential alignment in the poling direction (usually designated the 3 direction in the laboratory frame of reference), however the system is still isotropic in the plane perpendicular to this (the 1,2 plane). A direct result of this is that only three tensor components of $\chi^{(2)}_{IJK}$ are non-zero, $\chi^{(2)}_{333}$, $\chi^{(2)}_{311}$ and $\chi^{(2)}_{113}{}^{(x)}$. A further set of symmetry conditions, called Kleinman symmetry [16], may also be applied if the frequencies of the three electric fields are not on an electronic resonance. In this case the three subscripts, I, J and K may be permuted, without permuting the frequencies, resulting in the relation $\chi^{(2)}_{311} = \chi^{(2)}_{113}$. The number of independent tensor components can therefore been reduced to two, $\chi^{(2)}_{333}$ and $\chi^{(2)}_{311}$, in poled polymer systems such as these.

2.5.4 Types of Organic Polymeric Systems

There are several different ways in which chromophores can be introduced into a polymeric host. The four main classes are summarised below.

2.5.4.1 Guest-Host Polymers

By far the simplest way to introduce an active chromophore into a host media, and probably the most investigated, is to disperse the guest molecules throughout the polymer matrix. This is simply achieved by dissolving both the guest molecules and polymer into a common solvent. Thin films can then be prepared using the techniques described in chapter 4. One of the first nonlinear optical polymer systems to be investigated was one of this type, where the chromophore DANS was dissolved up into a liquid crystalline polymer [17]. Although guest host polymers are very easy to prepare, they do suffer from thermal relaxation of the polar alignment of the chromophores, quite a major problem which leads to a decay of the second order nonlinearity of the system. This relaxation is linked to various system parameters including the glass transition temperature of the polymer [18], the chromophore size [19], the amount of free volume within the polymer matrix [20] and the presence of any interactions between the guest and host, such as hydrogen bonding [21]. Although much work has been done in order to understand and counteract the

processes going on during realignment, it is quite clear that the problem will not be completely eliminated and as such it is unlikely that guest host systems are the material system most likely to be used in future devices. However, due to its simplicity, the guest-host method offers a very easy preparation technique if chromophore characterisation in the solid state only is required, particularly in view of the fact that many of the existing theoretical models used to characterise solid state systems are most appropriate for this class of material. As a result much of the understanding of nonlinear optical polymers has come from studying guest host systems.

2.5.4.2 Side Chain Polymers

After the early work on guest host polymer systems it was realised that improved thermal stability could be achieved if the active chromophore was chemically attached to the polymer backbone. The first of this type of polymeric system involved the incorporation of the active species as a side group, or pendant group, attached to the polymer backbone [23, 24]. Clearly, the relaxation of the aligned side chains would be expected to be much slower since the chromophore motion is hindered by its attachment to the polymer. Side chain polymers also have the advantage that higher doping levels can be achieved without any recrystallisation, phase separation or formation of concentration gradients, a problem quite prone to guest host systems if the doping level gets too high. The only disadvantage side chain polymers have compared with guest host systems is that the chemistry required to manufacture them is somewhat more complicated. Despite this, however, this class of polymeric media has a much more promising future with regard to its possible use as a material for the fabrication of devices.

2.5.4.3 Main Chain Polymers

Following on from the improved stability of chromophore alignment in side chain polymers, it became clear that polar order relaxation could be further restricted if the active species was chemically incorporated into the polymer backbone itself. Being attached now at both ends, large segmental motions are required if the polar alignment is to relax, making it a far more stable system. Secondly, a main chain

polymer may show improved tensile and mechanical properties [25]. The earliest main chain polymers were those where the active chromophores were attached in a head-to-tail arrangement along the backbone [26, 27]. It was originally thought that this would result in an enhancement of the resultant second order nonlinear response, however, the lack of linearity of the polymer chain and the reduction in polar alignment caused by chain entanglements reduces the expected enhancement. Other similar systems have also been tried, however many have suffered from insolubility problems. The origin of the high polar order stability in these main chain polymers also leads onto their main disadvantage. Initial orientation of the chromophores necessary to induce bulk noncentrosymmetry is very difficult due to the required segmental motions and chain entanglement. This has led in some cases to lower than predicted values for the nonlinearities in thin films fabricated from these materials [23]. This has been overcome to some extent by the fabrication of main chain polymers where the active chromophores are aligned perpendicular to the backbone [26]. It is thought that this is a result of the fact that smaller segments of the polymer backbone need only be oriented during the alignment procedure. Due to their very stable nature, main chain polymer systems are still an area of active research and are highly promising nonlinear optical materials.

2.5.4.4 Cross-Linked Systems

One method of obtaining the stable properties of the main chain polymers but allowing the initial orientation to occur with the ease of a side chain system is to use cross-linking side chain polymers [27, 28]. Following initial alignment, the polymers are cross-linked, usually by application of heat or light, to hold the alignment stationary. However, although this sounds ideal, it should be noted that on cross-linking, polymers suffer mechanically often becoming more brittle, less soluble and optically poorer. This is clearly a major disadvantage with regard to processibility and applications in low loss optical devices.

2.6 References

1.   P.N. Prasad and D.J. Williams, *Introduction to Nonlinear Optical Effects in Molecules and Polymers.* 1991: Wiley Interscience.

2.   D.M. Burland, R.D. Miller and C.A. Walsh, *2nd-Order Nonlinearity In Poled-Polymer Systems.* Chemical Reviews, 1994. **94**(1): p. 31-75.

3.   D.J. Williams, *Organic Polymeric and Non-Polymeric Materials With Large Optical Nonlinearities.* Angewandte Chemie-International Edition In English, 1984. **23**(9): p. 690-703.

4.   K.D. Singer, M.G. Kuzyk and J.E. Sohn, *2nd-Order Nonlinear-Optical Processes In Orientationally Ordered Materials - Relationship Between Molecular and Macroscopic Properties.* Journal Of the Optical Society Of America B-Optical Physics, 1987. **4**(6): p. 968-976.

5.   B. Dick, *Irreducible Tensor Analysis Of Sum-Frequency and Difference-Frequency-Generation In Partially Oriented Samples.* Chemical Physics, 1985. **96**(2): p. 199-215.

6.   S. Keilich, *Optical SGH by Electrically Polarised Isotropic Media.* IEEE J. of Quantum Electronics, 1969. **QE-5**: p. 562.

7.   C.J.F. Bottcher, *Theory of Electric Polarisation.* 1952.

8.   L. Onsager, *Electric Moments of Molecules in Liquids.* J. Am. Chem. Soc., 1936. **58**: p. 1486.

9.   Th. G. Scholte, *A Contribution to the Theory of the Dielectric Constant of Polar Liquids.* Physica, 1949, **XV** p. 437

10.   J. A. Stratton "Electromagnetic Theory" New York, London 1941 ch. 3

11.   H. Sasashi, Elec. Lett., 1977. **13**: p. 683.

12.   C.J. van Derpoel, J.D. Bierlein, J.B. Brown and S. Colak, *Efficient Type-I Blue 2nd-Harmonic Generation In Periodically Segmented Ktiopo4 Wave-Guides.* Applied Physics Letters, 1990. **57**(20): p. 2074-2076.

13.   E.J. Lim, M.M. Fejer, R.L. Byer and W.J. Kozlovsky, *Blue-Light Generation By Frequency Doubling In Periodically Poled Lithium-Niobate Channel Wave-Guide.* Electronics Letters, 1989. **25**(11): p. 731-732.

14.   U. Osterberg and W. Margulis, *Dye-Laser Pumped By Nd-Yag Laser-Pulses Frequency Doubled In a Glass Optical Fiber.* Optics Letters, 1986. **11**(8): p. 516-518.

15.   R. Kashyap, B.J. Ainslie and G.D. Maxwell, *2nd Harmonic-Generation In GeO₂ Ridge Wave-Guide.* Electronics Letters, 1989. **25**(3): p. 206-208.

16.   D. Kleinman, *Nonlinear Dielectric Polarisation of Optical Media.* IEEE J. Quantum Electron, 1969. **QE-5**: p. 562-568.

17.   G.R. Meredith, J.G. Vandusen and D.J. Williams, *Optical and Non-Linear Optical Characterization Of Molecularly Doped Thermotropic Liquid-Crystalline Polymers.* Macromolecules, 1982. **15**(5): p. 1385-1389.

18.   M. Stahelin, D.M. Burland, M. Ebert, R.D. Miller, B.A. Smith, R.J. Twieg, W. Volksen and C.A. Walsh, *Reevaluation Of the Thermal-Stability Of Optically Nonlinear Polymeric Guest-Host Systems.* Applied Physics Letters, 1992. **61**(14): p. 1626-1628.

19.   G.T. Boyd, C.V. Francis, J.E. Trend and D.A. Ender, *2nd-Harmonic Generation As a Probe Of Rotational Mobility In Poled Polymers.* Journal Of the Optical Society Of America B-Optical Physics, 1991. **8**(4): p. 887-894.

20.   H.L. Hampsch, J. Yang, G.K. Wong and J.M. Torkelson, *2nd Harmonic-Generation In Doped Glassy Polymer-Films As a Function Of Physical Aging and Dopant Size.* Polymer Communications, 1989. **30**(2): p. 40-43.

21.   K.D. Singer, M.G. Kuzyk, W.R. Holland, J.E. Sohn, S.J. Lalama, R.B. Comizzoli, H.E. Katz and M.L. Schilling, *Electro-Optic Phase Modulation and Optical 2nd-Harmonic Generation In Corona-Poled Polymer-Films.* Applied Physics Letters, 1988. **53**(19): p. 1800-1802.

22.   C. Ye, T.J. Marks, J. Yang and G.K. Wong, *Synthesis Of Molecular Arrays With Nonlinear Optical-Properties - 2nd-Harmonic Generation By Covalently Functionalized Glassy-Polymers.* Macromolecules, 1987. **20**(9): p. 2322-2324.

23.   M.A. Mitchell, J.E. Mulvaney, H.K. Hall, C.S. Willand, H. Hampsch and D.J. Williams, *New Main Chain Nonlinear Optical Polymers With High Glass-Transition Temperatures.* Polymer Bulletin, 1992. **28**(4): p. 381-388.

24.   G.D. Green, H.K. Hall, J.E. Mulvaney, J. Noonan and D.J. Williams, *Donor-Acceptor-Containing Quinodimethanes - Synthesis and Copolyesterification Of Highly Dipolar Quinodimethanes.* Macromolecules, 1987. **20**(4): p. 716-722.

25.   H.K. Hall, T.M. Kuo and T.M. Leslie, *New Ab Polyesters and a Polymethacrylate Containing Dipolar Para- Phenyleneazo Groups.* Macromolecules, 1989. **22**(9): p. 3525-3529.

26.   I. Teraoka, D. Jungbauer, B. Reck, D.Y. Yoon, R. Twieg and C.G. Willson, *Stability Of Nonlinear Optical Characteristics and Dielectric Relaxations Of Poled Amorphous Polymers With Main-Chain,Chromophores.* Journal Of Applied Physics, 1991. **69**(4): p. 2568-2576.

27.   D.R. Robello, C. Willand, M. Scozzafava, A. Ullman and D.J. Williams, *Materials for Nonlinear Optics, Chemical Perspectives,* , S.R. Marder, J. Sohn and G. Stucky, Editors. 1991, ACS. p. 279.

28.   R.J. Morgan, *Advances in Polymer Science,* . 1985, Springer-Verlag: Berlin. p. 72.

CHAPTER 3

ELECTRIC FIELD POLING

3.1 Introduction

As discussed in chapter 2, a material must not possess a centre of symmetry if it is to have a finite second order susceptibility. Typical polymeric systems, where the active chromophore has been introduced through molecular dispersion or attachment to the polymer chains, are usually centrosymmetric and as such must be treated to induce some form of asymmetry. This is usually achieved through the technique of electric field poling whereby the dipolar nature of the chromophores is exploited and a dc electric field is applied to align them. There are several ways in which this can be done and this chapter will begin with a brief overview of these. This will be followed by a summary of the theory used to model the orientation of the chromophores, necessary if the second order nonlinear susceptibility of the material is to be calculated.

3.2 Electric Field Poling Techniques

There exist several ways in which electric field poling can be achieved, although only differing in the way in which the field is applied. Common to all of the techniques, the polymer is heated to around its glass transition temperature (T_g), such that it softens and allows the chromophores to move. Following this, the dc field is administered causing the dipolar molecules to align. Once the alignment has reached

31

equilibrium, the polymer is then cooled, with the field still applied, and thus freezing in the polar order.

The technique of employing an electric field to remove the centre of inversion of a material system is not new as it was first used over thirty years ago to induce a second order nonlinear response in a centrosymmetric calcite crystal [1]. Following this however, studies on these electric field induced polarisations were mainly confined to liquids [2, 3]. The first studies which provided evidence that a net polarisation could be frozen in to a polymer system were carried out about twenty years ago when it was discovered that piezoelectricity could be induced in polyvinylidine fluoride (PVF) and other dipolar polymers [4]. However, it was not until the studies by Havinga and Van Pelt on the electrochroism of dye-polymer blends [5, 6] that a quantified approach was taken to evaluate the frozen-in alignment. Following this study it was realised that if the incorporated dye molecules were optically nonlinear, a second order nonlinear response could be induced. Some of the earliest work investigating nonlinear polymers poled in this manner was performed by Meredith, Vandusen and Williams [7].

Early electric field poling was achieved by simply attaching two electrodes on either side of the polymer and applying an electric field. Since then, however, other techniques have been developed including in-plane poling and corona poling, and even the internal electric field generated by ferroelectric media has been exploited. A brief description of each of these methods will therefore follow including a short discussion on the relative merits of each.

3.2.1 Parallel Plate Poling

In early electric field poling experiments, the electric field was applied by means of two electrodes placed either side of the sample. This technique is known as parallel plate or contact poling and with thin film samples the electric field is applied across the film thickness (see figure 3.1). Clearly if complicated waveguiding experiments are to be avoided, at least one of these electrodes must be transparent if optical studies are to be carried out, and to this end most films are deposited onto a

DC Voltage Supply

Top Electrode

Polymer Film

ITO
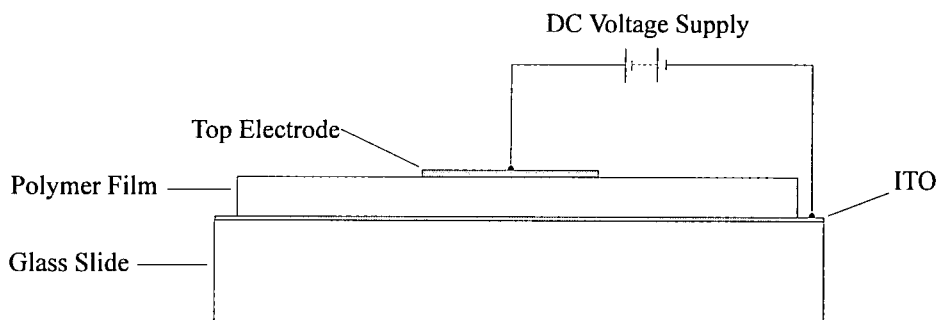
Glass Slide

Figure 3.1 Schematic of the arrangement required for parallel plate poling.

transparent conducting indium tin oxide (ITO) coated glass slide. The second contact is then either provided by an evaporated metal electrode, if optical measurements are to be done in reflection, or the film is sandwiched between two ITO coated slides, if optical transmission is required. Using this arrangement poling fields of up to 70 MVm^{-1} can be easily attained and if careful attention is given to material purity and film preparation then even higher fields can be reached.

The main advantage of this technique is that it is very simple, particularly if an evaporated metal top electrode is used. Field strengths are known, therefore allowing accurate modelling of the poling procedure. However, there are several disadvantages, the main one being that samples are very prone to short circuiting. The presence of any impurities, pinholes or dust, etc. within the film can lead to excessive charge injection, resulting in catastrophic breakdown and therefore sample failure. This is a particular problem if large poling fields are required since breakdown caused in this manner will become more common. Therefore if high poling fields are necessary, great care must be taken during sample preparation in order to make the film as pure as possible. If the ITO sandwich method is to be used, extra care must be taken to prevent short circuiting of the two electrodes since the quality of the films prepared this way tend to be rather poor at the edges. This can be avoided, however, through the use of patterned ITO electrodes which only apply the field to the centre of the sample.
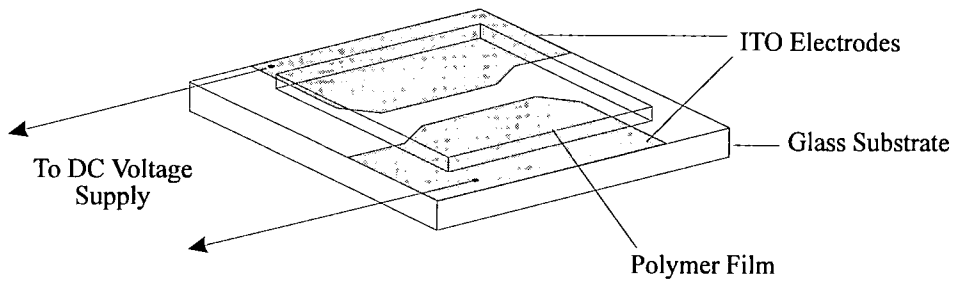
Figure 3.2 Schematic of arrangement required for coplanar poling.

These problems aside, this technique is very simple and is compatible with most methods used to characterise the nonlinear behaviour of polymer films and as such is still commonly employed. However, the attainable poling fields are generally quite low compared with other techniques and as such it is often not the method of choice.

3.2.2 In-Plane Poling

A recently developed method of applying the poling field is to use coplanar electrodes [8, 9]. The film is deposited on to an ITO substrate which has been patterned as shown in figure 3.2. The field is then applied in the film plane, aligning the dipoles parallel to the film surface. This has the distinct advantage that when using this configuration in a waveguide device the nonlinear response will be greatest when the optical field is polarised in the film plane (i.e. the TE mode), the most common operating mode of conventional waveguide devices. Poling fields of between 50 MVm⁻¹ to 100 MVm⁻¹ have been achieved using the configuration above, a slight improvement on the parallel plate method. Since the field is generated between the sharp electrode edges, charge injection has proven to be a major problem and the cause of the catastrophic breakdown observed at higher fields. A recent study of the breakdown processes involved, however, has revealed that, through the use of a substrate with a much higher resistivity, such as fused silica, and the application of a top cladding layer, much higher fields can be applied before breakdown [10]. Fields as great as 370 MVm⁻¹ have been achieved through this modification. Due to the requirement of two electrodes however, this technique, like the parallel plate method, still demands that the samples are very pure to reduce the

chance of breakdown. Great care therefore still needs to be taken when preparing such samples.

3.2.3 Internal Field Poling

A very new approach to electric field poling makes use of the very high internal electric fields generated by ferroelectric hosts such as poly(vinylidene fluoride), PVF. Following work which demonstrated the use of these internal fields to stabilise polar alignment [11], further studies were carried out to investigate the possibility of exploiting them to induce the alignment [12]. The nonlinear guest molecule is doped into a ferroelectric host polymer, such as a PVF and the sample is then poled to induce a ferroelectric polarisation in the host. The poling fields required to do this are usually low, typically around 50 -70 MVm^{-1}, and can be easily obtained using any of the techniques described in this chapter. The resultant internal electric field, brought about by this ferroelectric polarisation, is then strong enough to align the guest molecules. Electrochroism measurements have shown these fields to be as high as 250 MVm^{-1}, well in excess of the externally applied field used to induce the effect. Very high poling fields are therefore obtainable and the method has the added advantage that the internal field also acts to stabilise the resultant polar alignment. However there are also some disadvantages. The choice of host material is limited since a good ferroelectric polymer, compatible with the guest molecules and the sample fabrication methods, must be found. Often the optical quality of such polymers is slightly poorer due to their semi-crystalline nature, however this can be overcome by blending it with a high quality optical host such as PMMA. Finally, the concentration of guest molecules within the host must be kept low since the degree of order in the crystalline regions, from where the high internal fields are generated, is disrupted by the incorporation of the guest molecules, thus reducing the internal field. It has been shown that poling fields can be reduced by as much as 50% if the number density of the guest molecules is too high, a clear disadvantage if one is trying to raise the nonlinear activity of a material system by increasing the doping level, as is normally the case.
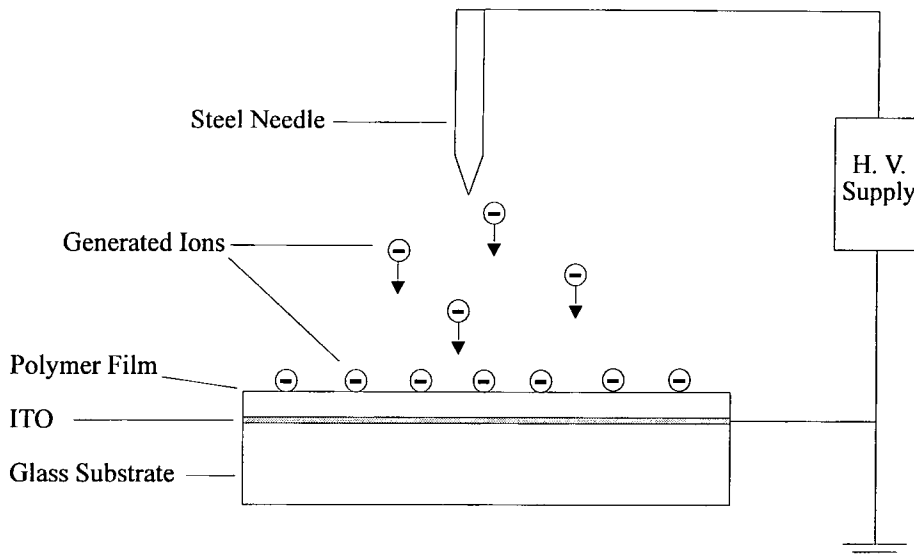
Figure 3.3 Schematic of a simple corona charger.

3.2.4 Corona Poling

Probably the most versatile poling technique for polymer films at present is corona poling [13, 14] and it is one of the few techniques which allows large scale manufacture of continuously poled media [15]. The poling fields in this case are a result of ions, generated from a corona discharge, deposited on to the polymer surface.

3.2.4.1 Corona Poling Apparatus

A corona discharge is a self sustainable, nondisruptive electrical discharge which occurs when a sufficiently high potential difference exists between asymmetric electrodes such as the needle and plate arrangement in the simple corona charger shown in figure 3.3. The high potential at the needle tip, typically set at around 5 - 10 kV, causes the surrounding gases to ionise. However the asymmetry of the field distribution, brought about by the electrode geometry, results in the ionisation remaining localised around the needle tip, ensuring no catastrophic breakdown occurs across the air gap. The generated ions, whose polarity are the same as that of the needle, drift towards regions of low potential and deposit themselves on the sample surface where they become trapped. A field is therefore established across

36

the sample thickness, values of which can be as high 400 MVm^{-1} [16]. The field values achieved using this method are only limited by the dielectric strength of the material and availability of surface traps at the poling temperature and as such far exceed those normally obtained using fixed electrode techniques. The absence of a top electrode also ensures that electric breakdown of the film, caused by impurities and imperfections, remains localised and does not cause sample failure. The advantages of this technique are therefore clear and its simplicity has made corona poling a very popular choice when aligning nonlinear optical films.

Despite the many advantages of this technique, however, there are some disadvantages associated with the experimental geometry shown in figure 3.3. Probably the most important of these is that there is no way of controlling or measuring the amount of charge deposited on the sample surface or the resultant poling fields. This is clearly a major problem particularly in view of the fact that the poling fields must be known if detailed quantitative analysis of the nonlinear response of the sample is to be carried out. Also, the distribution of the deposited surface charge, and therefore the poling field, is highly non-uniform across the sample surface, the charge density being far lower at the sample edges. The arrangement in figure 3.3 is therefore far from adequate if corona poling is to be used in any quantitative measurements.

This problem was overcome in 1976 when Moreno and Gross developed the corona triode [17]. Their idea was to place a biased metal grid between the needle and sample. The polymer film charges up to the potential of the grid, at which point there exists no potential difference between the sample and grid thus preventing further build up of charge. The completion of this process is indicated by the current flowing through the sample reducing to a steady value. This therefore allows one to pre-set the potential at which the sample is to be charged. Since the potential equalisation between the grid and sample occurs across the entire sample area, a much more uniform charge deposition is achieved. However, this geometry still did not permit the operator to monitor the potential build up and was therefore modified such that the sample was vibrated with respect to the grid. This arrangement then allows the

sample surface potential to be measured during charging using the vibrating capacitor technique [18], the two capacitor plates being the grid and sample. One of the disadvantages of this arrangement, however, is that the current flowing through the sample decreases as the surface potential increases. This was considered a problem since some of the charge transport equations used to characterise the behaviour of the sample could not be solved. As a result, versions of the corona triode were developed which kept the charging current constant. The first of these employed a feedback system which controlled the needle potential [19]. Varying the needle potential, however, results in small changes in the sample current and therefore imposing a maximum operating current of only 2 nA. At high grid voltages, the grid itself also begins to emit ions therefore limiting sample charging potentials. This high potential difference between the grid and sample during the early stages of poling also results in poor uniformity of the charge deposition, resulting in inaccurate measurements of sample potential. All of these problems were overcome with the introduction of a constant current corona triode which controls the sample current by varying the grid potential [20], described in detail in section **4.4.2**. Since in this mode the grid potential rises with the sample potential, the potential difference between the two remains low and therefore no grid emissions occur, even at high charging potentials. The low potential difference between the sample and grid also ensures that very good charge uniformities can be obtained throughout the charging process, allowing accurate surface potential measurements. The characteristics of this triode (see section **4.4.2.2**) mean that the sample potential can be determined directly from the grid potential without the need for the clumsy vibrating capacitor arrangement. This version of the constant current corona triode therefore solves many of the problems associated with the early corona chargers and as such has since become the apparatus of choice for quantified characterisation of corona poled nonlinear polymer films [21-23].

3.2.4.2 Characteristics of Corona Chargers

Although the charging process itself appears very simple, the mechanisms involved during the generation and storage of the ions can be quite complicated. As a result a number of studies have been carried out in an attempt to characterise the procedure.

It has been shown that not only the properties of the sample are important but also the atmospheric conditions under which the discharge takes place and the polarity of the needle.

Although positive and negative corona discharges appear to be very similar, the processes involved in generating them are very different. Under normal operating needle potentials, of typically 5 - 10 kV, negative discharges appear as short bursts from spots around the needle tip known as Trichel pulses [24]. The needle is intimately involved in sustaining the discharge avalanche, providing secondary electrons through secondary emission, ion impact and the photoelectric effect. As such negative coronae tend to be less stable, less uniform around the needle tip and very dependent on the chemical composition of the surrounding gases. Positive coronae on the other hand are much more uniform and exist as a continuous discharge [25], a direct result of the fact that the needle is not involved in sustaining the electron avalanche. In this case the ionisation processes occur entirely in the surrounding gas since the UV portion of the characteristic glow associated with positive coronae provides the secondary electrons by photoionisation. This difference in character results in the general observation that negative coronae are less stable than positive coronae, resulting in fluctuations which can lead to less efficient charge deposition and lower poling fields [14].

Clearly the different processes involved in generating positive and negative coronae will result in different types of ions deposited onto the film surface. Using mass spectrometer techniques it has been shown that the generated ions depend strongly on both the types of gas present and the relative humidity [26, 27]. For example, in air the dominant species for positive discharges are hydrated ions with the general formula $(H_2O)_nH^+$, where n is an integer that increases with relative humidity. If the humidity is very low then species such as $(H_2O)_nNO^+$ and $(H_2O)_n(NO_2)^+$ are generated. In negative coronas, the dominant ions are usually CO_3^- ions with about 10% of these appearing in their hydrated form, $(H_2O)_nCO_3^-$ at 50% relative humidity.

The marked differences observed when changing the polarity of the corona discharge is therefore a very important consideration when poling polymer films. The different ions generated will interact with the film in different ways and in some cases will cause chemical changes [21]. The mobility of the ions is also important and will effect the rate of charge build up and stability. Mobile charges will be able to penetrate through the bulk of the sample, if field strengths are high enough, and thus reduce the effective poling field. For a PMMA film in air for example, the mobility of ions associated with negative coronae is lower than the mobility of ions generated in a positive coronae, resulting in stronger poling fields and longer electric field lifetimes [14].

The properties of different gases will also affect the charging process. Discharges carried out in different atmospheres will result in different ions generated. One way of eliminating chemical changes within the sample when subjected to a corona discharge is to carry out the procedure in an inert gas where the resultant ions are usually far less active [21]. The free ion content of the atmosphere will also affect charging since charge neutralisation can occur. For example, charging carried out in a helium atmosphere produces a stronger and more stable field than in air due to the lack of neutralising charges in helium [14].

There can be many considerations, therefore, when poling polymer films with a corona discharge, however, the procedure is very simple and very high poling fields are obtainable.

3.3 Orientational Distributions

The determination of the degree of chromophore alignment after poling is essential if the second order nonlinear response of a system is to be interpreted. This can be seen clearly from equation 2.7 where the quantity $\langle \beta_{ijk} \rangle_{IJK}$ depends on the precise orientation of the chromophores in the polymer. A simple classical molecular theory, first developed by Keilich [28], is therefore presented which considers the interaction

40

between a strong electric field on dipolar species distributed randomly in a naturally isotropic medium.

On application of a strong electric field, not only do permanent dipoles undergo orientation but also field induced dipoles, brought about by the molecular polarisability, also orient themselves. The potential energy of each molecule is therefore given by [28]:

$$U(\Omega, F(0)) = -\mu_i F_i(0) - \frac{1}{2}\alpha_{ij}F_i(0)F_j(0) \qquad (3.1)$$

where μ_i is the *local* permanent dipole moment of the molecule, $F_i(0)$ and $F_j(0)$ are the components of the *local* applied dc electric field, α_{ij} is the molecular polarisability and Ω is the solid angle within the orientational distribution occupied by the molecule. In the cases considered here the macroscopic system is assumed to exhibit uniaxial symmetry and as such the Boltzmann distribution function of the molecules is only dependent on the polar angle θ between the molecular dipole axis (the z axis) and the poling axis (the 3 axis). The dipole moments of all the molecules considered are relatively large and thus the first term in equation (3.1) is dominant. As a result the second term in equation (3.1) is neglected and the Boltzmann distribution function is given by:

$$G(\theta, F_3(0)) = \frac{\exp(p\cos\theta)}{4\pi^2 \int_0^\pi \exp(p\cos\theta)\sin\theta.d\theta} \qquad (3.2)$$

where:

$$p = \frac{\mu_z F_3(0)}{k_B T_p} \qquad (3.3)$$

k_B is the Boltzmann constant and T_p is the poling temperature.

For measurements where β_{vec} (the component along the dipole moment) is the only component of β_{ijk} that need be considered and where a sample has uniaxial symmetry, the number of independent macroscopic nonlinear susceptibilities is reduced to two (as discussed in chapter 2) $\chi^{(2)}_{333}$ and $\chi^{(2)}_{311}$ can then be defined as follows[29]:

41

$$\chi^{(2)}_{333}(-\omega;\omega_1,\omega_2) = Nf(\omega)f(\omega_1)f(\omega_2)\beta_{vec}(-\omega;\omega_1,\omega_2)\langle\cos^3\theta\rangle \qquad (3.4)$$

and

$$\chi^{(2)}_{311}(-\omega;\omega_1,\omega_2) = Nf(\omega)f(\omega_1)f(\omega_2)\beta_{vec}(-\omega;\omega_1,\omega_2)\frac{1}{2}\left[\langle\cos\theta\rangle - \langle\cos^3\theta\rangle\right] \qquad (3.5)$$

where:

$$\langle\cos^n\theta\rangle = \int_0^\pi G(\theta,F_3(0)).\cos^n\theta.\sin\theta.d\theta \qquad (3.6)$$

and $f(\omega)$ is the optical local field factor at frequency ω defined in equation (2.11). Substituting equation (3.2) into equation (3.6) results in the following expression for $<\cos^n\theta>$:

$$\langle\cos^n\theta\rangle = L_n(p) = \frac{\int_0^\pi \cos^n\theta\exp(p\cos\theta)\sin\theta.d\theta}{\int_0^\pi \exp(p\cos\theta)\sin\theta.d\theta} \qquad (3.7)$$

where $L_n(p)$ are the set of functions known as Langevin functions. The nth solutions to equation (3.8) are the following n^{th} order Langevin functions [28]:

$$L_1(p) = \coth p - \frac{1}{p} \qquad (3.8)$$

$$L_2(p) = 1 + \frac{2}{p^2} - \frac{2}{p}\coth p \qquad (3.9)$$

$$L_3(p) = \left(1 + \frac{6}{p^2}\right)L_1(p) - \frac{2}{p} \qquad (3.10)$$

Therefore, the two independent second order nonlinear susceptibilities, defined in equations (3.5) and (3.6), can be expressed as follows:

$$\chi^{(2)}_{333}(-\omega;\omega_1,\omega_2) = Nf(\omega)f(\omega_1)f(\omega_2)\beta_{vec}(-\omega;\omega_1,\omega_2)L_3(p \qquad (3.11)$$

$$\chi^{(2)}_{311}(-\omega;\omega_1,\omega_2) = Nf(\omega)f(\omega_1)f(\omega_2)\beta_{vec}(-\omega;\omega_1,\omega_2)\frac{1}{2}[L_1(p) - L_3(p) \qquad (3.12)$$

The nonlinear susceptibilities are therefore only a function of the *local* dipole moment (μ_z), the poling temperature (T_p) and the *local* dc electric field ($F_3(0)$). As in the case of the optical electric fields, the dc electric field experienced by the

molecule differs from that applied externally due to the dielectric properties of the host media and that of the cavity. A dc local field correction factor therefore needs to be introduced to take account of this.

3.3.1 DC Local Field Correction Factors

The dc local field factors can be calculated in a similar manner to those for optical fields. It is common practice to employ the Onsager local field correction factor [30] which accounts for the dielectric properties of the guest molecules through the use of an isotropic spherical cavity. Unlike the theory outlined by Scholte [36], however, it does not account for the shape of the molecule or its anisotropy. The chromophore is assumed to be embedded within a spherical cavity contained within a uniformly polarisable host medium of relative permittivity $\varepsilon_h(0)$. The cavity is occupied by a medium of relative permittivity n_g^2, the three perpendicular components of which may be calculated using equation (2.17) employing an average molecular radius. The Onsager local field correction factor, $f_O(\omega)$ (where the subscript O refers to Onsager), can then be defined as:

$$f_O(\omega) = \frac{\varepsilon_h(0)\left[n_g^2 + 2\right]}{2\varepsilon_h(0) + n_g^2} \qquad (3.13)$$

The Onsager model describes the local fields in terms of two components, the cavity field and the reaction field. The cavity field is that described so far as being the field proportional to the applied external field. The reaction field, however, is brought about by polarisations in the surrounding media caused by the dipole moment field of the guest molecules. The presence of the reaction field has important consequences on the electronic properties of the guest molecules. The reaction field, being directed along the dipole moment axis, enhances the charge separation and as such the dipole moment can be expected to change when placed in different dielectric environments [30]. In a similar manner the molecular nonlinear polarisabilities will also be affected by the environment [32-35] resulting in a dependence of nonlinear performance on the host media. This stresses the

importance of quoting local values of molecular properties, such as dipole moment, in the analysis presented in section **3.3**.

As with the optical local field factor, the more general approach described by Scholte can be taken which defines the cavity in which the guest molecule is embedded as an ellipsoid [36]. The dc local field factor is calculated in an identical manner to that of the optical field factor using equations (2.10) to (2.16). However, the approximation that the relative permittivity of the host is equal to the square of its refractive index is no longer valid at low frequencies in the materials studied here due to their polar nature. Although optical local field factors change very little from those calculated using the Lorentz-Lorenz formula, the values of dc local field factor calculated using this formalism can differ greatly from those obtained using the standard Onsager formula particularly when considering large molecules with high polarisabilities. The approximations made in the original Onsager theory, therefore, may not necessarily be correct for some materials system.

Although the local field derivation outlined in section **2.3.1** may represent an improvement on what is used currently there still remain several uncertainties. Firstly, the polarisability of the molecules is required in the calculation. The modelling package used to determine α_{ij}, MOPAC (v.6), only calculates their value in a vacuum and cannot calculate local values. As mentioned above, the reaction field exerted on a molecule can have a considerable effect on its electronic properties, including the polarisability, and as a result could affect the local field factors. A second point is that the contribution from each of the three components of the local field (see equations (2.8) - (2.13)) will no longer be equal once the system starts to align in the poling field [36]. If the alignment efficiency of the system is high (ie. if the poling field and / or the molecular dipole moment is high) the local field factor will change further. Care must therefore be taken when applying local field factors, particularly for dc fields, as the models employed in their calculation are still very limited.

3.4 References

1.   R.W. Terhune, P.D. Maker and C.M. Savage, *Optical Harmonic Generation in Calcite*. Phys. Rev. Lett., 1962. **8**: p. 404.

2.   G. Hauchecorne, F. Kerherve and G. Mayer, *Mesure des Interactions Entre ondes Lumineuses dans Diverse Substances*. J. de Phys., 1971. **32**: p. 47.

3.   G. Mayer, *Even Harmonic light Radiation by Molecules in a DC Electric Field*. Compt. Rend. Acad. Sci. (Paris), 1968. **267B**: p. 54.

4.   H. Kawai, *Piezoelectricity of Poly(vinylidene fluoride)*. Jap. J. Appl. Phys., 1969. **8**: p. 975.

5.   E.E. Havinga and P. van Pelt, *Electrochroism of Substituted Polyalkenes in Polymer Matrixes: Influence of Chain Length on Charge Transfer*. Ber. Bunsenges. Phys. Chem., 1979. **83**: p. 816-821.

6.   E.E. Havinga and P. Van Pelt, *Intramolecular Charge Transfer Studied by Electrochroism of Organic Molecules in Polymer Matrices*. Mol. Cryst. Liq. Cryst, 1979. **52**: p. 145-156.

7.   G.R. Meredith, J.G. Vandusen and D.J. Williams, *Optical and Non-Linear Optical Characterization Of Molecularly Doped Thermotropic Liquid-Crystalline Polymers*. Macromolecules, 1982. **15**(5): p. 1385-1389.

8.   J.W. Wu, J.F. Valley, S. Ermer, E.S. Binkley, J.T. Kenney, G.F. Lipscomb and R. Lytel, *Thermal-Stability Of Electrooptic Response In Poled Polyimide Systems*. Applied Physics Letters, 1991. **58**(3): p. 225-227.

9.   S. Yitzchaik, G. Berkovic and V. Krongauz, *Charge Injection Asymmetry - a New Route to Strong Optical Nonlinearity In Poled Polymers*. Journal Of Applied Physics, 1991. **70**(7): p. 3949-3951.

10.   A. Otomo, G.I. Stegeman, W.H.G. Horsthuis and G.R. Mohlmann, *Strong-Field, Inplane Poling For Nonlinear-Optical Devices In Highly Nonlinear Side-Chain Polymers*. Applied Physics Letters, 1994. **65**(19): p. 2389-2391.

11.   N. Tsutsumi, G.T. Davis and A.S. Dereggi, *Measurement Of the Internal Electric-Field In a Ferroelectric Copolymer Of Vinylidene Fluoride and Trifluoroethylene Using Electrochromic Dyes*. Macromolecules, 1991. **24**(24): p. 6392-6398.

12. N. Tsutsumi, I. Fyjii, Y. Ueda and T. Kiyotsukuri, *2nd-Harmonic Generation From an Nlo Dye Aligned By the Internal Electric-Field In a Blend Of Poly(Vinylidene Fluoride) and Poly(Methyl Methacrylate).* Macromolecules, 1995. **28**(4): p. 950-955.

13. M.A. Mortazavi, A. Knoesen, S.T. Kowel, B.G. Higgins and A. Dienes, *2nd-Harmonic Generation and Absorption Studies Of Polymer Dye Films Oriented By Corona-Onset Poling At Elevated-Temperatures.* Journal Of the Optical Society Of America B-Optical Physics, 1989. **6**(4): p. 733-741.

14. H.L. Hampsch, J.M. Torkelson, S.J. Bethke and S.G. Grubb, *2nd Harmonic-Generation In Corona Poled, Doped Polymer-Films As a Function Of Corona Processing.* Journal Of Applied Physics, 1990. **67**(2): p. 1037-1041.

15. B. Hilczer and J. Malecki, *Electrets.* 1986, Warsaw: Elsevier.

16. A. Knoesen, N. Molcui, D. Yankelvich, N. Mortazavi and A. Dienes, *Corona Poled Nonlinear Polymeric Films: In Situ Electric Field Measurements, Characterisation and Ultrashort Pulse Applications.* Int. J. NLO Phys., 1992. **1**: p. 73.

17. R. Moreno and B. Gross, *Measurements of Potential Build up and Decay, Surface Charge Density and Charging Currents of Corona Charged Polymer Foil Electrets.* J. Appl. Phys., 1976. **47**: p. 3397.

18. C. Reedyk and M. Perlman, *The Measurement of Surface Charge.* J. Electrochemical Soc., 1968. **115**: p. 49.

19. B. Gross, J. Giacometti and G. Leal Ferreira. *Corona Method for Investigation of Charge Storage and Transport in Dielectrics.* in *Electrical Insulation and Dielectric Phenomena.* 1981.

20. J.A. Giacometti and J.S.C. Campos, *Constant Current Corona Triode With Grid Voltage Control - Application to Polymer Foil Charging.* Review Of Scientific Instruments, 1990. **61**(3): p. 1143-1150.

21. P.T. Dao, D.J. Williams and W.P. McKenna, *Constant Current Corona Charging As a Technique For Poling Organic Nonlinear Optical Thin-Films and the Effect Of Ambient Gas.* Journal Of Applied Physics, 1993. **73**(5): p. 2043-2050.

22. D. Healy, G.H. Cross and D. Bloor. *Guest-Host Polymeric Systems as Nonlinear Optical Materials.* in *ISE 8.* 1994, p.787.

23. D. Healy, D. Cross and M. Szablewski. *Molecular $\mu\beta$ Figure of Merit Studies of Solid Solutions.* in Proc. *SPIE, 2527,* 1995, p. 32 .

24. G. Trichel, *The Mechanism of the Negative Point to Plane Corona Near Onset.* Phys. Rev., 1938. **54**: p. 1078.

25. A. Goldman and J. Amoroux, *Electrical Breakdown and Discharges in Gases: Macroscopic Processes and Breakdown,* . 1981, Plenum Press. p.293.

26. M. Shahin, *Mass Spectrometric Studies of Corona Discharges in Air at Atmospheric Pressures.* J. Chem. Phys., 1966. **43**: p. 2600.

27. M. Shahin, *Nature of Charge Carriers in Negative Coronas.* Appl. Opt. Supp. Electr. Photogr., 1969. **82**: p. 106.

28. S. Keilich, *Optical Second Harmonic Generation by Electrically Polarised Isotropic Media.* IEEE J. of Quantum Electronics, 1969. **QE-5**: p. 562.

29. D.M. Burland, R.D. Miller and C.A. Walsh, *2nd-Order Nonlinearity In Poled-Polymer Systems.* Chemical Reviews, 1994. **94**(1): p. 31-75.

30. L. Onsager, *Electric Moments of Molecules in Liquids.* J. Am. Chem. Soc., 1936. **58**: p. 1486.

31. J.A. Osborn, *Demagnetisation Factors of the General Ellipsoid.* Phys. Rev., 1945. **67**: p. 351.

32. J.L. Brédas, F. Meyers, C. Dehu, B.M. Pierce and S.R. Marder, *Nonlinear-Optical Response Of Organic Conjugated Compounds - Theoretical Description Of Solvent Mediated Enhancement Of Hyperpolarizabilities.* Abstracts Of Papers Of the American Chemical Society, 1994. **208**(Pt1): p. 8-COMP.

33. F. Meyers, S.R. Marder, J.W. Perry, J.L. Brédas and B.M. Pierce, *Optimizing Molecular Polarizabilities In Linear Conjugated Organic- Molecules.* Abstracts Of Papers Of the American Chemical Society, 1994. **208**(Pt2): p. 169-POLY.

34. F. Meyers, S.R. Marder, B.M. Pierce and J.L. Brédas, *Tuning Of Large 2nd Hyperpolarizabilities In Organic Conjugated Compounds.* Chemical Physics Letters, 1994. **228**(1-3): p. 171-176.

35. F. Meyers, S.R. Marder, B.M. Pierce and J.L. Brédas, *Electric-Field Modulated Nonlinear-Optical Properties Of Donor- Acceptor Polyenes - Sum-Over-States Investigation Of the Relationship Between Molecular Polarizabilities (Alpha, Beta, and Gamma) and Bond- Length Alternation.* Journal Of the American Chemical Society, 1994. **116**(23): p. 10703-10714.

36. Th. G. Scholte, *A Contribution to the Theory of the Dielectric Constant of Polar Liquids.* Physica, 1949, **XV** p. 437.

CHAPTER 4

EXPERIMENTAL TECHNIQUES

4.1 Introduction

In this chapter the techniques used to prepare and characterise thin polymer films are described. Electric field poling was carried out using both the parallel plate and corona discharge methods, the latter employing a constant current corona triode which allowed control over the corona poling process. To establish the extent of the polar alignment in the contact poled samples the electro-optic response was measured using a simple reflection technique. The polar alignment and the nonlinear optical characteristics of the corona poled samples were determined through second harmonic generation (SHG) studies.

4.2 Sample Preparation

The thin polymer films were prepared using both the spin coating and substrate withdrawal, or 'dip-coating', technique. Both methods require the polymer and the guest material to be dissolved in a common solvent, the choice of which depends on the technique to be used. In order that the optical quality of the films was high and the probability of electric field breakdown during the poling process is minimised, each solution was filtered through a 5 µm pore size Millipore in-line filter before film preparation. Following the coating process excess solvent was removed from the films through drying in a vacuum oven over a period of time and at a temperature governed by the properties of both the solvent and the film.

48

4.2.1 Spin Coating

Spin coating is a technique wherein the polymer solution is poured onto the substrate which is subsequently rotated at a high velocity. This causes the solution to spread out uniformly across the entire substrate surface and form a thin layer which upon drying will leave a smooth film. Film thickness is governed by the viscosity of the solution and the angular velocity and time of spinning. Careful control of these factors can lead to film thicknesses ranging from sub-micron values to the order of 10's of microns. High quality films are only produced with non-volatile solvents and as such long drying times at high temperatures are required.

4.2.2 Substrate Withdrawal

The technique of substrate withdrawal or 'dip-coating' involves the steady withdrawal of the substrate from the polymer solution which results in the deposition of a thin polymer layer [1]. The apparatus used in this technique is shown in figure 4.1. Film thickness is governed by the viscosity of the polymer solution, the withdrawal speed of the substrate and the volatility of the solvent used. Through the careful control of these factors film thicknesses similar to those achieved in the spin coating technique can be realised. In order that the film does not distort after
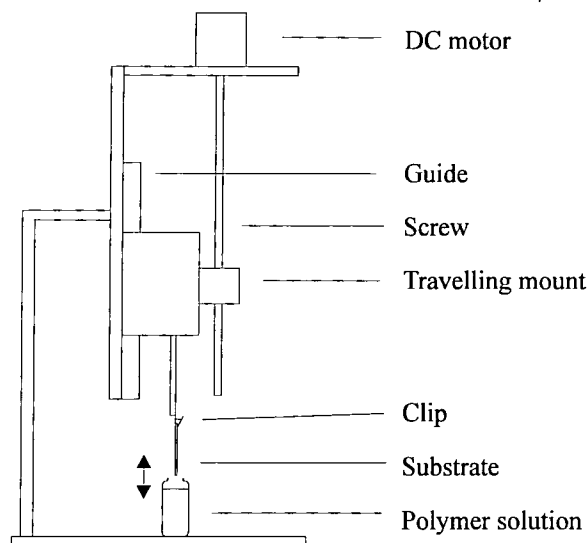
Figure 4.1 Apparatus used for the substrate withdrawal coating technique.

withdrawal, volatile solvents are more appropriate and as a result less severe film drying conditions are required.

4.3 Film Characterisation

In this section the methods used to characterise the physical and linear optical properties of the films are described.

4.3.1 Refractive Index

The technique of prism coupling [2] was used to determine the refractive index of the films. This is a method wherein radiation coupled into the film via a prism excites specific optical waveguide modes, the characteristics of which are governed by the refractive indices of the system components and the film thickness. As a result, the unknown properties of the system, i.e. the film refractive index and thickness, can be calculated. The experimental geometry used for this technique is shown in figure 4.2. In order that all possible waveguide modes are excited within the film, the refractive index of the prism should be larger than that of the film which in turn should have a refractive index larger than the substrate. For this reason the prisms are made from SF6 glass and the substrates are made from fused silica.

Figure 4.2 Experimental geometry for prism coupling

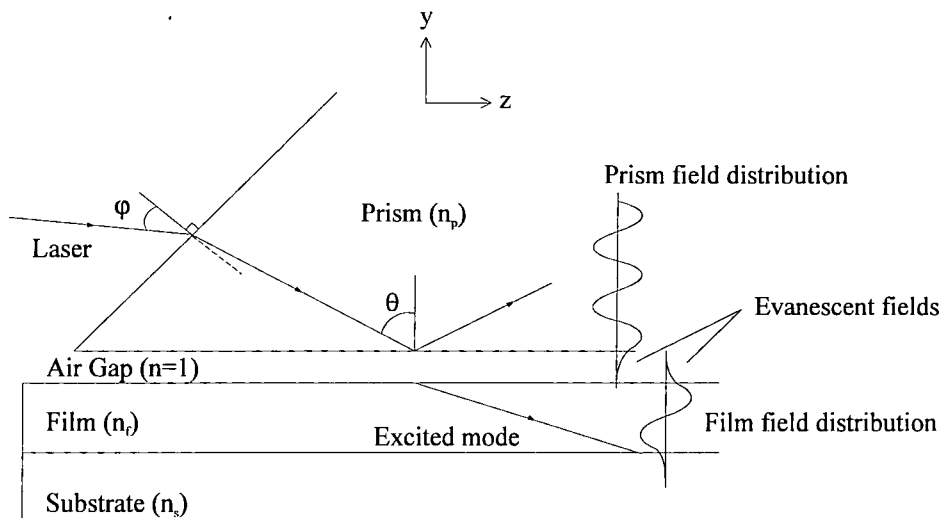Upon striking the base of the prism the laser beam is totally internally reflected, setting up an evanescent field which extends below the prism base and, if the air-gap is thin enough, into the film. For a resultant optical mode to be excited, the boundary conditions require that the z-directed wavevector in the prism (which is identical to the z-directed component of the evanescent field below the prism) matches the z-directed wavevector in the waveguide. In the waveguide a propagation constant, β_m, for the mth mode is defined such that:

$$\beta_m = k_0 n_{eff} \qquad (4.1)$$

where $k_0 = \omega / c$, ω is the angular velocity of the incident radiation, c is the velocity of light in a vacuum and n_{eff} is the effective index for the mode. Therefore at resonance when a mode is excited:

$$k_0 n_p \sin \theta = k_0 n_{eff} \qquad (4.2)$$

As a result the effective index of each mode can be determined by varying the incident angle of the laser beam and recording the angle at which the light is coupled into the guide.

The coupling angle, θ, of each mode was measured by placing a second prism along the waveguide in an opposite manner to the first, allowing the light in the film to be coupled out and displayed on a screen as a sharp bright line. Through the application of Snell's law, θ was then determined from the external coupling angle, φ. Knowing the refractive indices of the prism and the substrate and the wavelength of the laser used, the film refractive index and thickness was then calculated using the equations described by Kogelnik and Ramaswamy [3]. The results from these calculations provided a range of thicknesses and refractive indices, in the form of a curve, over which each waveguide mode could exist. Since all of the excitable modes must be supported by the waveguide, the curves for more than one mode were calculated and the unique film refractive index and thickness was determined from the crossing point of these curves. A set of curves for a typical polymer film are shown in figure

51

4.3. Since at least two modes are required, and preferably three, the film thickness must be tailored to achieve this.

The technique described above, known as two prism coupling, may only be used when there is no absorption in the film at the laser wavelength so as the out-coupled modes will not be too faint to observe. Therefore, when measurements are required at wavelengths where there is a small amount of absorption, the technique known as 'm-lining' must be used [4]. The principles of this technique are the same as the two prism method only the two right angled prisms are replaced with one equilateral prism. The reflection of the coupling spot on the base of the prism passes through the second face and is monitored on a screen. When a waveguide mode is excited a dark band will appear in the image of the coupling spot caused by the energy transfer from the incident radiation into the excited mode which is subsequently absorbed or scattered out of the propagation direction by the film. The angles at which this occurs correspond exactly with the angles measured using the two prism technique and therefore the same mathematical analysis can be used.
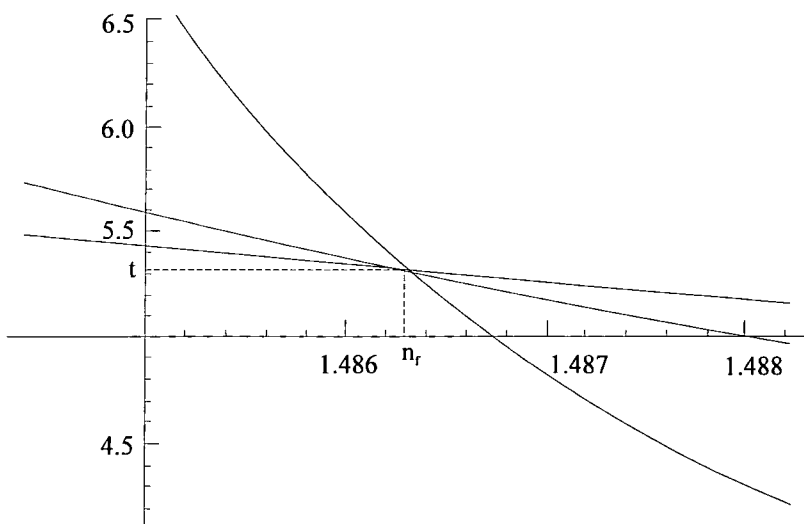
Figure 4.3 Mode index curves for a typical polymer film. The film refractive index (n_f) and thickness (t) are given by the crossing point.

4.3.2 Absorption Spectra

The UV-Visible absorption spectra were measured using a Perkin Elmer UV/VIS/NIR Lambda 19 spectrometer and IR spectra were measured on a Perkin Elmer 1420 Ratio Recording Spectrometer.

4.3.3 Glass Transition Temperature

The film glass transition temperature was determined using a Perkin Elmer DSC-7. After drying, the films were carefully removed from the substrate before insertion into the apparatus.

4.3.4 Thickness

Film thickness was determined using an Alpha Step surface profiler.

4.4 Electric Field Poling

In this section the experimental arrangements used to conduct contact poling and corona discharge poling are described. A detailed description of the theory and application of the constant current corona triode is also given.

4.4.1 Contact Poling

The experimental arrangement used to carry out the contact poling procedure is shown in figure 4.4. The films were deposited onto a transparent and conductive indium tin oxide (ITO) coated glass slide which acted as the ground electrode during poling. To provide a second electrode, a silver layer was evaporated onto the film surface following the drying procedure. The sample was mounted and held in position with two spring clips which provided the two electrode contacts. This was then placed on a heating stage, the temperature of which was controlled using a CAL 9000 RS temperature controller in conjunction with a thermocouple placed in the base of the hot plate. The film temperature was monitored using a thermocouple placed next to the electrode on the film surface. The entire assembly was placed in a
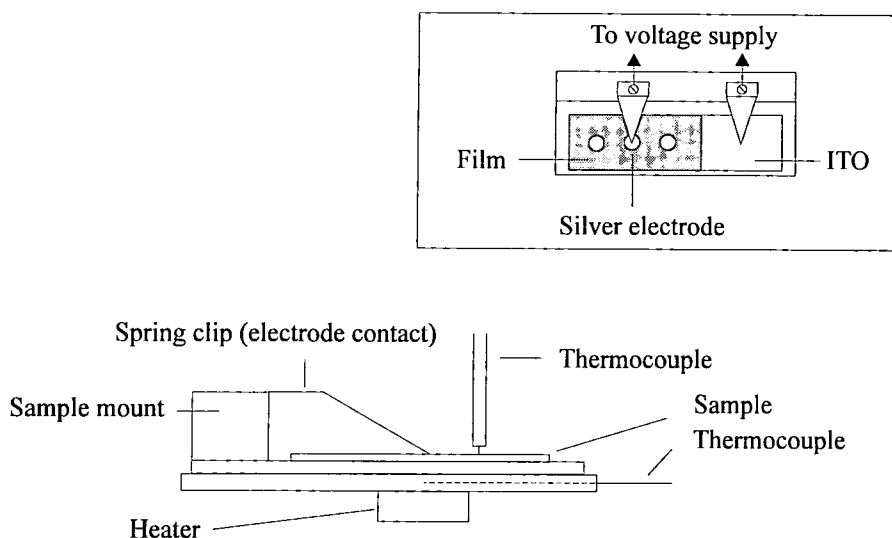
Figure 4.4 Experimental set-up used in contact poling. Inset shows sample arrangement

PERSPEX box in order that a stable thermal environment could be maintained. A dc. electric field was then applied using a Farnell 350 V voltage source (type E350). The current flowing through the sample (I_s) was monitored using a Keithley 601 electrometer and was used as an indication of the correct poling conditions since the dipolar alignment would be accompanied by a sharp increase in I_s.

4.4.2 Corona Discharge Poling and the Constant Current Corona Triode

As discussed in section **3.2.4**, the constant current corona triode (CCCT) is a recent development which overcomes many of the disadvantages associated with the standard corona chargers. The design not only ensures the charge is deposited far more evenly, but also enables the user to monitor and control the surface potential build-up. A description of the apparatus used is given in this section along with the theory and calibration required for its operation.

4.4.2.1 Experimental Arrangement of CCCT

A schematic of the constant current corona triode used, which is a modification of the charger designed by Giacometti and Campos [5], is shown in figure 4.5 (a). The apparatus consists of a sharp steel needle, biased at a potential of ±5 - 10 kV with a Brandenberg Alpha III high voltage supply (V_c), placed along the axis of an earthed

PVC Cylinder

Stainless Steel Needle

Earthed Metal Shield

Metal Grid

Guard Ring

Sample Holder

Heater

Teflon Insulators

Vertically Moving Stage

(a)

I_s

Metallic Shield

ITO Guard Ring

ITO Measuring Electrode

25 mm

18 mm

25 mm
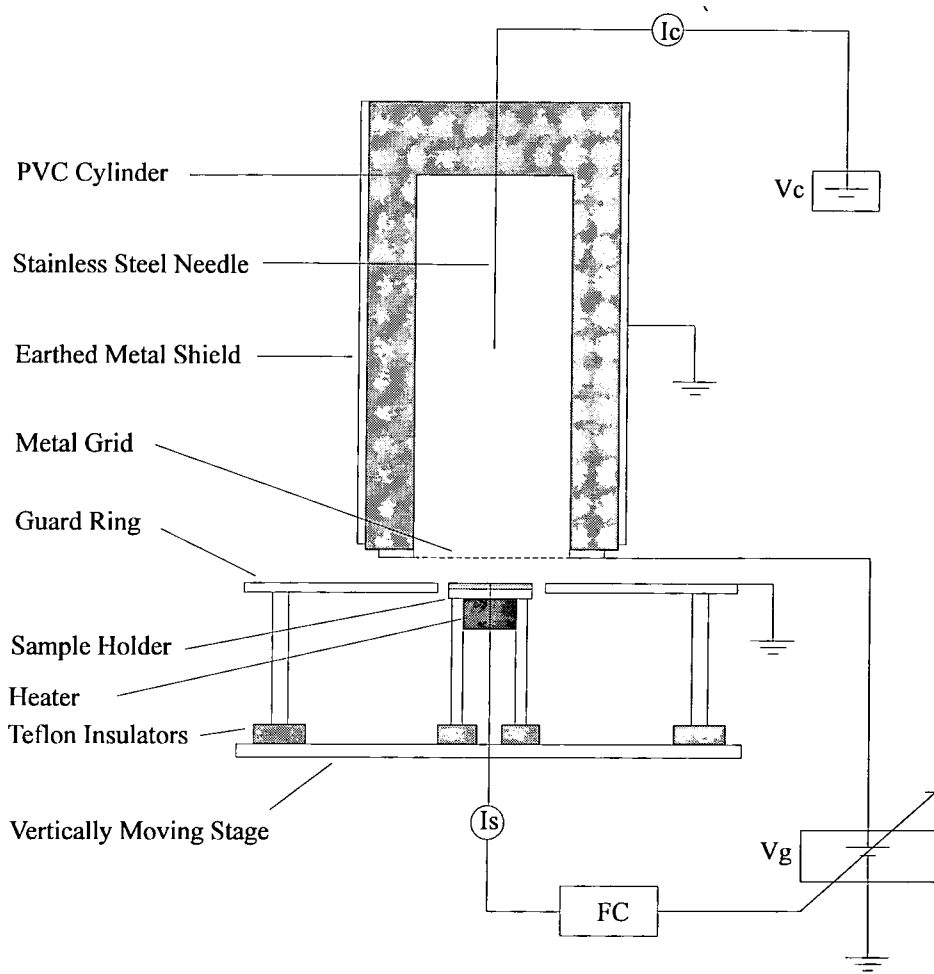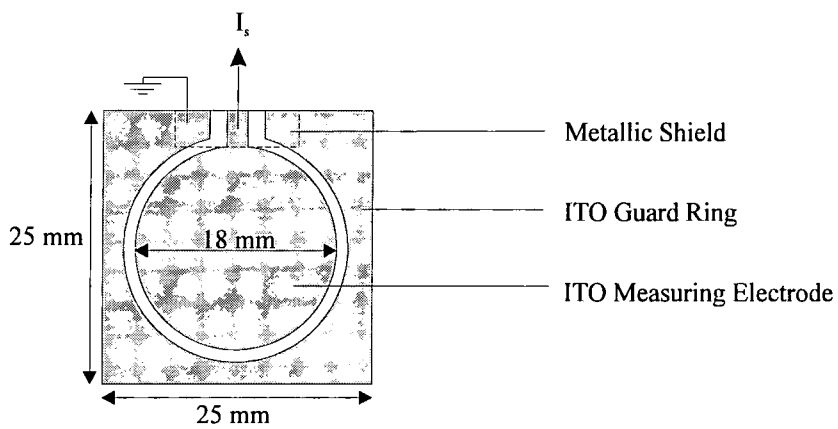
(b)

Figure 4.5 (a) Constant current corona triode apparatus.
(b) Diagram showing sample substrate design.
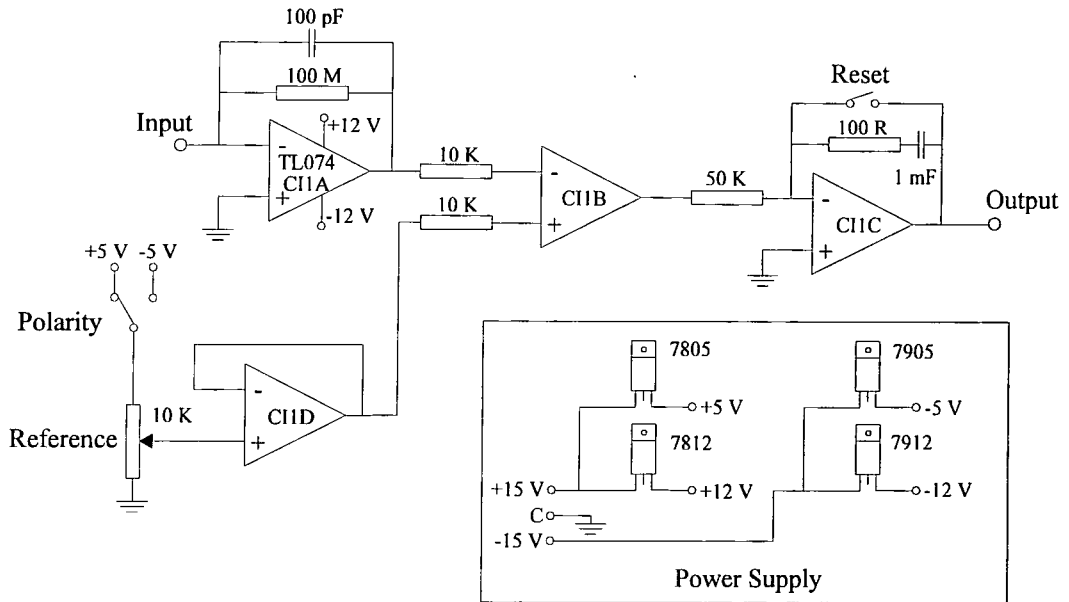
Figure 4.6 Feedback circuit used in the constant current corona triode.

PVC cylinder. A metal grid, with an approximate optical transparency of 0.8, lies at the end of the cylinder, approximately 5 cm from the needle tip, which can be biased with a Trek, model 610C, high voltage amplifier (V_g) and thus allowing control of the flow of ions onto the sample. The flow of ions is governed by the electrical transparency of the grid which in turn is directly related to the optical transparency [6]. Clearly this transparency should be kept at a maximum to ensure the available current is high. The sample is placed on a moveable stage, usually set at 5 mm below the metal grid, and the current flowing through the film (I_s) is monitored using a Keithley model 602 electrometer. In order that no surface currents contribute towards I_s, the films were deposited on specially patterned ITO coated glass substrates incorporating a guard ring arrangement as shown in figure 4.5 (b). The feedback circuit (FC) monitors I_s and adjusts V_g, and therefore the flow of ions onto the sample, such that I_s remains constant. The feedback circuit design is shown in figure 4.6. The polarities of both V_g and V_c can be reversed such that samples can be charged with currents of both polarities.

56

4.4.2.2 Theory of CCCT Operation

A detailed study of the characteristics of corona triodes and a description of how samples behave when charged in such a manner can be found in the work published by several authors [7-11]. The following description is specific to the apparatus design above and is based on the theory outlined by Giacometti and Campos [5].

In order that the following theory is simplified, the electric field quantities between the grid and sample are assumed to be independent of the lateral position in the air-gap. This is achieved through the use of the PVC cylinder which itself becomes charged and acts as a lens to collimate the generated ions uniformly onto the grid [7]. Alternatively, as on more modern designs, the same effect may be achieved by using a metal cylinder connected to a high voltage supply. Since the air gap conduction current is due to the transport of an ionic excess charge with a density of $\rho_g(x,t)$ [6, 7, 11], the total charging current density, $J(t)$, is given by equation 4.2.

$$J(t) = \frac{I(t)}{A} = [v + \mu E_g(x,t)]\rho_g(x,t) + \frac{\varepsilon_0 \delta E_g(x,t)}{\delta t} \qquad (4.2)$$

where t is time, ε_0 is the dielectric constant of the air gap, $E_g(x,t)$ is the electric field, μ is the ion mobility, A is the sample area and x is the position measured from the measuring electrode as indicated in figure 4.7. The $v\rho_g(x,t)$ term is the current density caused by the gas displacement as a result of the corona discharge (the corona wind), the second term is the conduction current and the final term is the
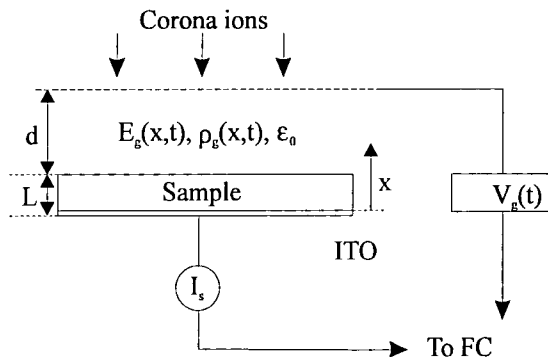

Figure 4.7 Schematic of grid sample region of CCCT

current density associated with the electric displacement. Integrating equation 4.2 over the air-gap thickness gives the following:

$$J(t) = \frac{1}{d} \int_L^{L+d} [v + \mu E_g(x,t)] \rho_g(x,t) dx + \frac{\varepsilon_0}{d} \frac{d}{dt} [V_g(t) - V(t)] \qquad (4.3)$$

where L is the combined sample and electrode thickness, d is the grid to sample thickness and $V_g(t) - V(t) = V_s(t)$ is the potential drop over the air gap as a result of the ionic space charge. $V_g(t)$ and $V(t)$ are the grid voltage and sample voltage respectively. Therefore, if the charging current is kept constant, experimentally achieved by operating the grid supply in constant current mode, V_s must be independent of time and the following equation must be satisfied:

$$V(t) = V_g(t) - V_s \qquad (4.4)$$

As a result, if V_s is known the sample potential throughout the charging process can be determined simply by recording the values of $V_g(t)$ necessary to maintain I_s at a constant value. Since the amount of gap space charge is dependent on the corona current, I_c, it is necessary to operate V_c in constant current mode. V_s can be determined using the calibration described in the next section.

4.4.2.3 CCCT Calibration

In order that the sample potential can be calculated, the air gap potential drop, V_s, must be determined. Since V_s is a function of the system parameters and measurement conditions, it must be determined prior to each charging experiment. By considering equation 4.4 it can be seen that V_s may be determined by simply recording V_g at the specific measurement conditions when no sample is present (i.e. $V(t) = 0$). Typical values obtained for V_s under different charging conditions are displayed in figure 4.8 in the form of calibration curves. It can be seen that I_s is a function of I_c since the electrical transparency of the grid is proportional to the electric field above it [6]. This highlights the need to maintain I_c at a constant value. It is noted that none of the curves cross the origin, a result of the presence of the corona wind which is proportional to the square root of the corona current [12].
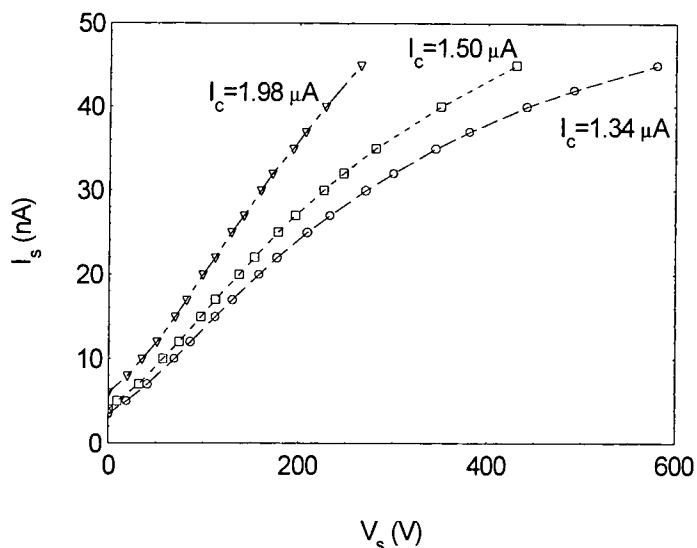
Figure 4.8 Calibration curves for CCCT

Since the air gap ionic conduction current is determined by Child's Law [13], which states that it is inversely proportional to cube of the grid-sample distance (d), it is important that the system is recalibrated following any changes to the value of d. It is also noted that changing the temperature also affects the CCCT calibration since increasing the temperature decreases the ion mobility and thus the air gap current.

4.4.2.4 CCCT Characteristics

The main feature of the CCCT which differs from other forms of corona triode is that the surface potential can be monitored throughout the charging procedure. A direct consequence of this is that, when using dipolar samples as in the case considered here, the alignment process can be monitored. An example is shown in figure 4.9 which shows the surface potential build up of a typical guest host polymer film poled well below its glass transition temperature. It can be seen that the surface potential initially builds up sharply and then levels off or even decreases for a period of time. This is then followed by a gradual rise in the surface potential to a plateau region where it remains steady. This effect was first observed by Giacometti and Campos when poling PVDF [5] and has since been seen by Dao and co-workers when poling the nonlinear optical side chain polymer SC1 [14]. The feature is attributed to the
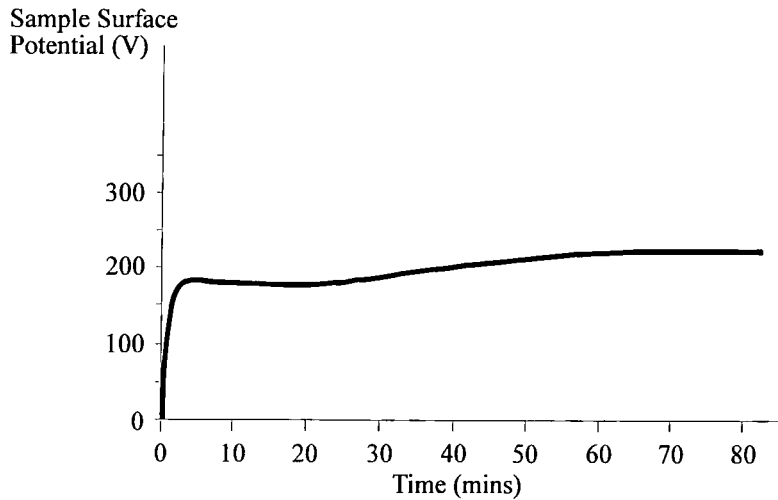
Figure 4.9 CCCT charging curve for a typical polymer film
poled below the glass transition temperature.

motion of the dipolar species within the film during the alignment procedure. The decrease or levelling off of the potential shortly after the initial deposition is caused by the realignment of the dipoles. The subsequent rise in potential to the plateau region therefore indicates the dipoles have stopped moving and the system is once again at an equilibrium. The extent of this effect is clearly dependent on the poling temperature relative to the polymer glass transition temperature, it being more pronounced and longer lasting the lower the temperature. This is an important feature of this apparatus if it is to be used to align nonlinear optical molecules since the system must have reached an equilibrium before any of the theoretical poling models can be employed.

The second important feature of the CCCT is that the resultant charge deposition is considerably more uniform than that produced by any other charging method. This is partly because of the PVC cylinder used, although largely a result of the existence of the ionic space charge in the air gap and the auto-compensation effect produced by the sample charges [5]. Characterisation of the CCCT by Giacometti and Campos has shown that better uniformity is achieved when I_s is low (i.e. low values of V_s) and the grid-sample distance is kept short [5].

4.5 Electro-Optic Measurements

Traditional methods used to determine the electro-optic coefficients of polymer films usually require the film to be fabricated in the form of a waveguide [15, 16]. This presents considerable problems since extensive research must be carried out in order to find suitable cladding materials which are compatible with the manufacturing and poling procedures. Secondly, due to the long path lengths within the waveguide, care must be taken in the choosing of the laser wavelength such that absorption losses are kept to a minimum. As a result of the very time consuming techniques used to couple the radiation into the wavequide, be it prism or end-fire coupling, quick measurements are almost impossible meaning that the waveguide method is unsuitable where monitoring of the dipole alignment efficiency within the film is required. These problems are overcome with the recent development of a simple reflection technique [17], described here, which requires no waveguide fabrication. The problems of film absorption, and therefore wavelength choice are also minimised since the path lengths are very short.

4.5.1 Experimental Arrangement

Figure 4.10 shows the experimental geometry and the optical configuration required to measure the electro-optic coefficients using the simple reflection technique. The sample is deposited onto an ITO coated glass substrate and, since two electrodes are also required to observe the electro-optic effect, is poled using the parallel plate technique. The laser beam is incident on the reverse of the sample, at an angle θ, and propagates through both the substrate and the film and is reflected back from the silver electrode. A polariser sets the polarisation angle of the incident radiation to 45° such that the intensities of the parallel (s wave) and perpendicular (p wave) components of the optical field are equal. A Soleil-Babinet compensator is then used to set the phase retardation between these two components to 90° (i.e. the field is circularly polarised). To cancel any film birefringence the Soleil Babinet compensator must be readjusted before every measurement. The reflected beam is then incident on an analyser and detector and its intensity monitored using a lock-in amplifier. When a modulation voltage is applied across the sample electrodes the

61
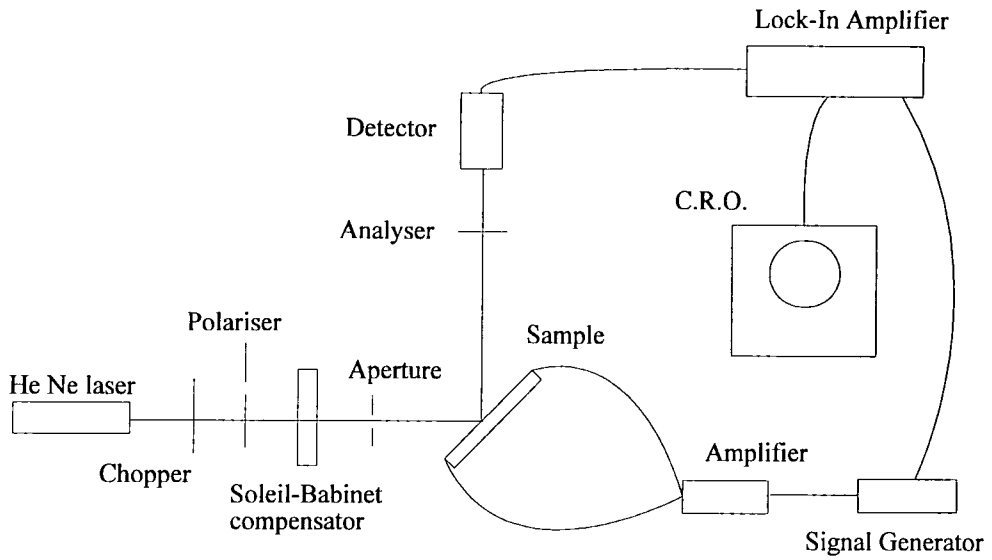
(a)
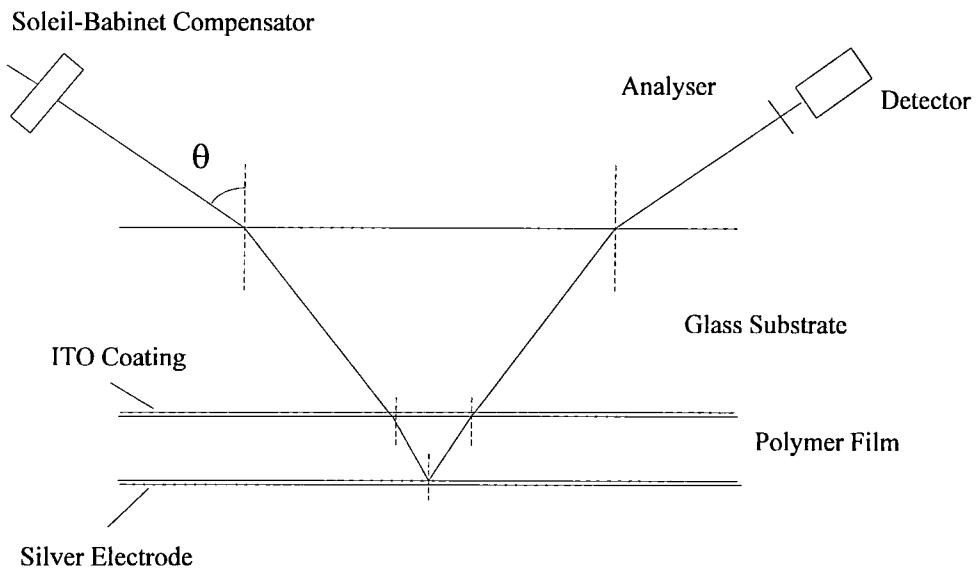
(b)

fig.4.2 Diagram showing the experimental set-up (a) and optical configuration (b) used in the measurement of the electro-optic coefficient

4·10

electro-optic effect induces refractive index changes which in turn induce a modulation in the phase angle between the s and p components of the optical field. This phase modulation can then be detected using the analyser detector arrangement described above.

4.5.2 Theory

When the modulation voltage, of the form $V_m \sin(\omega t)$, is applied across the film, a change in the phase angle, $\delta\psi$, in both the s and p components is induced by the change in refractive index δn. This change in refractive index also results in a change in the internal refraction angle, α, and therefore a change in path length, δs. Hence the phase difference can be expressed as:

$$\delta\psi = \left(\frac{2\pi}{\lambda}\right)(s\delta n + n\delta s) \tag{4.5}$$

Where d is the film thickness, λ is the wavelength and the path length, s, is given by:

$$s = \frac{2d}{\cos\alpha} \tag{4.6}$$

It is clear from equations (3.12) and (3.13) that the second order susceptibility tensors are related to the Langevin functions defined in equations (3.19) to (3.11). If the molecular dipole moment is low and the applied poling field of the order of 10's of MVm^{-1}, then the product $\mu\beta$ is much less than the product $k_B T_p$. As a result $p<<1$ and the ratio between χ_{311} and χ_{333} approximates to 1/3 (see section **6.6.11** for a more detailed discussion). These assumptions are certainly valid for the films studied using this technique (see Chapter 5) and as such $r_{33} = 3r_{31}$ where r is the electro-optic coefficient and the 3 and 1 represent directions perpendicular and parallel to the film plane respectively. If it is also assumed that the refractive indices seen by the extraordinary and ordinary ray are approximately equal (and equal to n) then the following equations can be derived [17]:

$$\delta\psi_{sp} = \delta\psi_p - \delta\psi_s = \Gamma_m \sin(\omega_m t \tag{4.7}$$

where:

$$\Gamma_m = \frac{2\pi n^3 V_m r_{33}}{3\lambda d}\left[s - \frac{4d^2}{sn^2}\left(\frac{\sin^2\theta}{\left(1 - \frac{\sin^2\theta}{n^2}\right)^2}\right)\right]\sin^2\alpha_p \qquad (4.8)$$

Since the Soleil Babinet compensator introduces a 90° phase shift between the s and p waves, the output intensity of the electro-optic modulator is at 50% which corresponds to a linear region of the modulator transmission curve [18]. Therefore, the ratio between the modulated beam intensity, I, and the 50% transmission intensity, I_c, can be approximated by the following:

$$\frac{I}{I_c} \approx \delta\psi_{sp} \qquad (4.9)$$

As a result the electro-optic coefficient, r_{33}, can be expressed as:

$$r_{33} = \frac{3\lambda I_m}{4\pi V_m I_c n^2}\left[\frac{\left(n^2 - \sin^2\theta\right)^{3/2}}{\left(n^2 - 2\sin^2\theta\right)}\right]\frac{1}{\sin^2} \qquad (4.10)$$

where I_m is the modulation amplitude. It is important to note that both I_m and V_m are expressed identically as peak-to-peak values.

4.6 Second Harmonic Generation Measurements

Until very recently the determination of the second harmonic nonlinear optical coefficients, d_{ij} (where $d_{ijk} = 1/2\chi_{IJK}$ and d_{IJK} is expressed in its contracted Voigt notation [19]), has been performed using the Maker Fringe technique [20], a detailed description of which was given by Jerphagnon and Kurtz in 1970 [21]. Assumptions made in this analysis, although valid when considering the transparent crystals studied then, are not necessarily valid for the coloured and strongly dispersive organic materials such as the poled polymers and liquid crystals, studied today.
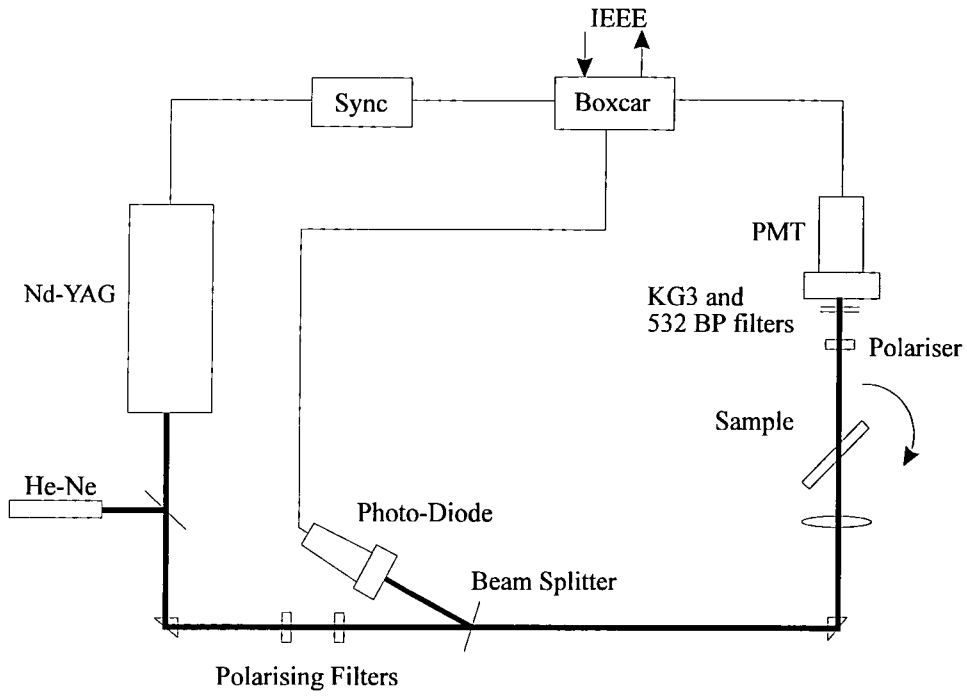
(a)
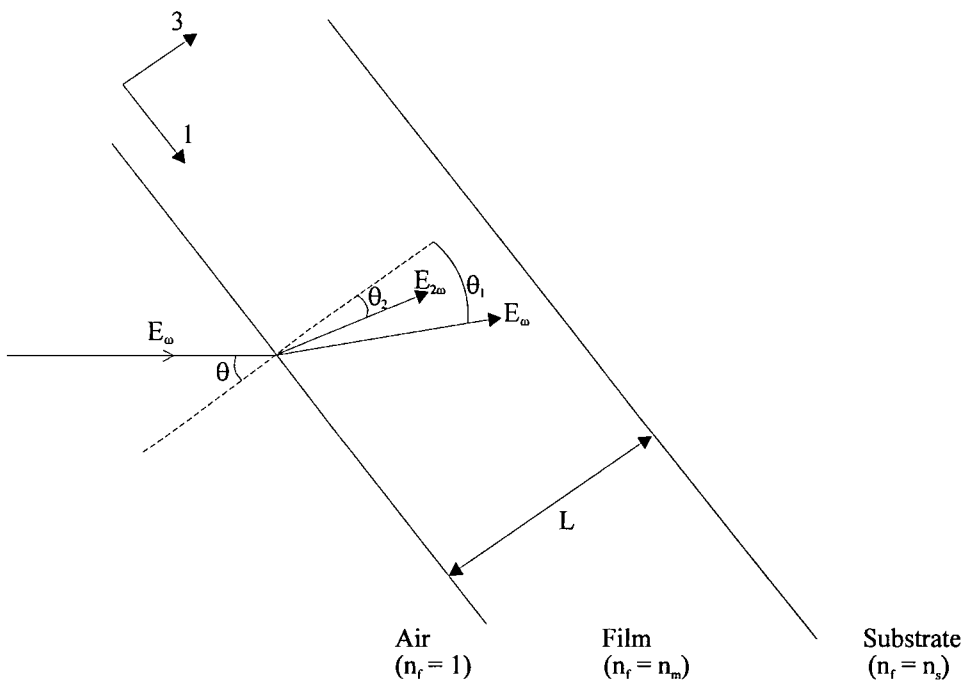
(b)

Figure 4.11 Experimental arrangement (a) and optical geometry (b)
used in SHG measurements.

Many of these materials have some residual absorption at the wavelengths typically used in SHG measurements, a factor not originally considered and has only been included recently as an approximate term valid only when the absorption coefficients are small [22]. As a result, the analysis presented here is a summary of that recently introduced by Herman and Hayden [23] which now removes the need for many of the original simplifying assumptions and takes into account absorption at both the fundamental and second harmonic wavelengths. As discussed in section **2.5.3**, the analysis is however simplified in the case of poled polymer films since only two second harmonic nonlinear optical coefficients, d_{31} and d_{33} are independent.

4.6.1 Experimental Arrangement

The experimental arrangement and the optical configuration used to measure the two independent d coefficients, d_{31} and d_{33} are shown in figure 4.11. The sample films were deposited on ITO substrates and poling was achieved using the CCCT. A Spectra Physics Nd : YAG laser of wavelength 1064 nm with a pulse duration of approximately 8 ns was used as the fundamental source. This was operated at a repetition rate of about 2-3 Hz and the beam energy was stopped down to about 0.1 mJ using a polariser / analyser arrangement. The second polariser of this arrangement also allowed control over the polarisation plane of the optical field incident on the sample. Following the polarisers a reference arm was split off using a beam splitter and the fundamental intensity (I_ω) monitored using a vacuum photo-diode. The fundamental was focused with a short focal length lens (approx. 30 cm) onto the sample which was mounted such that the poling direction is in the plane of incidence and is rotated about an axis perpendicular to the plane of incidence. An IR blocking filter (KG3) was used to remove the fundamental radiation and the intensity of the 532 nm second harmonic beam ($I_{2\omega}$) was measured using a photomultiplier tube (PMT) with a 532 nm band pass filter mounted on the front. A polariser was also placed between the sample and PMT such that the polarisation plane of the second harmonic radiation could be monitored. The intensities of both the reference arm and the second harmonic were measured using SR250 Standford Research box-car integrators and the data was normalised and collected on a PC.

4.6.2 Theory

Earlier theoretical analysis of second harmonic generation, based around that of Jerphagnon and Kurtz [21], has always made the assumption that the nonlinear medium is non-dispersive, i.e. the refractive indices at the fundamental frequency (n_1) and at the second harmonic frequency (n_2) are equal. In the case of many of the polymeric media studied today which are highly dispersive this assumption is largely incorrect and evidence has shown that making this assumption results in errors in the determination of the ratio d_{31} / d_{33} [23]. The modified theory below no longer makes this assumption and also takes into account the second harmonic wave reflected from the film-substrate interface, previously neglected and the cause of the non-standard Fresnel transmission coefficients which must have been previously calculated. Secondly, by introducing the refractive index of the nonlinear medium as a complex quantity before deriving the transmitted second harmonic intensity, absorption at both the fundamental and second harmonic frequencies can also be considered. This analysis then results in the following expression for the second harmonic intensity for the sample geometry in figure 4.11 (b) [23]:

$$\frac{I_{2\omega}}{I_\omega^2} = \left(\frac{128\pi^3}{c}\right)\left(\frac{t_\omega^4 t_{2\omega}^2 t_0^2}{n_2^2 c_2^2}\right)\left(\frac{2\pi L}{\lambda}\right)^2 d_{eff}^2 \exp\left[-2(\delta_1 + \delta_2)\right]\left(\frac{\sin^2\Psi + \sinh^2\Phi}{\Psi^2 + \Phi^2}\right)$$

$$(4.11)$$

where:

$$c_m = \left[1 - \left(\frac{\sin\theta}{n_m}\right)^2\right]^{\frac{1}{2}}$$

$$(4.12)$$

$$\delta_m = \left(\frac{2\pi L}{\lambda}\right)\frac{n_m \kappa_m}{c_m}$$

$$(4.13)$$

$$\Psi = \left(\frac{2\pi L}{\lambda}\right)(n_1 c_1 - n_2 c_2)$$

$$(4.14)$$

$$\Phi = \delta_1 - \delta_2$$

$$(4.15)$$

L is the film thickness, t_ω, $t_{2\omega}$ and t_0 are the standard Fresnel transmission coefficients at the air-film, film-substrate and substrate-air interface respectively and κ_m is the
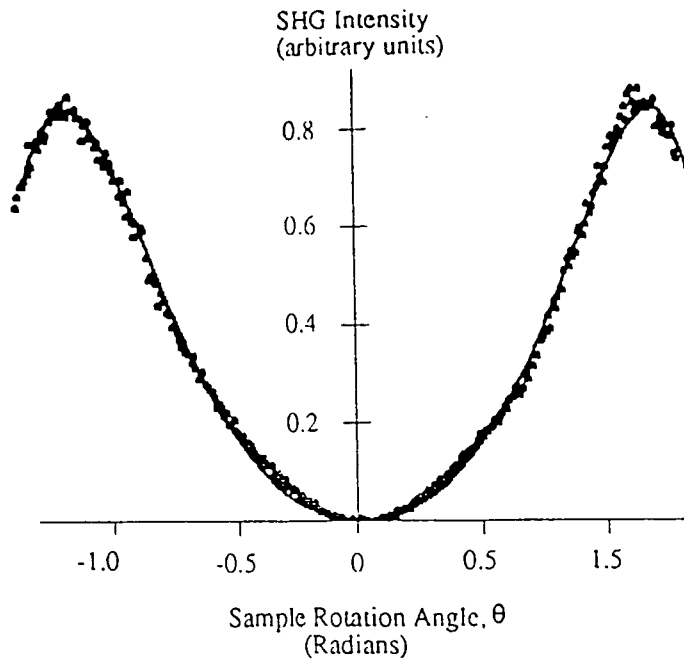
Figure 4.12 Plot showing equation 4.11 fitted to a typical set of data.
In the above case R = 0.19 ± 0.01.

extinction coefficient of the film. The subscript m (m = 1 or 2) refers to the value at frequency $m\omega$. d_{eff} is the effective second harmonic coefficient of the film and is dependent on the polarisation plane of the incident optical field and the symmetry of the nonlinear medium. In the case of media where the number of independent second order susceptibilities reduces to two (see section **2.5.3**) and the incident beam is polarised perpendicular to the plane of incidence (i.e. s-polarised) then d_{eff} is given by:

$$d_{eff} = d_{31} \sin\theta_2 \qquad (4.16)$$

If the incident beam is polarised in the plane of incidence and there is no in-plane anisotropy, then d_{eff} is given by:

$$d_{eff} = d_{33}\left\{ R\cos\theta_2\sin 2\theta_1 + \sin\theta_2\left(R\cos^2\theta_1 + \sin^2\theta_1 \right) \right\} \qquad (4.17)$$

where R is the ratio d_{31} / d_{33}. The second harmonic beam is always p-polarised and as such only the t_ω transmission coefficient should be adjusted to take into account the polarisation plane of the incident beam. In order to calculate accurate values of d_{33},

the value of R should be determined. When equation 4.17 is inserted into equation 4.11 the only unknown parameter amongst the angular dependent terms is R. Thus if the incident beam is p-polarised and the second harmonic intensity is recorded as a function of sample rotation angle, the angular dependent terms in equation 4.11 can be fitted to the experimental data and a value of R extracted. A typical set of fitted data is shown in figure 4.12.

In order that exact values of the d coefficients are measured, all calculations are done referenced to the d_{11} value of a y-cut quartz wedge (taken to be $d_{11} = 0.5$ pmV^{-1}.) Using equations 4.11 - 4.17 therefore allows the determination of the two independent second harmonic d coefficients and further, if used in conjunction with equations (3.11) and (3.12), estimates of the molecular hyperpolarisibilities of the active chromophores can also be made.

4.7 References

1.   C.C. Yang, J.Y. Josefowicz and L. Alexandru, *Deposition of Ultrathin Films by a withdrawal method.* Thin Solid Films, 1980. **74**: p. 117-127.

2.   P.K. Tien, *Light Waves in Thin Films and Integrated Optics.* Applied Optics, 1971. **10**: p. 2395.

3.   H. Kogelnik and V. Ramaswamy, Applied Optics, 1974. **13**: p. 1857.

4.   P.K. Tien and R. Ulrich, *Theory of Prism-Film Coupler and Thin Film Light Guides.* J. Opt. Soc. Am., 1970. **60**: p. 1325.

5.   J.A. Giacometti and J.S.C. Campos, *Constant Current Corona Triode With Grid Voltage Control - Application to Polymer Foil Charging.* Review Of Scientific Instruments, 1990. **61**(3): p. 1143-1150.

6.   R. Haug, J. Lebas and Y. Teisseyre, *Ion Current Calculation In a System Of Plane Grids In an Ionized-Gas Flow.* Journal Of Physics D-Applied Physics, 1984. **17**(2): p. 357-366.

7.   J.A. Giacometti, *Radial Current-Density Distributions and Sample Charge Uniformity In a Corona Triode.* Journal Of Physics D-Applied Physics, 1987. **20**(6): p. 675-682.

8.   J.A. Giacometti and O.N. Oliveira, *Corona Charging Of Polymers*. IEEE Transactions On Electrical Insulation, 1992. **27**(5): p. 924-943.

9.   G.F.L. Ferreira, D.L. Chinaglia, J.A. Giacometti and O.N. Oliveira, *Corona Triode Current-Voltage Characteristics - On Effects Possibly Caused By the Electronic-Component*. Journal Of Physics D-Applied Physics, 1993. **26**(4): p. 628-633.

10.   J.A. Giacometti and R. Coelho, *Further Speculations On the Natural Decay Of Corona Charged Insulating Films*. Physica Status Solidi a-Applied Research, 1987. **99**(1): p. K 45-K 48.

11.   O.N. Oliveira and G.F.L. Ferreira, *Grid-to-Plate Current-Voltage Characteristics Of a Corona Triode*. Review Of Scientific Instruments, 1985. **56**(10): p. 1957-1961.

12.   M. Robinson, *Movement of Air in the Electric Wind of the Corona Discharge*. Trans. Am. Inst. Electr. Eng., 1961. **80**: p. 143.

13.   M.A. Lampert and P. Mark, *Current Injection in Solids*. 1970, New York: Academic.

14.   P.T. Dao, D.J. Williams and W.P. McKenna, *Constant Current Corona Charging As a Technique For Poling Organic Nonlinear Optical Thin-Films and the Effect Of Ambient Gas*. Journal Of Applied Physics, 1993. **73**(5): p. 2043-2050.

15.   C.C. Teng and D. Stuetz, *U.S. Patent,* . 1988: USA.

16.   W.H.G. Horsthuis and G.J.M. Krijnen, *Simple Measuring Method For Electro-Optic Coefficients In Poled Polymer Wave-Guides*. Appl. Phys. Lett., 1989. **55**(7): p. 616-618.

17.   C.C. Teng and H.T. Man, *Simple Reflection Technique For Measuring the Electrooptic Coefficient Of Poled Polymers*. Appl. Phys. Lett., 1990. **56**(18): p. 1734-1736.

18.   A. Yariv, *Optical Electronics,* . 1985, CBS College Publishing: California. p. 293.

19.   D.M. Burland, R.D. Miller and C.A. Walsh, *2nd-Order Nonlinearity In Poled-Polymer Systems*. Chemical Reviews, 1994. **94**(1): p. 31-75.

20.   P.D. Maker, R.W. Terhune, N. Nisenhoff and C.M. Savage, *Effects of Dispersion and Focussing on the Production of Optical Harmonics*. Phys. Rev. Lett., 1962. **8**: p. 21.

21.   J. Jerphagnon and S. K. Kurtz, *Maker Fringes: A Detailed Comparison of Theory and Experiment for Isotropic and Uniaxial Crystals.* J. Appl. Phys., 1970. **41**: p. 1667.

22.   B.F. Levine and C.G. Bethea, *Second and Third Order hyperpolarisibilities of Organic Molecules.* J. Chem. Phys., 1975. **75**: p. 3572-3580.

23.   W.N. Herman and L.M. Hayden, *Maker Fringes Revisited - 2nd-Harmonic Generation From Birefringent or Absorbing Materials.* Journal Of the Optical Society Of America B-Optical Physics, 1995. **12**(3): p. 416-427.

CHAPTER 5

HYDROGEN BONDED GUEST-HOST POLYMERIC SYSTEMS

5.1 Introduction

The induced polar alignment in guest-host polymeric media is often unstable, often leading to a decay of the second order nonlinearity over a period of days or even hours. In recent years however, it has been reported that certain guest-host systems exhibit exceptional polar stability, more characteristic of side chain polymers. It was suggested that hydrogen bonding may be the origin of this stability, which in some cases has led to the polar alignment remaining stable for more than several months. This study was therefore an attempt to characterise fully the behaviour of these systems and investigate whether the stability can be attributed to hydrogen bonding. Through careful choice of host, an attempt was also made to further enhance their stability.

5.1.1 The Hydrogen Bond

A hydrogen bond is a weak chemical bond brought about by an associative interaction between the functional group A-H and another atom or group, B, specifically involving the hydrogen atom bonded to A. A hydrogen bond usually forms when A and B are closely spaced electronegative atoms such as oxygen or nitrogen. As a result, they normally form when the hydrogen is attached to an acidic group such as a hydroxyl, carboxyl or amide group. The bond forms through the donation of a free electron pair from atom B to the hydrogen resulting in a weak

chemical bond. A direct consequence of this is that the bonding electrons in the A-H group are drawn towards the hydrogen to compensate for the redistribution of charge and the bond weakens and lengthens. It is this change in the character of the A-H bond that is often exploited when investigating hydrogen bonding (see section **5.5**).

5.1.2 Hydrogen Bonding in Nonlinear Optical Polymers

The first evidence that hydrogen bonding may be affecting the nonlinear response of polymeric systems appeared in 1989 when Hampsch et al. reported that the second order nonlinearity of disperse orange-25, DO25, and disperse red-1, DR1, decayed considerably faster in poly(methyl methacrylate), PMMA, than in bisphenol A polycarbonate, BPA-PC [1]. This result at the time was attributed to a greater local mobility of the chromophores in PMMA than in BPA-PC. However, both chromophores contain the functional hydroxyl group which would clearly be capable of hydrogen bonding with a suitable group on the host. This hypothesis was first proposed in 1991 when Boyd et al. reported the same unusual stability in a similar guest-host system [2]. Lindsay et al. have also attributed a very high stability in the side-chain polymer poly(methyl methacrylate-co-coumaromethacrylate) to hydrogen bonding [3]. They observed only a 7% relaxation of second harmonic signal over 400 hours. In 1992 Karakus et al. reported very high stabilities of the polar alignment of 2-(N, N dimethylamino)-5-nitroacetanilide (DAN) doped into BPA-PC [4]. Both this, and an observed enhancement of nonlinear response, was accounted for by hydrogen bonding. This improved stability and enhancement of the nonlinear response was also observed by Wan et al. when conducting studies on disperse orange-3 (DO3) and DR1 doped into BPA-PC and again attributed to hydrogen bonding [5].

Common to all of the above studies is that all of the chromophores contain A-H functional groups suitable for hydrogen bonding. The high stabilities were all observed when the host BPA-PC was used which contains a carbonyl group, ideal for forming hydrogen bonds with an A-H group. However, the host PMMA also contains a similar carbonyl group and no enhancement of polar stability is observed in these systems. The mere presence of hydrogen bonds, therefore, may not be

sufficient to stabilise the polar alignment. Consequently, the effect may be more complicated and factors such as the strength of the hydrogen bond or other system properties may also play a role. The purpose of this study is therefore to ascertain whether hydrogen bonds are indeed present in both of these materials, and to investigate the possibility of other requirements necessary to produce the observed stability enhancements in the polycarbonate systems.

5.2 Material Systems

The guest molecule used in this investigation was DAN shown in figure 5.1. It can be seen that the acetanilide side group in DAN is capable of hydrogen bonding and highly stable polar alignment has been observed when it is dispersed in BPA-PC [4]. In DAN the dimethylamino group and the acetanilide side chain group combine to form a strong electron donor whereas the nitro group is the required electron acceptor. Experimental values for μ and β^0_{vec} in the solvent 1,4-dioxane have been measured at 9.2 D and 17 x 10^{-30} esu respectively [6]. The nonlinear properties of DAN were first reported by Tweig et al. [7] in 1983 and its good nonlinear optical response has since made it the subject of a number of studies [8, 9].

The host polymers used for this study were PMMA and BPA-PC, shown in figure 5.2. It is a common observation that dopant relaxation is related to the glass transition temperature (T_g) of the system [10]. To this end the high T_g polycarbonate, BPTMC-PC [11] (figure 5.2), was also used in order to investigate the possibility of improving the polar stability still further. The T_g of this polymer is 239 °C, 83 °C
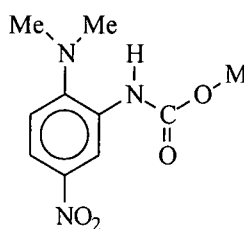
Figure 5.1. The chemical structure of DAN.

PMMA

BPA-PC

BPTMC-PC
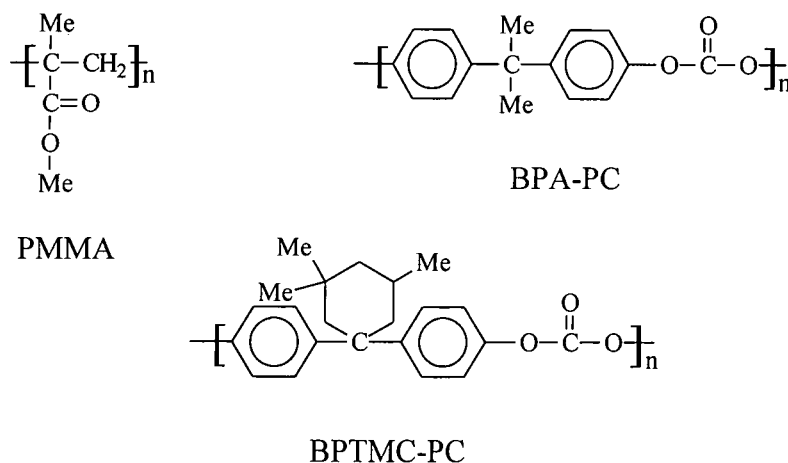
Figure 5.2 Chemical structures of the host polymers

higher than that of BPA-PC whose T_g is 155 °C. All of the above polymers are amorphous, that is they are optically homogenous and are characterised by a very high optical transparency. This has resulted in many applications in optical materials such as lenses and fibres and their good mechanical properties, particularly in the case of the polycarbonates, has led to their use as substrates for optical discs [11].

5.3 Sample Preparation

20% w/w solutions of DAN in each of the host polymers were prepared in dichloromethane (approx. 1 g of polymer to 5 ml of solvent). Once fully dissolved, the solutions were filtered through 5 μm in-line Millipore filters to remove undissolved contaminants. Films were deposited onto appropriate substrates using the substrate withdrawal technique (see section **4.2.2**). Withdrawal speeds of 40 mm min^{-1} were used resulting in film thicknesses of approximately 3 - 5 μm. Samples to be poled were deposited onto conductive ITO coated glass substrates and films to be used in refractive index measurements were deposited onto fused silica. The films were dried under vacuum for 2 - 5 hrs at temperatures ranging between 40 and 80 °C to remove excess solvent.

75
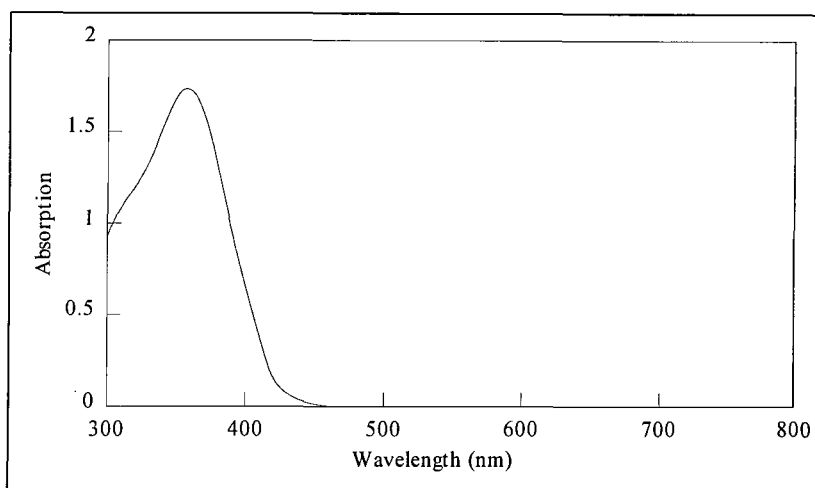
Figure 5.3 Absorption spectrum of a DAN-doped polymer film.

5.4 Film Characterisation

The UV-visible absorption spectrum of a DAN-doped polymer film is shown in figure 5.3. Refractive index measurements at 632.8 nm were carried out using the prism coupling technique (section **4.3.1**) with a helium-neon laser. The glass transition temperature of the undoped and doped polymers was also determined as described in section **4.3.3**. The results of these measurements are given in table 5.1.

Polymer	Refractive Index (632.8 nm)	T_g (°C)
PMMA	1.492	105
20% DAN / PMMA	1.494	55
BPA-PC	1.578	155
20% DAN / BPA-PC	1.58	82
BPTMC-PC	1.548	239
20% DAN / BPTMC-PC	1.568	139

Table 5.1 Film characteristics of DAN-doped polymers.

76

5.5 Infra-Red Spectroscopic Studies

One of the most common and simplest of techniques used to detect the presence of hydrogen bonds is IR spectroscopy which reveals the characteristic frequencies of molecular vibrations. These frequencies are governed by the masses of the vibrating atoms, the molecular geometry, and the restraining forces holding the atoms in their equilibrium positions. As a result, this is a very powerful technique used to probe chemical bonding and molecular structure.

When considering hydrogen bonding in DAN the vibrational resonance of importance is the amido group, N-H, stretching mode which, in the absence of hydrogen bonding, occurs at around 3400 - 3500 cm^{-1} [12]. As discussed briefly in section **5.1.1**, bond formation at the proton in the N-H group perturbs the N-H bond and weakens it. Such a change will not only have a considerable effect on the resonant frequency of the stretching mode, but also other spectral changes may be observed. The following is a summary of the more important changes that can be expected in the N-H stretch as a result of hydrogen bond formation:

(1)   *Frequency Shift*: A shift of the mode to lower frequencies.

(2)   *Half-Width Change*: A broadening of the mode.

(3)   *Intensity Change*: An increase in the integrated absorption coefficient.

In many cases these changes can be considerable, and in particular shifts of the resonant frequency of the A-H stretch are typically in excess of 100 cm^{-1}. IR spectroscopy is therefore a very powerful, and yet simple technique capable of detecting hydrogen bond formation.

5.5.1 Experimental

Following drying, each DAN-doped polymer film was carefully removed from the substrate such that IR absorption of the glass could be eliminated. The films were then suspended from a frame to allow easy insertion into the spectrometer. For comparison, a spectrum of pure DAN also had to be determined. Crystalline DAN

was ground up with potassium bromide (KBr), which is transparent to infra-red radiation in the region of interest, in a mortar and pestle. The powder was pressed at 10 tonnes for 10 mins resulting in a small thin solid disc which could then be inserted into the spectrometer.

5.5.2 Results and Discussion

The IR spectra of crystalline DAN, DAN-doped BPA-PC and DAN-doped PMMA are displayed in figure 5.4. The N-H stretch is positioned at 3260 cm^{-1} in the crystalline sample and at 2960 cm^{-1} and 2940 cm^{-1} in the BPA-PC and PMMA film samples respectively. In all cases the N-H band appears to be shifted from the 3400 - 3500 cm^{-1} region where it would be expected if no hydrogen bonds were present. This alone is very strong evidence that hydrogen bonds are present in all of the samples studied.

If the crystalline sample is considered first, it can be seen that the N-H stretch has shifted by approximately 200 cm^{-1} to 3260 cm^{-1}. It is very common in compounds such as DAN, where hydrogen bonding groups are present, to observe shifts in the N-H band to lower frequencies in the solid state [12]. Typically these shifts are of the order of 200 cm^{-1} and result in the N-H stretch appearing at approximately 3180 - 3350 cm^{-1}. It is clear that this is the case in this crystalline sample indicating the presence of inter-molecular hydrogen bonding between the DAN molecules.

If the DAN-doped polymers are now considered, it can be seen that the N-H stretch has shifted from the 3400 -3500 cm^{-1} region by approximately 500 cm^{-1}, some 300 cm^{-1} from its position in the crystalline sample. This is a very large shift and cannot be attributed to hydrogen bonds of the type present in the crystalline sample. The further shift therefore suggests that stronger hydrogen bonds are forming between the DAN and the polymer. The relatively small differences between the two IR spectra implies that the guest-host hydrogen bonds in both the PMMA and BPA-PC systems are of similar strength and character. These small differences do however suggest that the interactions are host dependent and provide further evidence that the hydrogen bonds are forming between the DAN and the polymer.
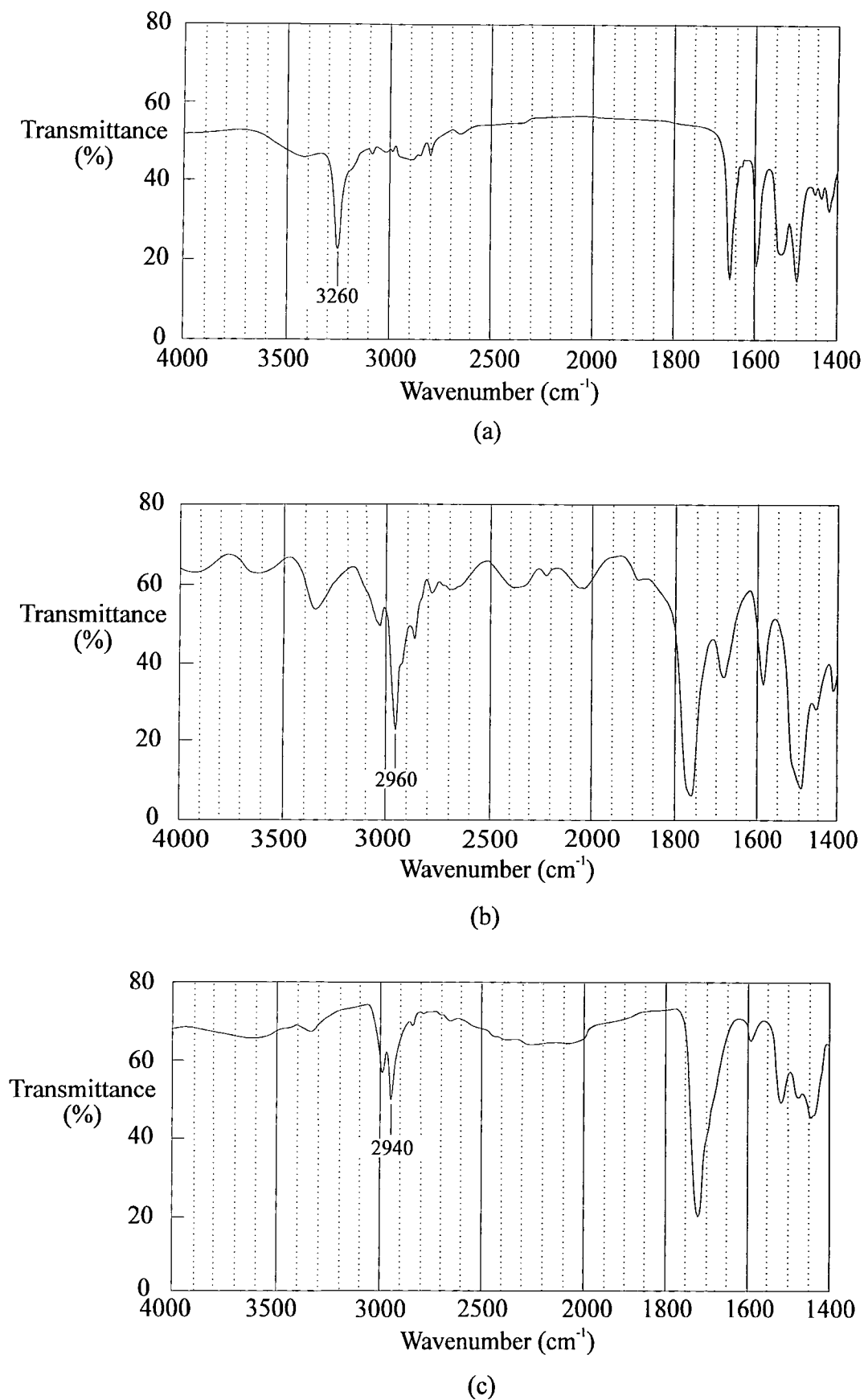
(a)

(b)

(c)

Figure 5.4 I.R spectra of (a) crystalline DAN, (b) DAN doped BPA-PC and (c) DAN doped PMMA

5.6 Electric Field Poling Studies

The presence of hydrogen bonds in both systems may suggest that the polar alignment should remain stable in both. However, electro-optic measurements on DAN-doped PMMA films indicate that the polar alignment is lost after less than 24 hrs [13]. Based on these observations, therefore, it is quite clear that hydrogen bonding alone cannot explain the high polar stabilities observed in the polycarbonate systems. Although hydrogen bonding may play an important role in stabilising the polar alignment, it is clear that it is only part of the mechanism involved. Since the only difference between the two polymer systems studied above is the host, this mechanism must therefore be the result of a property of BPA-PC which is absent in PMMA.

One major difference between the two polymers studied here is that, unlike PMMA, the polycarbonates may be formed as stable main-chain nonlinear optical polymers [14]. Although the dipole in PMMA may also orient in a poling field, local chain motion is persistent at room temperature and allows immediate relaxation. It may be in this property, therefore, that the origins of the observed polar stabilities in polycarbonates lie. If this is the case, a difference in the alignment mechanisms, during poling of the two systems, may be apparent. An important characteristic of the constant current corona triode, CCCT (see section **4.4.2.4**), is that through monitoring of the surface potential build up on the sample, polarisation currents brought about by dipolar alignment can be studied. Any differences between the alignment mechanisms of the two polymer systems, may therefore be revealed.

5.6.1 Experimental

Films of both the PMMA and BPA-PC systems were prepared on the patterned ITO substrates described in section **4.4.2.1**. The samples were poled with a charging current (I_s) of 10 nA and a corona current (I_c) of 1.5 μA. The poling temperature was set to 5 °C below the T_g in the case of the PMMA films (ie. 50 °C) and 7 °C below the T_g in the case of the BPA-PC films (ie. 75 °C). This permitted both free

movement of the chromophores during alignment and a reasonably high poling field to build up. Poling was continued until the grid voltage traces indicated alignment was complete (see section **4.4.2.4**) and then the sample was cooled over a period of half an hour while constant current charging was maintained.

5.6.2 Results and Discussion

Curves showing the build up of surface potential on each of the samples are compared in figure 5.5. The curves show a marked difference in the behaviour of the two polymer systems during poling, indicating a difference in the alignment mechanisms involved. The proximity of the poling temperature to the system T_g in these experiments means that dipoles capable of free rotation will respond to the electric field over a very short space of time, almost instantaneously. The alignment of freely moving dipoles will therefore occur at the same rate as charge deposition and the poling curve will be characterised by a fast but uniform increase of the surface potential to a steady value. This is certainly evident in the DAN-doped PMMA curve (curve (a)) which shows a uniform rise of the surface potential to a constant value of approximately 150 V in under 8 mins. This therefore suggests that there is no restriction of motion of the DAN molecules in PMMA during poling. Likewise there would be no restrictions of dipolar relaxation following poling which would result in the lack of polar stability observed in these systems, despite the presence of hydrogen bonds.
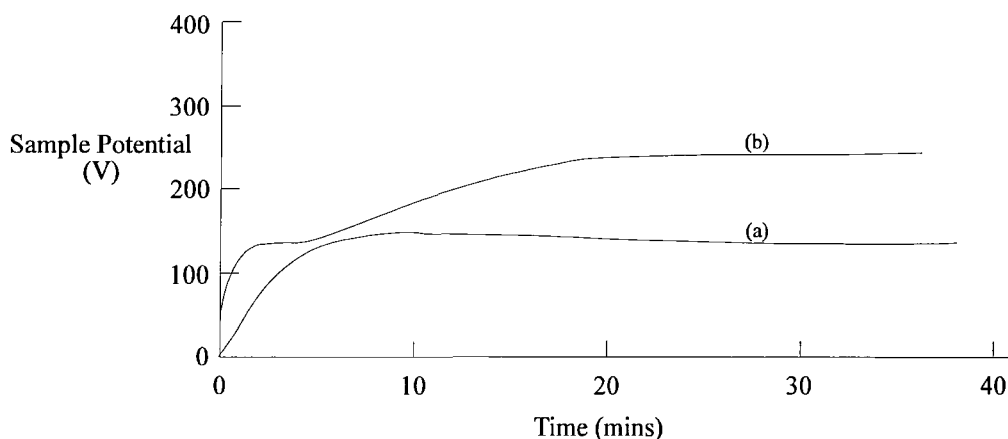
Figure 5.5 Surface voltage characteristics of (a) DAN doped PMMA and
(b) DAN doped BPA-PC during constant current corona charging.

81

This observation can easily be explained if the chemical structure of PMMA (figure 5.2) is examined and the position of the hydrogen bonding group, the carbonyl group, is considered. The carbonyl group is a relatively mobile side group of the polymer main chain. Consequently, movement of the carbonyl group, and the DAN molecule hydrogen bonded to it, is achieved relatively easily without the need of slow segmental motions of the polymer. This would explain why the presence of hydrogen bonds has no effect on the stability of polar order of these systems.

The behaviour of the DAN-doped BPA-PC system is somewhat different (see curve (b)). The curve is characterised by a very rapid rise in surface potential to approximately 60 V, after which the surface potential levels off and remains steady at 120 V for about 5 mins. Following this the surface potential very gradually increases to approximately 250 V over a period of 25 mins after which it appears to reach an equilibrium. As discussed in section **4.4.2.4** the levelling off of the surface potential and subsequent slow increase is an indication of polarisation currents caused by the rotation of dipoles. Their presence, along with the long time required for an equilibrium to be reached, suggests that the motion of the dipolar species is far more gradual in these materials. As discussed above, at the temperatures at which poling was carried out, dipoles normally free to move would align almost instantaneously resulting in an absence of these extra features on the surface voltage characteristics. The motion of dipoles in these materials is therefore restricted by their environment resulting in the long poling times required. This hypothesis can be further supported if the surface potential characteristics at the very start of poling are examined in greater detail. It can be seen that the surface potential rises almost instantaneously, suggesting that virtually no polarisation currents begin to flow until the potential reaches approximately 60 V. This would suggest that dipolar rotation is very restricted when the electric field induced torque on the dipoles is low. This is in complete contrast to the case of DAN-doped PMMA where it would appear that the dipolar species are able to move under all applied fields. This is a clear indication that the motion of the dipoles in the BPA-PC materials is considerably more impeded than in the PMMA system. These forces restricting dipolar rotation present in the BPA-PC systems during poling will also be present after poling and thus

maintain the induced polar stability. The origins of these restricting forces can be explained by studying the chemical structure of the polycarbonates (figure 5.2). Unlike PMMA, the polycarbonate backbone itself contains the polar carbonyl group [14] and thus will align in the electric field along with the DAN molecules hydrogen bonded to it. Considerable segmental motion is required if polymer backbones are to align and it is this that restricts the alignment processes during poling. It is clear therefore the same segmental motions must also occur if the polar alignment is to relax, thus resulting in the very good polar stabilities observed.

5.7 Nonlinear Optical Characterisation of High T_g Polycarbonates

It is a common observation that polar stability improves as the glass transition temperature of the system rises [10]. The high T_g polycarbonate, BPTMC-PC, was therefore investigated as a possible alternative host, which, being a polycarbonate, would be expected to behave in a similar manner to BPA-PC. Indeed, the IR spectrum and poling characteristics of DAN-doped BPTMC-PC are identical to DAN-doped BPA-PC and as such the same polar stability would be expected. In this section, therefore, the nonlinear optical properties of DAN-doped BPTMC-PC are determined using electro-optic and second harmonic generation (SHG) measurements, and the results are compared with the DAN-doped BPA-PC system.

5.7.1 Experimental

All of the films to be used in these measurements were deposited onto ITO coated glass substrates. Samples to be characterised using electro-optic measurements were poled using fixed electrode poling (section **4.4.1**) and thus had silver electrodes evaporated onto the film surface prior to poling. Those to be used in SHG measurements were poled using the CCCT (section **4.4.2**). The poling conditions for both the BPA-PC samples and BPTMC-PC systems for each poling technique are summarised in table 5.2. Following poling all samples were cooled for 30 minutes while the field was still applied. The nonlinear optical measurements began within 5 minutes of removing the electric field.

5.7.2 Electro-Optic Measurements

Electro-optic measurements were carried out using the simple reflection technique described in section 4.5. The purpose of these measurements was to ascertain whether the use of the high T_g polycarbonate improves the stability of the electro-optic response observed in DAN-doped BPA-PC [4]. The electro-optic response provides a simple method of monitoring the alignment of the chromophores since magnitude of the response is directly related to the orientation of the dipoles. As discussed in section **4.4.2** the corona poling technique used to prepare samples for SHG measurements deposits charge on to the film surface which generates the required poling field. As will become clear in section **5.7.3** the decay of this charge is very unpredictable, varying from sample to sample. As a result, comparing relaxation data from samples poled in this way, such as SHG data, may be over-complicated by the decay of this residual surface charge. It is for this reason that the electro-optic technique was chosen to compare the polar order stability of these material systems.

Figure 5.6 shows a plot of the normalised electro-optic coefficient of the two polycarbonate systems. For comparative purposes the relaxation of the electro-optic coefficient of DAN-doped PMMA (obtained from reference [13]) is also shown. It is quite clear from the figure 5.6 that *both* polycarbonate samples exhibit a considerably more stable electro-optic response than the PMMA sample, as might be expected. It is also clear that the use of the high T_g polycarbonate, BPTMC-PC, enhances the stability of the electro-optic coefficient to a greater extent than the standard BPA-PC. Indeed, after 6 months at room temperature the BPTMC-PC

Poling Technique	Material System	Poling Temp. (°C)	Poling Time (mins)	Poling Field $(V\mu m^{-1})$
Contact Poling	BPA-PC	75	10	25
	BPTMC-PC	125	10	25
Corona Poling	BPA-PC	75	40	67
	BPTMC-PC	125	40	70

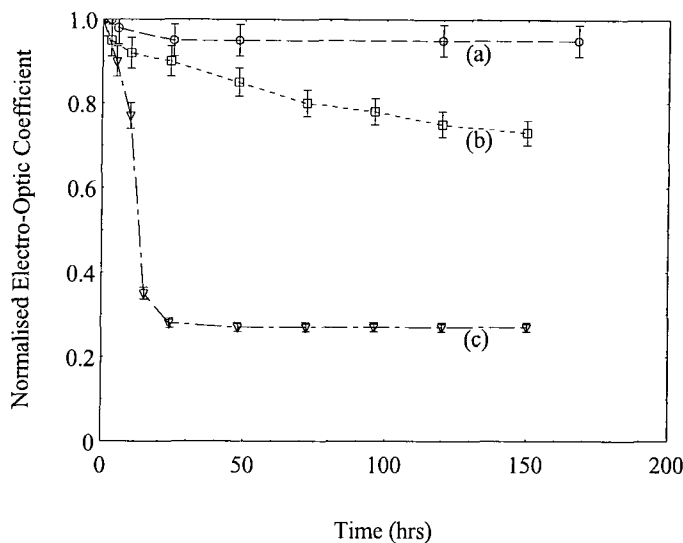Table 5.2 Summary of poling conditions used in nonlinear optical characterisations.

Figure 5.6 Relaxation of electro-optic coefficient of (a) DAN-doped BPTMC-PC,
(b) DAN-doped BPA-PC and (c) DAN-doped PMMA*.
(* Data obtained from reference [4])

sample showed no more than a 10% relaxation compared with a relaxation of approximately 30% for the DAN-doped BPA-PC sample over a similar period [13]. This is quite a considerable effect since the stability of the BPTMC-PC system is now equivalent to a good side chain polymer.

The use of a host with a high T_g therefore improves the stability of the polar order considerably. This can be improved still further by reducing the doping level of the guest molecules which would increase the system T_g to even higher values. However, the nonlinear optical response would clearly reduce due to the lower number density of the active chromophores. Increasing the T_g to greater values also increases the temperature at which the samples must be poled. If this poling temperature gets too high, the guest molecules begin to evaporate from the film and may even thermally decompose, thus reducing the nonlinear response. A compromise must therefore be reached and system components with high thermal stabilities must be synthesised if the polar stability is to be further enhanced in this manner.

5.7.3 Second Harmonic Generation Measurements

Second harmonic generation measurements were carried out using the technique described in section **4.6**. The purpose of these measurements was to obtain accurate values of the nonlinear susceptibilities and hyperpolarisibilities of the DAN-doped polycarbonate materials and also compare signal relaxation with the data obtained using the electro-optic technique. There is no simple relationship between the electro-optic coefficient and the nonlinear susceptibility, only an approximate expression employing various simplifying assumptions and the two-level model can be obtained. Accurate expressions for the nonlinear susceptibility can, however, be obtained from SHG results using the analysis described in sections **3.3** and **4.6.2**. SHG measurements are therefore essential if accurate characterisation of the nonlinear response of a material system is required.

Values of the two independent second harmonic coefficients of the two polycarbonate systems are displayed in table 5.3 along with their ratio, R (d_{31}/d_{33}), obtained by fitting equation 4.11 to the experimental data (see section **4.6.2**). Using equation 3.12, values of the component of the dynamic first hyperpolarisibility of DAN along its dipole moment axis ($\beta^{(\omega)}_{vec}$) can be obtained and these are also shown in table 5.3. The value of $\beta^{(\omega)}_{vec}$ for DAN obtained in a solution of 1, 4-dioxane was 34×10^{-30} esu[6]. Such that direct comparisons of this solution measurements can be made with the results in table 5.3, the local field models employed in both studies must be the same. To this end the more familiar Lorentz-Lorenz and Onsager local field correction factors (equations (2.9) and (3.13)) respectively were employed.

It is clear that the values of $\beta^{(\omega)}_{vec}$ in table 5.3 are higher than the values obtained in solution and are consistent with the enhancements of the nonlinear response observed previously in such hydrogen bonded systems [4, 5]. The enhancements observed in these earlier studies were attributed to the suspected guest-host interactions. However recent theoretical calculations have shown that the nonlinear response of a molecule shows a marked dependence on the dielectric nature of its environment [15-18]. This was mentioned briefly in section **3.3.1** and will be discussed in more detail in chapter **6** with respect to very polar molecules where the

Material System	R	d_{31} (pmV^{-1})	d_{33} (pmV^{-1})	$\beta^{(\omega)}_{vec}$ (x 10^{-30} esu)
DAN-doped BPA-PC	0.33 ± 0.02	0.98 ± 0.1	3.36 ± 0.3	58 ± 10
DAN-doped BPTMC-PC	0.33 ± 0.02	0.67 ± 0.05	2.35 ± 0.2	45 ± 10

Table 5.3 Results of the SHG analysis on the DAN-doped polycarbonates.

implications are far greater. The calculations show that for environments where the relative permittivity is low, such as in the case of most polymers and non-polar solvents such as 1, 4-dioxane, $\beta^{(\omega)}_{vec}$ will increase with increasing relative permittivity. The relative permittivity of 1, 4-dioxane is very low, indeed it is this reason that it is chosen as a solvent for solution characterisation of new nonlinear molecules since it is hoped the molecules best represent their gas phase electronic and structural configurations. The polycarbonates on the other hand, due to their higher relative permittivity and dipole moment might provide a considerably more polar environment. As a result it would be expected that the values of $\beta^{(\omega)}_{vec}$ in polycarbonate are higher. This may therefore account for the enhancement of the nonlinear response observed in this and previous studies. It should be noted that the values of $\beta^{(\omega)}_{vec}$ in table 5.3 can not be considered to be absolute since no consideration was given to the local field correction factors used or the effects of a field enhanced dipole moment. For comparative purposes a spherical cavity shape was assumed in their calculation which in light of recent publications [19] may not be the best approximation. It can be shown that the choice of cavity shape can have considerable effect on the calculated values of dipole moment and $\beta^{(\omega)}_{vec}$. However, a comparison of the results obtained in this study and those obtained from solution measurements was sufficient and as a result absolute values of $\beta^{(\omega)}_{vec}$ were not required. This problem of local fields and the cavity shape used to determine them will, however, be addressed in chapter 6.

The relaxation of the second harmonic signal of the two polycarbonate systems is shown in figure 5.7. It would appear from these results that the DAN-doped BPTMC-PC is less stable than the DAN-doped BPA-PC, in complete contrast with the results obtained from the electro-optic studies. This difference is caused by the different methods of poling used. The electric fields generated during corona poling arise from the accumulation of free charge trapped on the surface of the film. The lifetimes of these surface traps can be very long and vary considerably between materials. As a result the decay of the poling field after the corona discharge is turned off is by no means instantaneous and, due to the many decay processes involved, can be quite complicated and prolonged. This is indicated by the very large initial decay of the second harmonic coefficient of the material, an effect not observed in the electro-optic measurements. Remanent fields are therefore common in corona poled samples and can affect the stability of the dipolar order. Based on the results in figure 5.7, it would therefore appear that the remanent field is far more stable in the DAN-doped BPA-PC system accounting for the greater stability of the second harmonic signal. It is for this reason that electro-optic measurements were chosen to monitor the polar stability of these DAN-doped systems since the same effect does not occur with contact poled samples. Despite these complications, however, it is clear that the stability of both material systems is still very good with
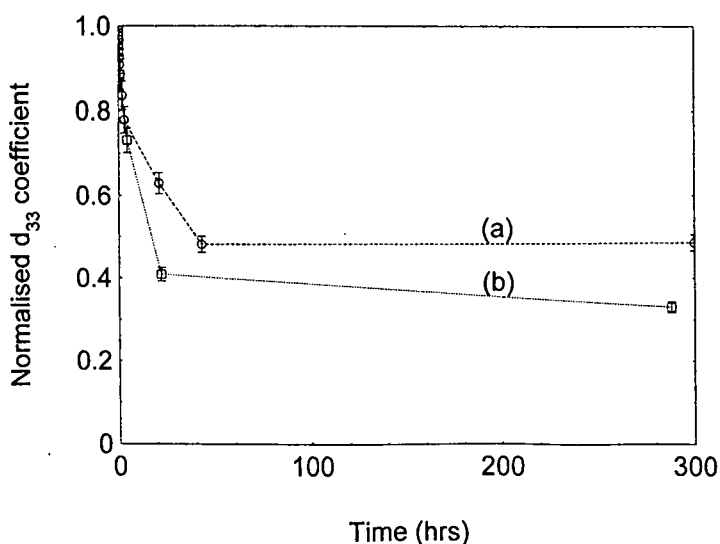

Figure 5.7 Relaxation data for the second harmonic response of (a) DAN-doped BPA-PC and (b) DAN-doped BPTMC-PC.

high second harmonic signals obtainable after as long as 2 years at room temperature.

5.8 Summary and Conclusions

The high stability of the polar order observed in particular guest-host polymeric media was investigated using IR spectroscopy and through the application of a constant current corona triode used to monitor the alignment mechanisms during poling. It was found that two system requirements are necessary to account for the high polar stabilities observed. Firstly, both the guest and host must contain functional groups suitable for hydrogen bond formation between them. Secondly, the functional group on the host must be directly attached to the polymer backbone such that the polymer backbone itself aligns in the poling field along with the guest. The origin of the polar stability lies in the fact that considerable segmental motion in the polymer backbone is necessary if it is to move. The motion of the polymer backbone is therefore severely restricted and as such stabilises the alignment of the chromophores attached to it via hydrogen bonding.

The polar stability of one such system was further enhanced through the use of a host with a high glass transition temperature. A polycarbonate variant (whose T_g is 85 °C higher than the standard BPA-polycarbonate) was used to increase the 20% loaded system T_g from 85 °C to 139 °C. The resultant film showed only a 10% drop in electro-optic coefficient over 7 months compared with a 30% drop for the standard polycarbonate system. SHG relaxation data indicated that the high T_g polycarbonate system was less stable, however this was attributed to remanent fields brought about by surface charge remaining from the corona poling process.

5.9 References

1. H.L. Hampsch, J. Yang, G.K. Wong and J.M. Torkelson, *2nd Harmonic-Generation In Doped Glassy Polymer-Films As a Function Of Physical Aging and Dopant Size.* Polymer Communications, 1989. **30**(2): p. 40-43.

2. G.T. Boyd, C.V. Francis, J.E. Trend and D.A. Ender, *2nd-Harmonic Generation As a Probe Of Rotational Mobility In Poled Polymers.* Journal Of the Optical Society Of America B-Optical Physics, 1991. **8**(4): p. 887-894.

3. G.A. Lindsay, R.A. Henry, J.M. Hoover, A. Knoesen and M.A. Mortazavi, *Sub-T(G) Relaxation Behavior Of Corona-Poled Nonlinear Optical Polymer-Films and Views On Physical Aging.* Macromolecules, 1992. **25**(19): p. 4888-4894.

4. Y. Karakus, D. Bloor and G.H. Cross, *Enhanced Linear Electrooptic Response and Enhanced Stability Of Thermo-Poled Guest Host Polycarbonate Thin-Films.* Journal Of Physics D-Applied Physics, 1992. **25**(6): p. 1014-1018.

5. F. Wan, G.O. Carlisle, K. Koch and D.R. Martinez, *Enhanced 2nd-Harmonic Response and Stability Of Corona-Poled Guest- Host Polycarbonate Thin-Films.* Journal Of Materials Science-Materials In Electronics, 1995. **6**(4): p. 228-234.

6. D. Gray, *Molecular Organic Photonics*, in *Dep't of Physics.* 1994, University of Durham: Durham.

7. R. Tweig, 1983.

8. P. Kerkoc, M. Zgonik, K. Sutter, C. Bosshard and P. Gunter, *Optical and Nonlinear Optical-Properties Of 4-(N,N-Dimethylamino)-3-Acetamidonitrobenzene Single-Crystals.* Applied Physics Letters, 1989. **54**(21): p. 2062-2064.

9. P.A. Norman, D. Bloor, J.S. Obhi, S.A. Karaulov, M.B. Hursthouse, P.V. Kolinsky, R.J. Jones and S.R. Hall, *Efficient 2nd-Harmonic Generation In Single-Crystals Of 2-(N,N- Dimethylamino)-5-Nitroacetanilide.* Journal Of the Optical Society Of America B-Optical Physics, 1987. **4**(6): p. 1013-1017.

10. M. Stahelin, D.M. Burland, M. Ebert, R.D. Miller, B.A. Smith, R.J. Twieg, W. Volksen and C.A. Walsh, *Reevaluation Of the Thermal-Stability Of Optically Nonlinear Polymeric Guest-Host Systems.* Applied Physics Letters, 1992. **61**(14): p. 1626-1628.

11. D. Freitag, G. Frengler and L. Morbitzer, *Routes to New Aromatic Polycarbonates with Special Material Properties.* Angew. Chem. Ed. Engl., 1991. **30**: p. 1598.

12. R.M. Silverstein, G.C. Bassler and T.C. Morrill, *Spectrometric Identification of Organic Compounds (4th Ed.).* 1981: John Wiley and Sons.

13. Y. Karakus, *Nonlinear Optical Properties of Poled Polymeric Thin Films*, in *Dep't of Physics.* 1993, University of Durham: Durham.

14. R.J. Gulotty, C.A. Langhoff and S.E. Bales. *Nonlinear Response of Bisphenol A Polycarbonate and Related Copolymers.* in *SPIE.* 1990.

15. J.L. Bredas, F. Meyers, C. Dehu, B.M. Pierce and S.R. Marder, *Nonlinear-Optical Response Of Organic Conjugated Compounds - Theoretical Description Of Solvent Mediated Enhancement Of Hyperpolarizabilities.* Abstracts Of Papers Of the American Chemical Society, 1994. **208**(Pt1): p. 8-COMP.

16. F. Meyers, S.R. Marder, J.W. Perry, J.L. Bredas and B.M. Pierce, *Optimizing Molecular Polarizabilities In Linear Conjugated Organic- Molecules.* Abstracts Of Papers Of the American Chemical Society, 1994. **208**(Pt2): p. 169-POLY.

17. F. Meyers, S.R. Marder, B.M. Pierce and J.L. Bredas, *Electric-Field Modulated Nonlinear-Optical Properties Of Donor- Acceptor Polyenes - Sum-Over-States Investigation Of the Relationship Between Molecular Polarizabilities (Alpha, Beta, and Gamma) and Bond- Length Alternation.* Journal Of the American Chemical Society, 1994. **116**(23): p. 10703-10714.

18. F. Meyers, S.R. Marder, B.M. Pierce and J.L. Bredas, *Tuning Of Large 2nd Hyperpolarizabilities In Organic Conjugated Compounds.* Chemical Physics Letters, 1994. **228**(1-3): p. 171-176.

19. C. Dehu, F. Meyers, E. Hendrickx, K. Clays, A. Persoons, S.R. Marder and J.L. Bredas, *Solvent Effects On the 2nd-Order Nonlinear-Optical Response Of Pi- Conjugated Molecules - a Combined Evaluation Through Self-Consistent Reaction Field Calculations and Hyper-Rayleigh Scattering Measurements.* Journal Of the American Chemical Society, 1995. **117**(40): p. 10127-10128.

CHAPTER 6

HIGH DIPOLE GUEST-HOST SYSTEMS

6.1 Introduction

The subject of this chapter concerns the nonlinear characterisation of a series of zwitterionic nonlinear optical chromophores. The high dipole moments of zwitterionic molecules can lead to high alignment efficiencies during electric field poling resulting in large nonlinear susceptibilities. Until recently, molecular characterisation of such materials has been confined to the liquid state, employing either EFISH or Hyper Rayleigh Scattering techniques, and molecular monolayers, or Langmuir-Blodgett (LB) films. Although these techniques provide a means of comparison between new molecules, they do not provide an accurate representation of their nonlinear response in a device format which would undoubtedly be in the solid state. To this end this chapter is concerned with the characterisation of the zwitterionic chromophores in the solid state. A new technique is described which makes use of angular dependent SHG measurements to determine the molecular dipole moment of the chromophores while doped into thin polymer films. The method is largely free of the requirement to know the chromophore concentration. The high dipole moment of these molecules often results in the dimerisation of a large proportion reducing the effective number density. However, this effective number density can be determined through electrochroism studies. Quantitative analysis of the SHG data can therefore be carried out providing an estimate of the molecular first hyperpolarisability of the chromophores. The values of dipole moment and nonlinear polarisability obtained are very sensitive to the choice of
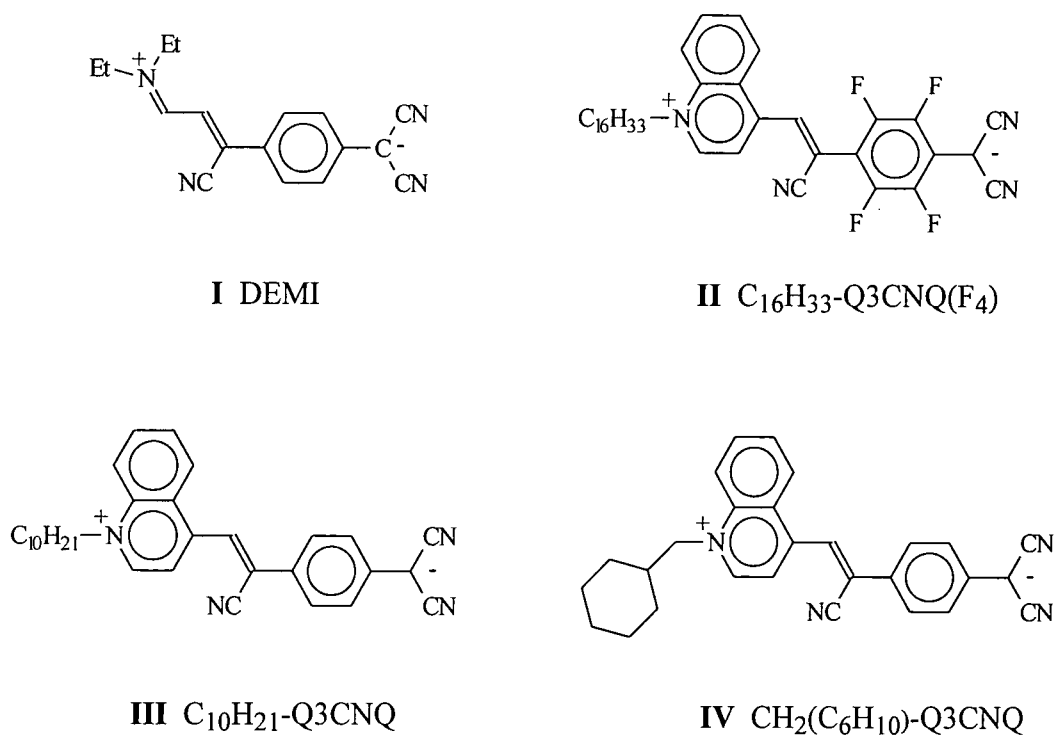
Figure 6.1 Molecular Structures of the zwitterionic chromophores investigated.

dielectric cavity shape when deriving the local field correction factors. The experimental results obtained in this study are therefore compared with theoretical calculations and a possible local field cavity shape is proposed.

6.2 Material Systems

All of the guest molecules used throughout this study (shown in figure 6.1) are zwitterionic derivatives of 7,7,8,8-tetracyanoquinodimethane (TCNQ). TCNQ was first discovered in 1960 [1] and has been used to form stable charge transfer salts with a variety of electron donors [2]. However in 1984 it was discovered that TCNQ could be reacted to a form zwitterionic donor-π-acceptor adduct [3]. This discovery led to a variety of similar molecules being synthesised [4-6] whose properties could lead to applications in molecular rectification, photochromism and nonlinear optics.

Molecule I in figure 6.1 results from a novel reaction of TCNQ with a tertiary amine reported in 1994 [6] and believed to be the first of its kind. The resultant zwitterionic molecule, known as DEMI, has a very distinctive absorption spectrum (shown in figure 6.2) and the transmission window at around 460 nm makes it a very promising candidate for use in frequency doubling devices based on anomalous dispersion phase matching [7]. Theoretical calculations using the modelling package MOPAC (version 6), result in ground state values of the dipole moment and first hyperpolarisability component along the dipole axis (β^{gs}_{vec}) of 10.1 D and 39 x 10^{-30} esu respectively. Experimental solution values for μ_t of DEMI, when dissolved in the solvent dichloromethane (DCM), has been determined, using a spherical local field cavity shape and found to be 32 ± 10 D [8].

Molecules II to IV were all zwitterionic chromophores originally synthesised for LB studies, with the long hydrophobic carbonyl chains attached to allow film deposition. Not only have the nonlinear optical properties of these LB films been investigated [4], but they have attracted considerable attention with regard to molecular rectification [9, 10]. However, these molecules are yet to be experimentally characterised in a form other than an LB film, where the uncertainty of molecular ordering during film deposition makes it difficult to determine their NLO properties. Theoretical calculations using MOPAC (version 6) result in ground state dipole moment values of 15.4 D for molecule II and 12.4 D for molecules III and IV. Ground state calculations of the first hyperpolarisability component along the dipole moment axis result in values of 86 x 10^{-30} esu for molecule II and 91 x 10^{-30} esu for the remaining two. Theoretical calculations on this class of molecule in the crystalline form have also been carried out and result in dipole moment values of 45 D [11].

6.3 Sample Preparation

Solutions of all the above guest molecules in the host polymer PMMA (see figure 5.2) at concentrations ranging from 0.2% w/w (for molecules II - IV) to 1% w/w (for

94

DEMI) were prepared in anhydrous DMF (approx. 1 g of polymer to 5 ml of solvent). As a result of the solvation effects caused by the presence of water on all of the guest molecules, anhydrous solvents had to be used and solutions were prepared in a glove box. The solutions were left stirring for approximately 12 hrs to dissolve and were then filtered through 5 μm Millipore in-line filters to remove undissolved contaminants. Films were deposited onto the appropriate substrates using the spin coating technique (section **4.2.1**). The films were spun at approximately 2000 rpm for 5 -10 seconds resulting in film thicknesses of 2 - 4 μm. Care had to be taken to ensure the films did not dry in air since moisture may be absorbed by the remaining solvent leading to cloudy films. For this reason, spinning times were kept below 10 seconds and the films were placed directly into the vacuum oven following removal from the spinning apparatus. The films were dried under vacuum at a temperature of 75 °C for 5 days to remove the solvent.

6.4 Film Characterisation

The UV-Visible absorption spectrum of DEMI-doped PMMA is shown in figure 6.2. DEMI exhibits a very large solvatochromic shift when placed into different
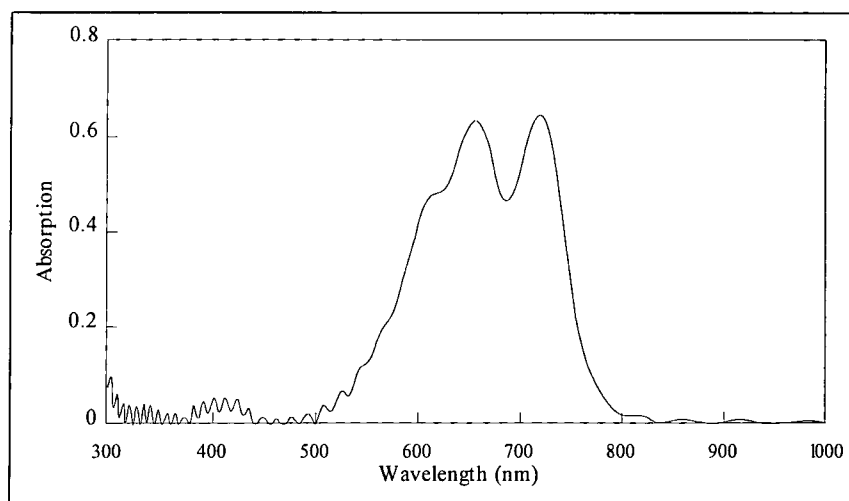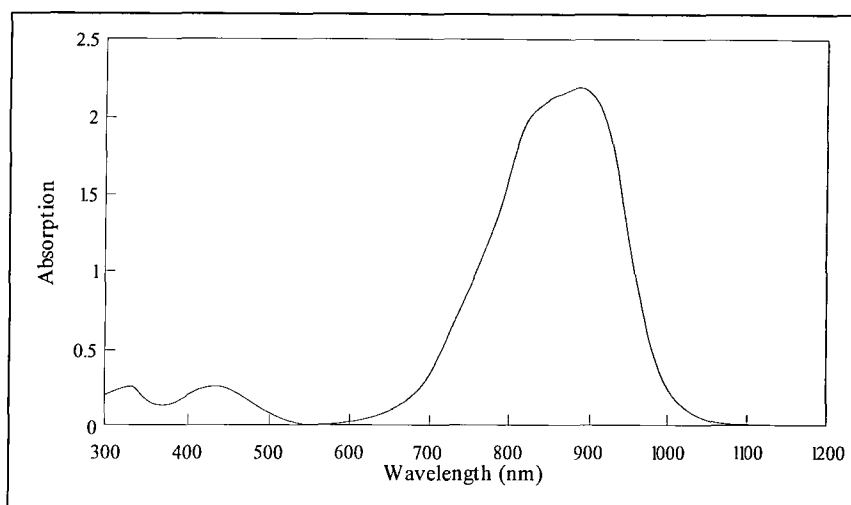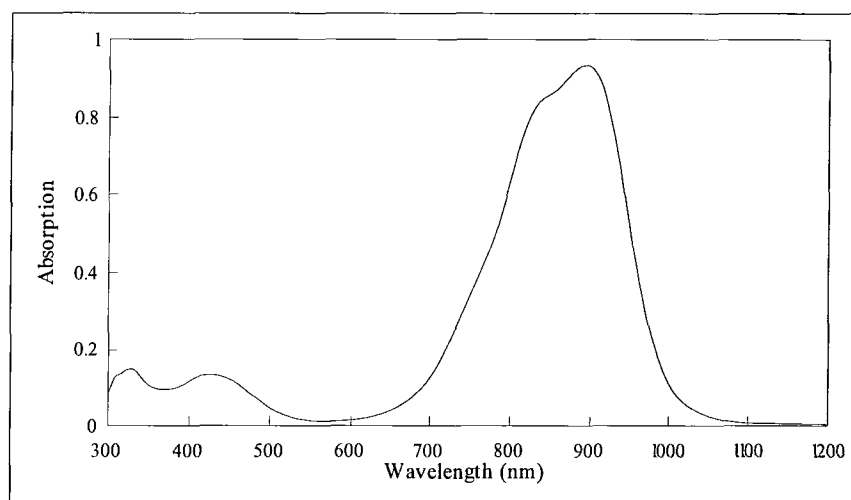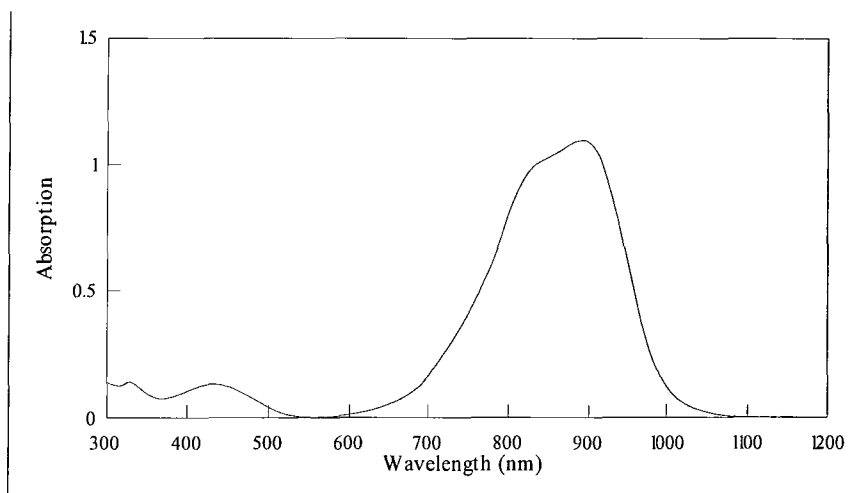

Figure 6.2 UV-Visible absorption spectrum of DEMI doped PMMA.

(a)

(b)

(c)

Figure 6.3 UV-Visible Absorption Spectra of (a) molecule II,
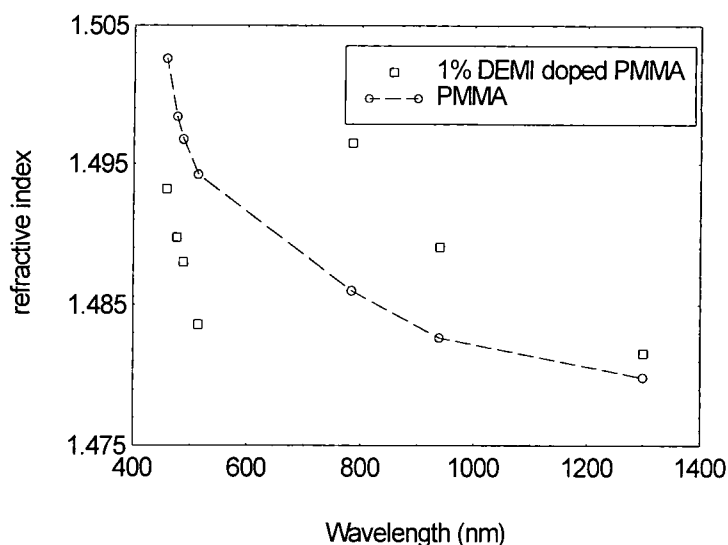(b) molecule III and (c) molecule IV.

Figure 6.4 Refractive index dispersion curve for 1% DEMI doped PMMA.

environments, with the position of the low energy band varying from 720 nm in dichloromethane (DCM) and PMMA to 690 nm in acetonitrile and DMF. Unfortunately the spectrometer was not sensitive enough to detect the absorption bands of the films containing the remaining three molecules due to the weak concentrations used. However experience has shown that the UV-Visible absorption spectrum of these molecules in PMMA is very similar to that of a DCM solution. The absorption spectra of molecules II - IV dissolved in DCM are therefore shown in figures 6.3(a) - (c). The solvatochromic shifts exhibited by these molecules are far greater than that of DEMI with the low energy band moving by as much as 180 nm.

The refractive index of PMMA and 1% DEMI-doped PMMA was measured at a variety of wavelengths using the prism coupling technique described in section **4.3.1**. The results are displayed in the form of the dispersion curves shown in figure 6.4. The anomalous dispersion region can be clearly seen through the wavelengths of the low energy absorption band (approx. 600 - 800 nm). It is in this region that phase matching can be achieved through careful control of the guest doping levels and, with the window at 460 nm in the UV-Visible absorption spectrum, may be used in a frequency doubling device to generate blue light.
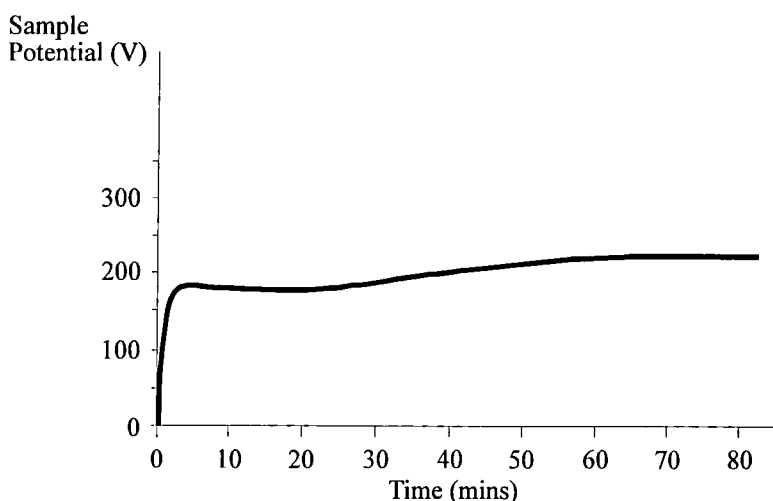
Figure 6.5 CCCT charging curve for a 1% DEMI doped PMMA film poled 25 °C below the film T_g. The curve indicates that equilibrium is reached after approximately 70 mins.

6.5 Electric Field Poling

Electric field poling of all of the films investigated in this study was carried out using the corona poling technique employing the CCCT described in section **4.4.2**. The samples were poled at temperatures in the region of 70 - 80 °C, approximately 20 - 30 °C below the T_g of the samples and with a charging current of 10 nA. The low poling temperatures enabled high electric fields to be obtained during poling. At such low poling temperatures, however, dipole alignment is very restricted and can take some time. This can be monitored by studying the evolution of the film surface voltage on the CCCT and as is indicated in a typical voltage plot (figure 6.5) takes approximately 70 mins. It is therefore important when poling at such low temperatures to monitor the alignment procedure in this manner and highlights once again the value of the CCCT. The electric fields generated ranged from approximately 50 - 200 MVm^{-1} and varied with the poling temperature chosen and the film quality.

6.6 Second Harmonic Generation Measurements

The second harmonic generation measurements served two purposes, allowing the determination of both the local molecular dipole moment of the guest chromophores (μ_l) and the resonant first hyperpolarisability component along the dipole moment ($\beta^{(\omega)}_{vec}$).

6.6.1 Experimental Methods

6.6.1.1 Dipole Moment Determination

The technique used to determine the molecular dipole moment of the guest chromophore relies on the measurement of the interaction strength between a known poling field and the dipole moment. Incidence angle resolved second harmonic generation is employed to measure the orientational distribution of the aligned dipoles following poling which, in the regime of large fields and dipole moments, is very sensitive to this interaction strength.

If equations 3.12 and 3.13 are considered and knowing that $\chi^{(2)}_{IJK} = 2\, d_{ij}$, the ratio R ($d_{31}$ / d_{33}), determined through the fitting of the experimental SHG data to equation 4.11 as described in section **4.6.2**, can be expressed in the following form:

$$R = \frac{1}{2}\left[\frac{L_1(p)}{L_3(p)} - 1\right] \qquad (6.1)$$

where $L_1(p)$ and $L_3(p)$ are the first and third order Langevin functions defined in equations (3.8) and (3.10) respectively. Since p is a function of the local dipole moment, local poling field and poling temperature only (see equation 3.3), the local dipole moment can be determined if the remaining two parameters are known. The poling field is obtainable from the CCCT characteristics (see section **4.4.2.2**) and clearly the temperature can be determined using a thermocouple. R can therefore be expressed as a function of the local dipole moment and figure 6.6(a) shows a plot of R against dipole moment at a variety of poling fields. Figure 6.6(b) shows the derivative of R with respect to μ_l and is a measure of the precision with which the
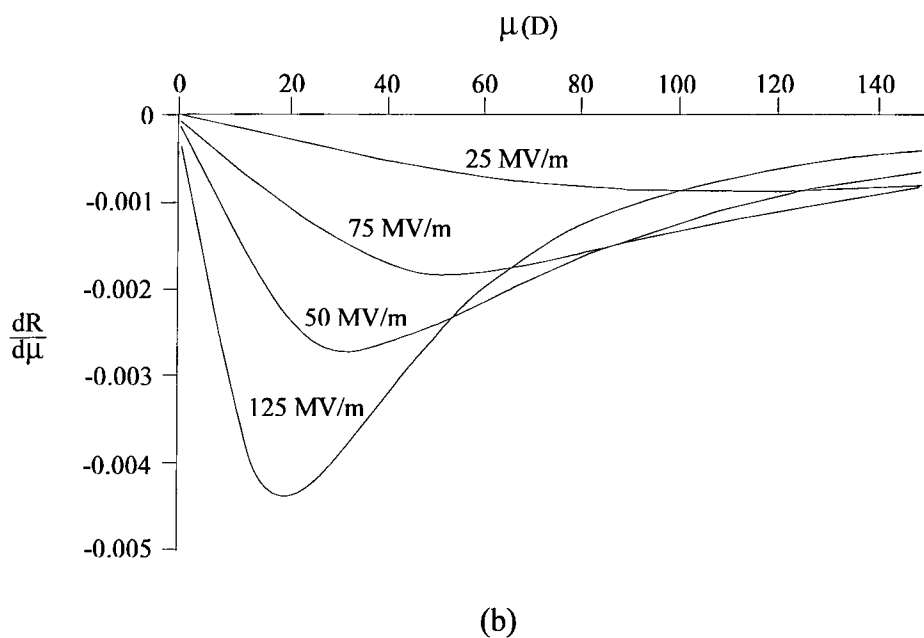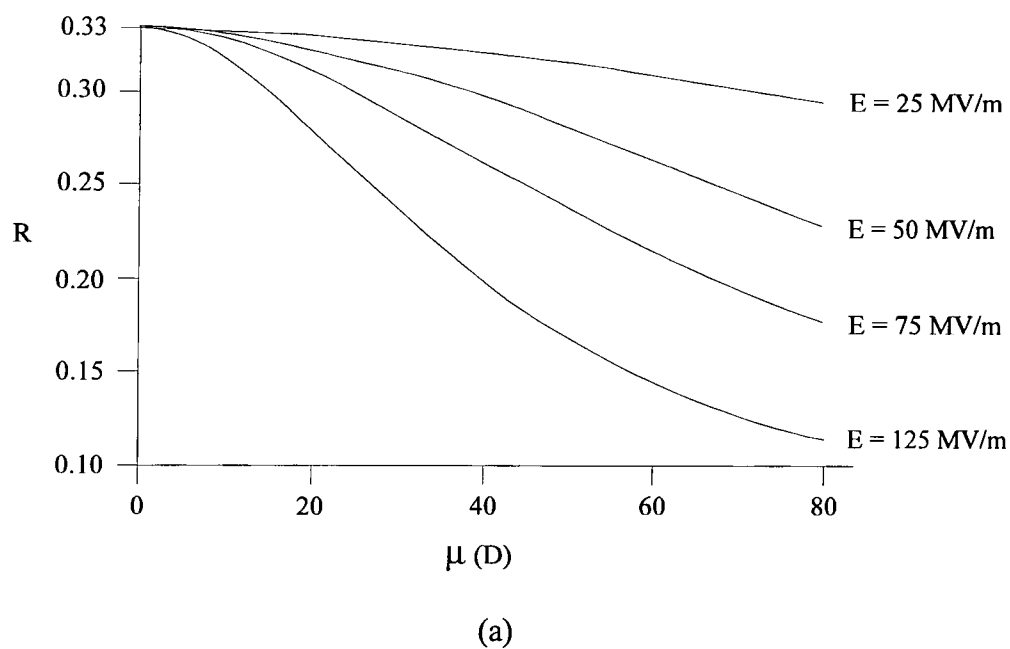
(a)

(b)

Figure 6.6 Plots showing (a) dependence of R on μ_1 and (b) derivative of R with respect to μ_1 at a variety of poling fields.

100

dipole moment may be obtained by this method. It is clear from the figures in 6.6 that R only becomes sufficiently sensitive to μ_l when the interaction strength between the dipole moment and local field is moderately large. This therefore limits this measurement technique to molecules whose dipole moments are greater than approximately 15 D, below which the experimental errors become too great. Similarly, the poling fields applied to the film must be sufficiently large and, for zwitterionic molecules of the type studied here whose dipole moments are expected to be of the order of tens of Debyes, should be at least 40 - 50 MVm^{-1}. As has already been discussed in chapter 3, this is easily achievable with the corona poling technique used in these studies. One final point clearly shown by equation (6.1) is that this technique allows the determination of the dipole moment independent of the chromophore concentration. This is very important particularly in view of the high probability of forming non-polar dimer species when working with such molecules.

6.6.1.2 Electrochroism Measurements and Determination of $\beta^{(\omega)}_{vec}$

Once the local dipole moment of the guest molecules has been determined it is possible to calculate the resonant first hyperpolarisability component along the dipole moment axis ($\beta^{(\omega)}_{vec}$). The two independent second harmonic coefficients (d_{31} and d_{33}) and therefore the second order nonlinear susceptibilities ($\chi^{(2)}_{311}$ and $\chi^{(2)}_{333}$), are calculated as described in section **4.6.2** and equations (3.11) and (3.12) can then be used to calculate $\beta^{(\omega)}_{vec}$. As can be seen in equations (3.11) and (3.12), the calculation of $\beta^{(\omega)}_{vec}$ requires knowledge of the number density of active chromophores. Although the number density of chromophores added to each film is known from the weight fractions used to prepare the initial solutions, experience has shown that a significant amount of polar molecules such as these form dimer species whose symmetry render them inactive with regard to a second order NLO response. If this is not accounted for, calculations will lead to an overestimate of the number density of active species and therefore an under estimate of $\beta^{(\omega)}_{vec}$. The effective number density of monomer species must therefore be calculated to allow an accurate determination of $\beta^{(\omega)}_{vec}$.
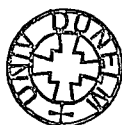
It has been well known for a number of years that the technique of electrochroism may be used to determine the extent of chromophore alignment following the electric field poling of thin films [12, 13]. Since the non-polar dimer species do not align in electric fields they will not contribute to the absorption changes observed in the electrochroism measurements. The theoretically predicted absorption changes can therefore be compared with the experimental changes and an estimate of the number of monomer species present can be made. A typical example of the UV-Visible spectral changes observed is shown in figure 6.7. If the absorbance of the unpoled sample is A_0 and A_p is the absorbance of the poled sample then the magnitude of the effect is given by:

$$\frac{A_p}{A_0} = 1 - \frac{1}{2}\left(3\cos^3\xi - 1\right)\left(1 - \frac{3\coth p}{p} + \frac{3}{p^2}\right) \tag{6.2}$$

where p is as previously defined in equation (3.3) and is calculated using the experimentally determined concentration independent values of μ_1, and ξ is the angle between the ground state dipole moment and the transition moment of the measured absorption band. If we assume ξ is zero, as is normally the case, then equation (6.2) can be simplified to the following:

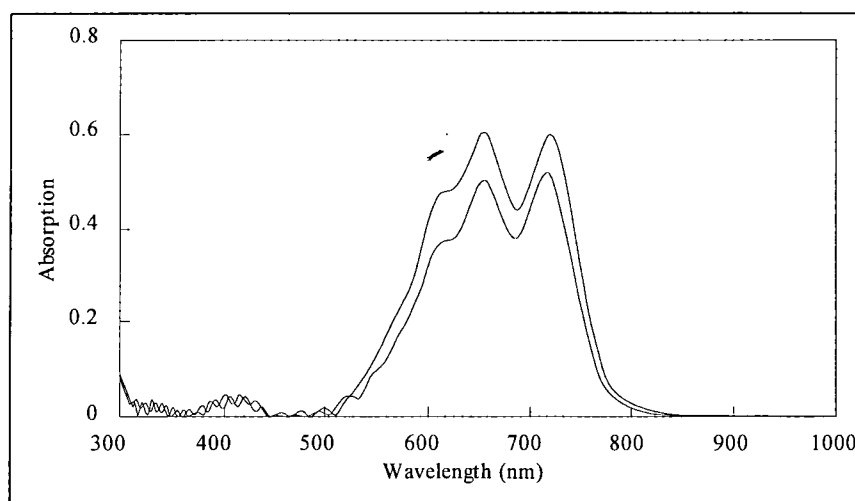$$\frac{A_p}{A_0} = \frac{3}{p^2} - \frac{3\coth p}{p} \tag{6.3}$$

Figure 6.7 Absorption spectra of 1% DEMI doped PMMA before and after poling.

Thus the expected absorption change obtained from equation (6.3) can be compared with the experimental change and an estimate of the non-dipolar content of the dopant calculated. The number density, N, in equations (3.11) and (3.12) can therefore be modified accordingly and a more accurate value of $\beta^{(\omega)}_{vec}$ may then be determined.

6.6.2 Results and Discussion

Typical values of R obtained from these samples are significantly lower than 0.33 and range from 0.19 to 0.28 as figure 6.6(a) would indicate for guest molecules with large dipole moments. The resultant local dipole moments calculated from equation (6.1) are given in table 6.1. In view of recent work carried out by Dehu et al. [14] who have proposed that the dielectric cavity must be ellipsoidal when calculating the reaction field acting on a molecule, two dipole moment values are presented for each molecule corresponding to the two local field models used (see section **2.3.1**). The first of these models is the Onsager local field model (see section **3.3.1**) which employs, what has been up to now, the more conventional spherical cavity. The second, and that considered by Dehu et al. to calculate reaction fields employs an ellipsoidal cavity whose shape is governed by the molecule. Dynamic values for the first hyperpolarisability, $\beta^{(\omega)}_{vec}$, employing each of the two local field models are also presented. The electrochroism measurements suggest that the effective number density of dipoles in the 1% DEMI doped PMMA films is only 1/3 of that of the

Molecule	μ (D) (spherical)	μ (D) (ellipsoidal)	β^{ω} (x 10^{-30} esu) (spherical)	β^{ω} (x 10^{-30} esu) (ellipsoidal)
I	32 ± 5	46 ± 5	330 ± 70	480 ± 100
II	38 ± 10	47 ± 10	600 ± 120	800 ± 180
III	35 ± 5	44 ± 5	600 ± 120	1000 ± 200
IV	35 ± 5	44 ± 5	600 ± 120	1000 ± 200

Table 6.1 Dipole moment and dynamic $\beta^{(\omega)}_{vec}$ values for molecules I - IV determined from SHG measurements using the spherical and elliptical cavity local field models.

total concentration of dopant molecules. It should be noted, however that due to the very low doping levels and the resultant weak absorption bands observed in films containing molecules II - IV, only the values of $\beta^{(\omega)}_{vec}$ for molecule I (DEMI) have been corrected for dimer formation. Therefore the values obtained for molecules II - IV should be considered minimum values since the number density of contributing molecules is expected to be lower.

Despite the large differences between the values of μ_1 obtained using the two local field cavity models it is quite clear that the molecules in PMMA exists predominantly in a zwitterionic ground state and possess a dipole moment far in excess of those expected for a neutral quinoidal structure. The values obtained for β_{vec} are also very large and are much greater than the ground state values calculated on MOPAC (see section **6.2**). The molecules therefore show great promise with regard to second order nonlinear optical devices particularly in the case of DEMI whose spectral properties are very favourable for a frequency doubling blue light generator.

6.6.2.1 Comparison with Theoretical Calculations

It is clear from the results in table 6.1 that the experimentally determined values of μ_1 and $\beta^{(\omega)}_{vec}$ are very sensitive to the choice of dielectric cavity shape employed when deriving the local field correction factors. In order to establish which cavity shape is more favourable, the results were compared with theoretical calculations which model the dipole moment and first hyperpolarisability under the influence of an applied field. It has been shown recently that the values of μ_1 and the static first hyperpolarisability, $\beta^{(0)}_{vec}$, depend markedly on the dielectric nature of the environment in which the molecule is embedded [17-19]. This has been accounted for in terms of a reaction field which is an electric field generated by the polarisable dielectric medium surrounding the molecule resulting from the presence of that molecule [20]. This field, which is directed opposite to the dipole moment, redistributes the charge on the molecule and enhances μ_1. Clearly this redistribution of charge will also have a considerable effect on the hyperpolarisability of the molecule. The theoretical calculations involve applying fields of the order of that

expected of a typical reaction field and modelling the response of the dipole moment and first hyperpolarisability. The influence of this field on molecule I (DEMI) has been studied by Malgoli et al. [21] at the semi-empirical INDO (Intermediate Neglect of Differential Overlap) level. Once the field was applied the molecular geometries in the presence of the field were optimised at the SCF (Self Consistent Field) level and calculations of $\alpha_{ij}(\omega)$ and $\beta^{(0)}_{ijk}(\omega)$ were performed by means of the Sum Over States (SOS) formalism (40 States) on the basis of state energies, state dipole moment and transition moments computed with a Single Configuration Interaction (SCI) calculation [22]. Figures 6.8(a) and (b) show the evolution of the theoretical dipole moment and $\beta^{(0)}_{vec}$ values for DEMI as a function of the applied field. It is clear that these calculations further support the assertion that these molecules exist in a charge separated state in these films and that the large dipole moments measured experimentally are of the correct order of magnitude.

Dehu et al. have already stated that the reaction field exerted on a molecule must be calculated using an ellipsoidal cavity model. Using the model outlined by Scholte [24], the reaction field can be calculated using the following equation:

$$R = \frac{3}{abc} \frac{A_1(1-A_1)(\varepsilon_h - 1)}{\varepsilon_h + (1 - \varepsilon_h)A_1} \mu_1 \qquad (6.4)$$

where a, b, c, A_1 and ε_h are defined in section **2.3.1**. If the ground state dipole moment of the molecule is μ_{gs} then the local dipole moment within the cavity (μ_l) is given by:

$$\mu_l = \frac{1}{(1 - f_R\alpha_1)}\mu_{gs} \qquad (6.5)$$

where $f_R = R / \mu_l$ and α_1 is the molecular polarisability component along the dipole moment axis. For DEMI in PMMA the reaction field calculated using equation (6.4) is 0.0036 au which results in a local dipole moment of 25.9 D. A quick comparison of this theoretical dipole moment with the measured dipole moments for DEMI in table 6.1 clearly indicates that the experimental results are in far more agreement with theory if a spherical cavity model is employed when determining the local field

105
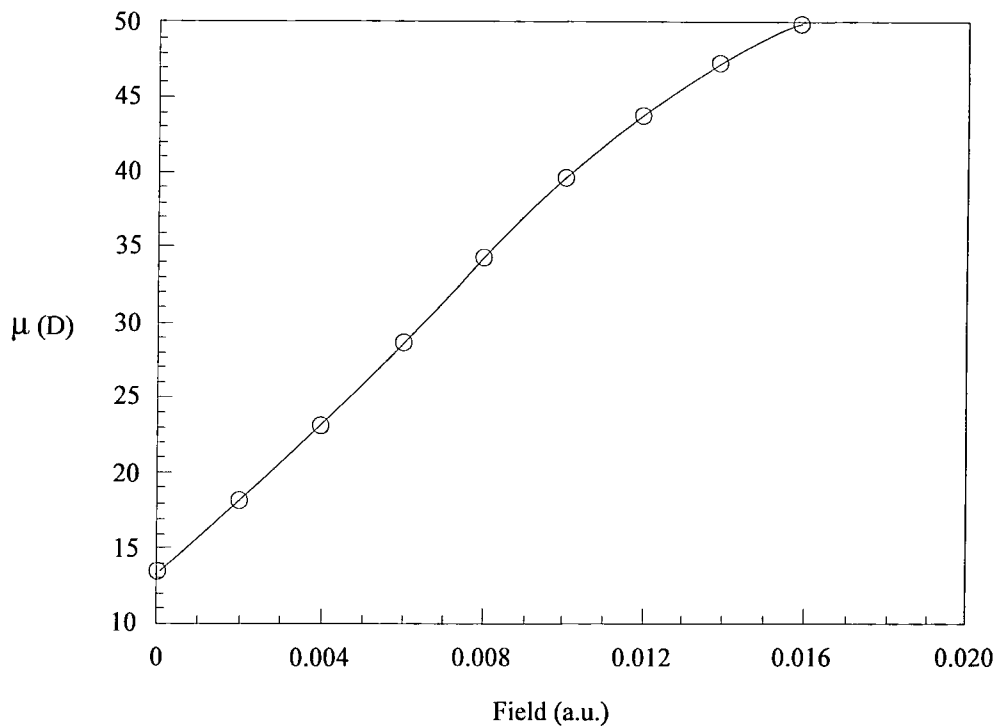
(a)
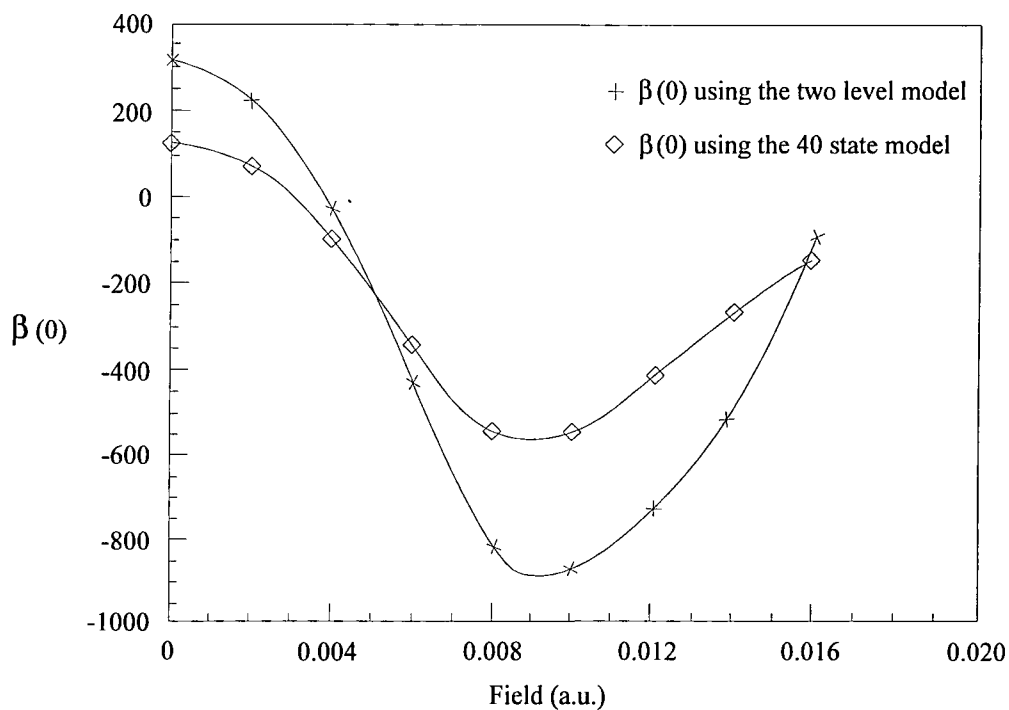
(b)

Figure 6.8 Graphs showing the theoretical evolution of (a) the dipole moment
and (b) the non-resonant molecular hyperpolarisibility with electric field.

106

correction factors. Using the elliptical local field model results in dipole moment values which are far too high. Further support for the dipole moments obtained using the spherical local field model comes from comparison with the value obtained from solution calculations. Thomas et al. have determined the dipole moment of DEMI dissolved in DCM using a spherical cavity local field model to be 34 D [8]. The position of the low energy absorption band of DEMI in DCM in the UV-Visible absorption spectrum is 720 nm. This resonance is in a very similar position to that of DEMI in PMMA (see figure 6.2) and suggests that the DEMI molecules reside in very similar local environments within the two host media. It might be expected therefore that similar dipole moment values will be obtained. The spherical cavity local field model was employed in the solution calculations with greater certainty since its use to calculate gas phase values of the dipole moment of DEMI proved more accurate than calculations employing an elliptical cavity [8]. It would therefore appear that despite the necessity to calculate the reaction field using an ellipsoidal cavity model as shown by Dehu, a spherical cavity model is favoured when calculating the local field correction factors.

Despite the evidence which suggests that a spherical cavity must be employed to determine the local fields, the dipole moment values calculated using equation (6.5) are far from equal to those measured experimentally. Figure 6.8(a) would suggest that for a dipole moment of 32 D a reaction field of approximately 0.007 au is operating which is double the calculated value. The value obtained from figure 6.8(a) is a measure of all reaction field effects acting on the molecules including local interactions not accounted for in the above Scholte model. It would therefore appear that the fields acting on the guest molecules are far more complicated than can be described using the above simple model and may include local effects such as intermolecular interactions.

Although the local field correction factors and the reaction fields are calculated using the same theoretical model, it would appear that two different dielectric cavity shapes are required for each calculation. This may seem somewhat strange at first,

but if the behaviour of the chromophores during poling and the nature of the two fields in question are considered in more detail this observation may be rationalised.

During electric field poling two energies must be considered, that of the molecule in the applied electric field and its thermal energy. The thermal energy has the effect of disorganising the distribution of the molecules causing them to move and vibrate randomly. It is this thermal motion which prevents the dipoles from aligning fully during poling resulting in an averaged cone distribution of the molecules with respect to the applied poling field. Averaged over time, therefore, the shape of this molecular distribution would appear to be far more spherical than that of an individual molecule and it may be the shape of this that must be accounted for in the local field correction factor calculations. This is not unreasonable since the poling time is far in excess of the time periods over which thermal motions occur. In the case of the reaction field this is certainly not the case. Since the reaction field originates from the dipole moment field of the molecule it is always directed anti-parallel to the dipole moment axis (this is indicated in equation (6.6) by only using the components of A and α_{ij} directed along the dipole moment axis). As a result at every instant in time, regardless of the orientation of the molecule with respect to the poling field, the reaction field is applied along one molecular direction and therefore the molecular shape must be accounted for in its calculation.

Similar conditions will apply to the optical local field correction factors and as such the calculation of the first hyperpolarisability for each molecule employing a spherical local field model should be used. This would suggest therefore that the lower values for the dynamic hyperpolarisability of each molecule in table 6.1 is favoured.

6.6.2.2 High Poling Field Regime

The results in table 6.1 were consistently obtained for a number of different poling fields up to a value of approximately 100 MVm^{-1}. However, higher poling fields resulted in a gradual reduction of the calculated dipole moment as displayed in figure 6.9. The graph shows a plot of the measured dipole moment of molecule IV,
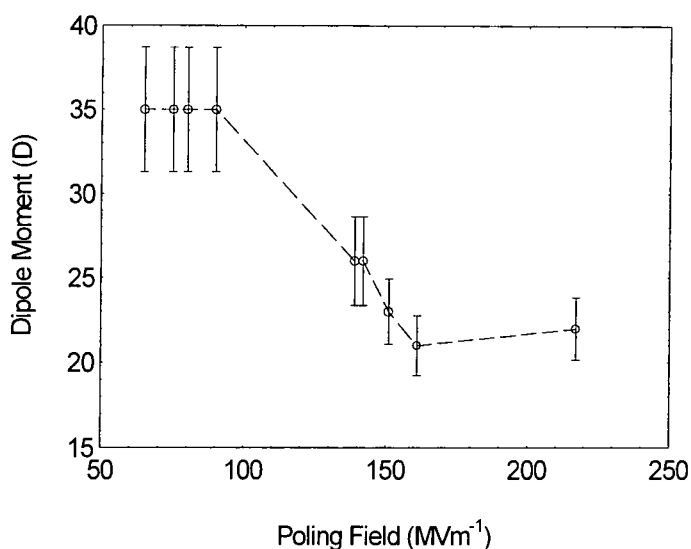
Figure 6.9 Graph showing the measured dipole moment, using a spherical local field cavity model, as a function of the applied poling field.

calculated using an elliptical cavity model, against the external poling field as measured by the CCCT. It clearly indicates a drop in the dipole moment of some 13 D between fields of 100 MVm^{-1} to 150 MVm^{-1} beyond which it levels out and remains steady at about 22 D. The origin of this effect is as yet unknown, however up to now three possible explanations have been considered.

The first possible explanation for the observed high field anomalies is that through some mechanism, the alignment field exerted on each molecule is reducing relative to that which is measured. This could be explained in two ways, both of which arise through consideration of the effects of charge injection. Under normal conditions and moderate poling fields, ions generated as a result of a corona discharge do not possess enough energy to penetrate the sample [25] and as such remain on the surface applying a field across the entire sample thickness. However, as the generated field increases, some of the ions may start to progress through the sample surface under the influence of this high field and become trapped within the bulk, thereby reducing the magnitude of the poling field. Due to the very small sample thicknesses used in these studies, the CCCT is unable to differentiate between surface and bulk trapped charge and as a result would overestimate the poling field leading to a decrease in the calculated values of dipole moment. The second route by

which errors may be introduced into the measured field values is through alteration of the local fields. Recent studies by Risser and Ferris have provided evidence indicating that the presence of defects within a media, which would include trapped charge, can alter the local fields [26]. This effect once again could reduce the effective field exerted on the guest molecules resulting in an underestimate of the dipole moment.

The consideration of charge injection leads onto a second possibility, that being the dipole moment is itself reducing. Recent work has highlighted the strong dependence of the electron affinity of an organic polar molecule with its dipole moment [27]. Models employing the Hartree-Fock method and second order perturbation theory used to study the electronic structures of various organic molecules have shown that the electron affinity grows rapidly for those molecules whose dipole moments exceed about 4 D. Clearly the molecules in this study will therefore have very large electron affinities and the presence of any free charge brought about by charge injection could easily alter their electronic state and thus reduce the dipole moment. If this were the case evidence would be apparent in their optical spectra, however this has yet to be observed. It is important to note that if this phenomenon is occurring the injected free charge is not directly attacking the molecules as this would be indicated by degradation of the optical spectrum.

Probably the most likely explanation concerns discussion in the previous section regarding the use of a spherical cavity in calculating the local field correction factors. It was concluded that it should be the shape of the time averaged dielectric cavity, defined by the thermal motion of the molecules, which should be accounted for in the local field calculations. Under moderate poling fields (ie. < 100 MVm^{-1}), even with dipole moments of 32 D, this time averaged cavity is approximately spherical in shape since the internal cone half angle of the molecular distribution remains large. However, as the poling fields increase still further and the alignment efficiency rises, the shape of the time averaged cavity will begin to elongate and approach that of the molecule itself as the cone half angle of the molecular distribution decreases. This

would result in the true local field correction factor being lower than that calculated leading to an underestimate of the dipole moment.

Further to the above effect, as the cavity becomes ellipsoidal in shape another effect will reduce the local field factor still further as a result of the high degree of alignment of the ellipsoids. This effect concerns the derivation of the Scholte local field correction factors in section **2.3.1**. The local field in Scholte's equation is expressed in terms of three perpendicular components (see equations (2.10) - (2.16)) which in the case of randomly oriented ellipsoids are averaged to obtain the net local field. However, if the ellipsoids are not randomly oriented then this simple averaging is not valid and distribution terms for each of the components have to be introduced [24]. At poling fields of a few 10's of MVm^{-1} where the alignment efficiencies are low, an averaged spread of ellipsoids is a good approximation even with high dipole chromophores. However, with guest molecules possessing a large dipole moment, alignment efficiencies can increase substantially when the poling fields become large as indicated by the considerable reduction in R (see figure 6.6(a)). As a result the local field will gradually reduce and for these highly anisotropic and polarisable molecules, approach that of the external field, as alignment efficiencies increase. This would lead to further underestimate of the poling field and clearly lead to an apparent reduction in the measured dipole moment.

Although the results in figure 6.10 are as yet unexplained the most likely cause is the final explanation discussed above regarding the change of the effective cavity shape along with the effects of orienting ellipsoids as the poling field increases. Existing local field models should therefore be examined in detail to give a greater understanding of this subject. However the possibility of injected charge affecting the system in some manner should not be discounted particularly in view of the high probability of its presence at such high poling fields. Thermally stimulated current (TSC) studies at different poling fields would allow investigation of this, revealing if deposited surface charge is indeed redistributing itself through the sample at high fields. One result that is clear from these studies is that models used to describe

electric field poling, particularly the subject of local fields, may still be limited and care should be taken when modelling these systems under extreme poling conditions.

6.7 Summary and Conclusions

The dipole moments of a series of zwitterionic chromophores doped into the polymer PMMA have been determined using a new technique based on angle resolved SHG measurements. The values obtained, along with the calculated values of $\beta^{(\omega)}_{vec}$, were shown to be very sensitive to the shape of the dielectric cavity used in the derivation of the local field correction factors. By comparison of the μ_l values obtained using different cavity shapes with theoretical calculations, evidence is found which supports, in this case, a model cavity describing a sphere. Although this appears at first to contradict the results of Dehu on reaction field theory, the observations are explained in terms of thermal motion of the chromophores which leads to a more spherical time averaged dielectric cavity. This thermal motion need not be accounted for in the calculation of the reaction field since it is always directed anti-parallel to the dipole moment, irrespective of the orientation of the molecule with respect to the poling field.

It is also shown that the accuracy of the dipole moment measurement technique described in this chapter cannot be guaranteed when the poling fields are higher than approximately 100 MVm^{-1}. It is thought that the very high alignment efficiencies achieved at very high poling fields may reduce the effect of the thermal motion and change the shape of the time averaged dielectric cavity. This would lead to a reduction of the local field and an underestimate of the dipole moment. Although the origin of the apparent reduction in measured dipole moment is not fully understood these results highlight the care that must be taken when modelling systems such as these, particularly under extreme poling conditions.

6.8 References

1.   D.S. Acker, R.J. Harder, W.R. Hertler, W. Mahler, l.R. Melby, R.E. Benson and W.E. Mochel, *7,7,78-Tetracyanoquinodimethane and its Electrically Conducting Anion-radical Derivatives.* J. Am. Chem. Soc., 1960. **82**: p. 6408.

2.   L.R. Melby, R.J. Harder, W.R. Hertler, W. Mahler, R.E. Benson and W.E. Mochel, *Substituted Quinodimethanes II. Anion-Radical Derivatives and Complexes of 7,7,8,8-Tetracyanoquinodimethane.* J. Am. Chem. Soc., 1962. **84**: p. 3374.

3.   R.M. Metzger, N.E. Heimer and G.J. Ashwell, *Crystal and Molecular-Structure and Properties Of Picolyltricyanoquinodimethan, the Zwitterionic Donor-Pi-Acceptor Adduct Between Li&TCNQ- and 1,2-Dimethylpyridinium Iodide.* Molecular Crystals and Liquid Crystals, 1984. **107**(1-2): p. 133-149.

4.   G.J. Ashwell, *Photochromic and Nonlinear Optical-Properties Of C16H33-P3CNQ and C16H33-Q3CNQ Langmuir-Blodgett-Films.* Thin Solid Films, 1990. **186**(1): p. 155-165.

5.   G.J. Ashwell, E.J.C. Dawnay, A.P. Kuczynski, M. Szablewski, I.M. Sandy, M.R. Bryce, A.M. Grainger and M. Hasan, *Langmuir-Blodgett Alignment Of Zwitterionic Optically Nonlinear D-π- A Materials.* Journal Of the Chemical Society-Faraday Transactions, 1990. **86**(7): p. 1117-1121.

6.   M. Szablewski, *Novel Reactions Of TCNQ - Formation Of Zwitterions For Nonlinear Optics By Reaction With Enamines.* Journal Of Organic Chemistry, 1994. **59**(5): p. 954-956.

7.   T.C. Kowalczyk, K.D. Singer and P.A. Cahill, *Anomalous-Dispersion Phase-Matched 2nd-Harmonic Generation In a Polymer Wave-Guide.* Optics Letters, 1995. **20**(22): p. 2273-2275.

8.   P. Thomas and G. H. Cross, University of Durham, *Private Communication.*

9.   G.J. Ashwell, J.R. Sambles, A.S. Martin, W.G. Parker and M. Szablewski, *Rectifying Characteristics Of Mg/(C16H33-Q3CNQ LB Film)/Pt Structures.* Journal Of the Chemical Society-Chemical Communications, 1990(19): p. 1374-1376.

10.   A.S. Martin, J.R. Sambles and G.J. Ashwell, *Molecular Rectifier.* Physical Review Letters, 1993. **70**(2): p. 218-221.

11. A. Broo and M.C. Zerner, *Electronic-Structure Of Donor-Spacer-Acceptor Molecules Of Potential Interest For Molecular Electronics .4. Geometry and Device Properties Of P3CNQ and Q3CNQ.* Chemical Physics, 1995. **196**(3): p. 423-436.

12. E.E. Havinga and P. Van Pelt, *Intramolecular Charge Transfer Studied by Electrochroism of Organic Molecules in Polymer Matrices.* Mol. Cryst. Liq. Cryst, 1979. **52**: p. 145-156.

13. S. Hu, G.O. Carlisle and D.R. Martinez, *Absorption Studies Of Polymer-Dye Films Oriented By Corona Poling.* Journal Of Materials Science Letters, 1992. **11**(11): p. 794-796.

14. C. Dehu, F. Meyers, E. Hendrickx, K. Clays, A. Persoons, S.R. Marder and J.L. Bredas, *Solvent Effects On the 2nd-Order Nonlinear-Optical Response Of Pi- Conjugated Molecules - a Combined Evaluation Through Self-Consistent Reaction Field Calculations and Hyper-Rayleigh Scattering Measurements.* Journal Of the American Chemical Society, 1995. **117**(40): p. 10127-10128.

15. D. Rinaldi, M.F. Ruizlopez and J.L. Rivail, *Ab initio SCF Calculations On Electrostatically Solvated Molecules Using a Deformable 3 Axes Ellipsoidal Cavity.* Journal Of Chemical Physics, 1983. **78**(2): p. 834-838.

16. J.A. Osborn, *Demagnetisation Factors of the General Ellipsoid.* Phys. Rev., 1945. **67**: p. 351.

17. J.L. Bredas, F. Meyers, C. Dehu, B.M. Pierce and S.R. Marder, *Nonlinear-Optical Response Of Organic Conjugated Compounds - Theoretical Description Of Solvent Mediated Enhancement Of Hyperpolarizabilities.* Abstracts Of Papers Of the American Chemical Society, 1994. **208**(Pt1): p. 8-COMP.

18. F. Meyers, S.R. Marder, J.W. Perry, J.L. Bredas and B.M. Pierce, *Optimizing Molecular Polarizabilities In Linear Conjugated Organic- Molecules.* Abstracts Of Papers Of the American Chemical Society, 1994. **208**(Pt2): p. 169-POLY.

19. F. Meyers, S.R. Marder, B.M. Pierce and J.L. Bredas, *Tuning Of Large 2nd Hyperpolarizabilities In Organic Conjugated Compounds.* Chemical Physics Letters, 1994. **228**(1-3): p. 171-176.

20. L. Onsager, *Electric Moments of Molecules in Liquids.* J. Am. Chem. Soc., 1936. **58**: p. 1486.

21. M. Malgoli, F. Meyers and J.L. Bredas, *Private Communication, .* 1995.

22.   F. Meyers, S.R. Marder, B.M. Pierce and J.L. Bredas, *Electric-Field Modulated Nonlinear-Optical Properties Of Donor- Acceptor Polyenes - Sum-Over-States Investigation Of the Relationship Between Molecular Polarizabilities (Alpha, Beta, and Gamma) and Bond- Length Alternation.* Journal Of the American Chemical Society, 1994. **116**(23): p. 10703-10714.

23.   N. Bloembergen, *Nonlinear Optics*. 1965: Benjamin.

24.   Th. G. Scholte, *A Contribution to the Theory of the Dielectric Constant of Polar Liquids.* Physica, 1949, **XV** p. 437

25.   R. Moreno and B. Gross, *Measurements of Potential Build up and Decay, Surface Charge Density and Charging Currents of Corona Charged Polymer Foil Electrets.* J. Appl. Phys., 1976. **47**: p. 3397.

26.   S.M. Risser and K.F. Ferris, *Enhancements Of Local Electric-Fields In Inhomogeneous Dielectric Media By Microstructural Defects.* Materials Letters, 1992. **14**(2-3): p. 99-102.

27.   G.L. Gutsev and L. Adamowicz, *Relationship Between the Dipole-Moments and the Electron-Affinities For Some Polar Organic-Molecules.* Chemical Physics Letters, 1995. **235**(3-4): p. 377-381.

CHAPTER 7

CONCLUDING REMARKS

It is clear at present that within the field of nonlinear optics research must be concentrated on the development of new materials. Along with this, however, an understanding of the properties and behaviour of the new molecules within their environment must also be gained if their suitability for device applications is to be evaluated fully. It is with this aspect of the field that the work contained within this thesis is concerned.

If the device suitability of new materials is to be evaluated, techniques must be developed which can characterise the nonlinear optical properties of new compounds in a device format. The sensitivity to environment of the relevant molecular parameters has already been demonstrated and the results obtained in this work regarding the hyperpolarisability measurement of DAN in PMMA highlights further the necessity of characterising molecules in the solid state. The development of a new technique by which the dipole moment of polar molecules can be determined in the solid state is therefore very important. Unfortunately the technique is limited only to those molecules whose dipole moments are expected to be of the order of tens of Debyes. However, if poled polymer systems are to be used in optical devices, it is clear that only those systems containing highly polar chromophores will interact with the poling field sufficiently to induce the high alignment efficiencies required.

Although the approach taken during the course of this research to characterise molecules in the solid state may be the more appropriate there still remains a number of uncertainties with the current theoretical models used. The value of the local field factors has the most severe effect on the measured values of dipole moment and it is with this calculation that the majority of uncertainties lie. Whether the Onsager model or the more detailed Scholte model is employed to calculate the local field factors and reaction fields, both the local molecular polarisability and molecular volume of the guest chromophores must be known. Throughout the calculations made in this study gas phase values of the molecular polarisability have been used and the molecular volume has been determined from the van-der-Waals dimensions measured on a computer modelling package. The sensitivity of the molecular polarisability to environment has already been demonstrated and as such relatively small changes in the dielectric nature of the environment may have a considerable effect on the local field values when modelling highly polarisable molecules such as zwitterions. The determination of the molecular volume can have an even greater effect on resultant local field calculations. Depending on how the molecular dimensions are measured, the local field values for the molecules investigated in this study can vary by as much as 10 %. Both of these factors could introduce errors into the measured dipole moment values as great as 15 %.

The comparison of measured dipole moments with theoretically calculated values using the reaction field model highlights a further uncertainty to the measured dipole moment values. It would appear that there is the possibility of local molecular interactions influencing the local fields by a considerable amount. Clearly these interactions would be difficult to characterise and as such neither of the local field models employed took account of them. As a result they could introduce further errors into the values of measured dipole moment.

Although the concern of this discussion lies with the solid state dipole moment measuring technique described above, the same arguments and uncertainties apply to the more familiar solution techniques. The calculation of the dipole moment in solution relies on the understanding of the dielectric behaviour of the solution and as

a result models similar to those used in describing the local fields are employed. Many of the assumptions made in these local field models are valid for a large number of existing molecules. However, with materials research being concentrated on the larger, more polarisable molecules, these assumptions may no longer be valid and as such the theory must be analysed once again. Further to this an investigation into the presence and the effects of local molecular interactions on the local fields should also be carried out. It is clear, therefore, that a great deal of research still needs to be conducted if dipole moment measurement techniques are to be considered reliable for many of the large highly polarisable molecules investigated currently.

Despite the many uncertainties in the results of this study the nonlinear optical properties of the zwitterionic chromophores investigated are still highly promising. All of the molecules studied possessed large dipole moments and molecular hyperpolarisabilities well in excess of many of the previously reported molecules. There still exists, however, several problems with this class of material which would severely limit their application at present. Probably the most important of these and one which is common to many of the highly nonlinear molecules, is that of chemical stability. Upon exposure to light these chromophores degrade under the process of photo-induced oxidation. Further to this the alignment of the chromophores following poling remains only for a few days at most for DEMI and a few weeks for the remaining zwitterionic systems. From a device point of view, therefore, a considerable amount of work needs to be carried out if the nonlinear optical properties are to remain stable long enough to be of any practical use. If these obstacles were to be overcome, however, the class of materials investigated during the course of this research would be very strong contenders for possible device applications and as such further characterisation of their properties and behaviour in a device format should continue.